Excitations in Holographic Quantum Liquids

Richard A. Davison

Christ Church, University of Oxford

Trinity Term 2012

Submitted for the degree of Doctor of Philosophy in Theoretical Physics

Acknowledgements

I am deeply indebted to Andrei Starinets for both his guidance and patience over the last four years, as well as for the countless hours he has spent explaining physics to me which have made this thesis possible. I am also grateful to Danny Brattan, Simon Gentle, Sašo Grozdanov, Nikos Kaplis and Andy O'Bannon for their collaboration on the work herein and elsewhere, and to the Science and Technology Facilities Council for their financial support. On a more personal note, I would like to say thank you to my parents, grandparents and siblings for their support over the last 25 years, and muchas gracias to Mónica. Finally, I would like to thank all of my other teachers, colleagues and friends in Cambridge, Oxford and around the world who have helped me along the way.

Abstract

In this thesis we review the gauge/gravity duality and how it can be used to compute the thermodynamic properties and low-energy excitations of holographic quantum liquids — strongly-interacting field theories with a non-zero density of matter. We then study in detail the charge density excitations of two such liquids, the D3/D7 theory and the RN-AdS_4 theory, by computing the poles of their charge density Green's functions, and their charge density spectral functions. Although it is not a Landau Fermi liquid, the charge density excitations of the D3/D7 theory display many of the same properties as one, including a collisionless/hydrodynamic crossover as the temperature is increased. In contrast to this, the charge density (and energy density) excitations of the RN-AdS_4 theory do not share these properties but behave in a way that cannot be explained by Landau's theory of interacting fermionic quasiparticles. This is consistent with other results which indicate that this is not a Landau Fermi liquid.

Contents

Chapter 1

Introduction

1.1 Overview

String theory is a theory which incorporates both gravity and gauge field theories. For this reason, it has been studied extensively for many decades as a possible 'theory of everything' — a unified description of all known forces and matter. In 1997 it was realised that in addition to unifying gravity and gauge field theories, string theory provides a startling link between these two apparently distinct phenomena [1]. This link, which became known as 'the AdS/CFT correspondence' or, more generally, 'gauge/gravity duality', is the subject of this thesis.

Heuristically, the existence of such a link may not seem too surprising since both gravitational degrees of freedom and gauge field degrees of freedom arise from stringy dynamics. Gauge/gravity duality is, however, tremendously more powerful than one might anticipate. A formal statement of the duality for a particular example will be given in the following section, but its essence can be understood as follows. A given configuration of stringy degrees of freedom may be constructed in two ways, each of which is valid in a different range of a parameter λ. When $\lambda \ll 1$, the stringy degrees of freedom at low energy are just those of a gauge field theory whereas when $\lambda \gg 1$, the stringy degrees of freedom at low energy are those of gravity. Gauge/gravity

duality is the conjecture that these two different theories are actually equivalent for all values of λ.

A key feature of gauge/gravity duality is that the gravitational theory lives in a spacetime with a greater number of spatial dimensions than its 'dual' gauge theory. Because of this, gauge/gravity duality is a manifestation of the holographic principle — that a gravitational system in a certain volume can be described in terms of degrees of freedom living on the area bounding that volume [2–4]. It is worthwhile to note that the duality does not rely upon the experimental verification of string theory as a true description of nature, but simply on the theoretical fact that certain gauge field theories and gravitational theories may be constructed within string theory.

The work in this thesis will exploit one particularly startling feature of gauge/gravity duality. In the limit $\lambda \to \infty$, the gravitational theory reduces to a classical theory of gravity. In the dual gauge theory, λ is the coupling constant. Thus one manifestation of gauge/gravity duality is that some specific classical theories of gravity are equivalent to some specific infinitely strongly-interacting gauge field theories. As will be described in more detail below, this allows one to compute the Green's functions of some strongly-interacting field theories by doing relatively simple calculations in the dual, classical gravitational theory.

Although they are certainly realised in nature, strongly-interacting field theories are, in general, poorly understood because the usual perturbative computational methods are not applicable to them. Gauge/gravity duality is therefore invaluable as it enables calculations to be done precisely in this strongly-coupled limit. Let us emphasise, however, that the duality applies only to specific field theories, and their specific gravity duals. There is no experimentally-accessible strongly-coupled field theory for which the dual gravitational theory is known and thus a more speculative approach is taken. This involves studying the field theories for which a gravitational dual *is* known and asking what kind of behaviour is possible for this class of field

theories, and if this behaviour is similar to that of the strongly-coupled materials which can be investigated experimentally.

A priori, this approach could have proven fruitless. However, it was found that some properties (for example, the ratio of shear viscosity to entropy density) of certain strongly-coupled thermal field theories, calculated from their gravitational duals, were not only universal amongst this class of theories but also agreed approximately with those measured for the quark-gluon plasma (a strongly-interacting material composed of a large number of quarks and gluons) [5–7]. Motivated by this success, investigations of the properties of strongly-interacting field theories at low temperature and with a large density of matter present have been performed. The ultimate aim of these investigations is to obtain an insight into the unexplained phases of matter observed in condensed matter systems.

The work contained in this thesis will be along these lines. In particular, we will study the low-energy bosonic excitations of some of the simplest examples of 'holographic quantum liquids' — strongly-interacting field theories at high density and low temperature which have a classical gravitational dual. We will discover that in some cases these agree with the corresponding excitations in the standard perturbative theories describing quantum liquids, whereas in other cases they differ.

There remains much work to be done to show that gauge/gravity duality is useful for this purpose, but there are promising signs that theories with a gravitational dual may possess some features of the aforementioned unexplained phases of matter (see [8] for a recent review of the current state of the field). The ultimate goal is to find agreement between a wide variety of the low-energy properties of a holographic quantum liquid and those of a real material. Such an agreement would, in principle, allow for the determination of the strongly-coupled effective field theory governing these mysterious materials.

In the rest of this chapter, a more formal definition of gauge/gravity duality will be presented along with the 'dictionary' for computing properties of a strongly-

coupled field theory from its dual classical gravitational theory. Following that, an introduction to Landau Fermi liquid theory — a conventional theory of condensed matter describing a large density of interacting fermions — is given, with particular attention paid to its bosonic excitations. In the following chapters, we give a brief introduction to holographic quantum liquids before describing in detail the bosonic excitations of some holographic quantum liquids with a particular emphasis placed on how these compare to those of Landau Fermi liquids.

We note here that throughout this thesis, we work in units in which the speed of light c, the reduced Planck's constant $\hbar$, and Boltzmann's constant k_B, are equal to one.

1.2 Gauge/gravity duality

In this section, we begin by describing the simplest realisation of gauge/gravity duality (which is also commonly known as the AdS/CFT correspondence). This is the duality between the (3+1)-dimensional $\mathcal{N} = 4$ supersymmetric Yang-Mills theory with gauge group $SU(N_c)$, and type IIB supergravity in the (9+1)-dimensional $AdS_5 \times S^5$ background. We then explain the basics of the gauge/gravity 'dictionary' for determining properties of the strongly-interacting field theory — in particular its Green's functions — from the dual gravitational theory. We conclude the section by exploring the gravitational duals of field theory states with a non-zero temperature and/or density.

1.2.1 The simplest example of gauge/gravity duality

The key to gauge/gravity dualities lies in the properties of D-branes of string theory (or M-branes in M-theory). A Dp-brane is an excitation of string theory which is extended in p spatial dimensions (and one temporal dimension) and which is charged under the Ramond-Ramond (p+2)-form field strength (see, for example, [9–11]).

The simplest example of gauge/gravity duality can be motivated by considering N_c coincident D3-branes embedded in flat, (9+1)-dimensional spacetime. Such a configuration is a state of type IIB superstring theory. We denote the string coupling constant g_s and consider the case $g_s \ll 1$.[1]

Firstly, we can describe this configuration in terms of the open strings moving on the (3+1)-dimensional worldvolume of the D3-branes, the closed strings moving in the (9+1)-dimensional flat spacetime ("the bulk"), and the interaction between these two sectors. Taking the low energy limit, we find that the open strings on the D3-brane decouple from the closed strings in the bulk and that only the massless string states survive. To be more precise, the low energy limit is the limit in which the string length $l_s \to 0$ with all other energy scales fixed. The result of taking this limit is the $\mathcal{N} = 4$ supersymmetric Yang-Mills theory in (3+1)-dimensional Minkowski spacetime with gauge group $SU(N_c)$ (from the massless open string states on the D3-brane), decoupled from free, type IIB supergravity in (9+1)-dimensional flat spacetime (from the massless closed string states in the bulk) [17–19]. $\mathcal{N} = 4$ supersymmetric Yang-Mills is the maximally supersymmetric field theory in (3+1)-dimensions. Its field content is one gauge field, four Weyl fermions and six real scalar fields which are all massless and which all transform in the adjoint representation of the gauge group. The action of the theory is completely fixed by supersymmetry up to one dimensionless constant — the coupling g_{YM} — and the rank of the gauge group N_c. This theory is conformal i.e. the coupling g_{YM} does not run. A nice introduction to this theory may be found in [20].

An equivalent description of this configuration is given by a solution to type IIB supergravity, which arises upon taking the low energy limit of type IIB superstring theory. The action of type IIB supergravity (in Einstein frame) is

$$S_{IIB} = \frac{1}{2\kappa_{10}^2} \int d^{10}x \sqrt{-g} \left[\mathcal{R} - \frac{1}{2} \partial_\mu \Phi \partial^\mu \Phi - \frac{1}{4 \times 5!} F_{\mu\nu\alpha\beta\gamma} F^{\mu\nu\alpha\beta\gamma} + \dots \right], \qquad (1.1)$$

[1] We note here that there are numerous good introductory lecture notes on gauge/gravity duality, including [12–16].

where $\mathcal{R}$ is the Ricci scalar of the metric g, Φ is the scalar dilaton field and the ellipsis denotes terms involving other fields which will not be relevant in what follows. This action must be supplemented by the self-duality condition of the five-form field $F_{(5)} = *F_{(5)}$. The coupling constant is $2\kappa_{10}^2 = (2\pi)^7 \alpha'^4 g_s^2$, where α' is related to the string length l_s via $\alpha' = l_s^2$. The solution we are interested in has the form [21]

$$\begin{aligned} ds_{D3}^2 &= f_{D3}(\rho)^{-1/2}\left(-dt^2 + dx^2 + dy^2 + dz^2\right) + f_{D3}(\rho)^{1/2}\left(d\rho^2 + \rho^2 d\Omega_5^2\right), \\ F_5 &= (1+*)\, dt \wedge dx \wedge dy \wedge dz \wedge df_{D3}^{-1}, \qquad f_{D3}(\rho) = 1 + \frac{R^4}{\rho^4}, \\ R^4 &= 4\pi g_s l_s^4 N_c, \end{aligned} \tag{1.2}$$

where $d\Omega_5^2$ is the metric on S^5. Note that this solution has translational symmetry in (3+1)-dimensions and carries N_c units of 5-form charge, as one would expect for N_c coincident D3-branes. Again we wish to look at only the lowest energy excitations in this background. From the point of view of an observer at $\rho \to \infty$ there are two classes of low energy excitations. In addition to excitations with a low proper energy, excitations with an arbitrary proper energy which are localised near $\rho = 0$ will be redshifted such that they have a low energy as measured by the observer at infinity. These two classes of excitations decouple from one another at low energies. Thus we are left with two decoupled sectors: free, type IIB supergravity in the (9+1)-dimensional flat spacetime present in the $\rho \to \infty$ region of (1.2), and type IIB supergravity (including its excited states) in the $\rho \to 0$ region of (1.2):

$$ds^2 = \frac{r^2}{R^2}\left(-dt^2 + dx^2 + dy^2 + dz^2\right) + \frac{R^2}{r^2} dr^2 + R^2 d\Omega_5^2. \tag{1.3}$$

This metric is that of $AdS_5 \times S^5$. The co-ordinates (t, x, y, z) span the D3-brane worldvolume directions where the dual field theory degrees of freedom live. We have relabelled the radial co-ordinate $\rho \to r$ for convenience later. The radial co-ordinate of the full D3-brane metric is ρ whereas r denotes the radial co-ordinate of the $AdS_5 \times S^5$ spacetime, which is the $\rho \to 0$ limit of the full D3-brane spacetime.

By comparing these two theories describing N_c D3-branes, we see that their equivalence requires that $\mathcal{N} = 4$ $SU(N_c)$ supersymmetric Yang-Mills theory in (3+1)-dimensions is equivalent to type IIB supergravity in $AdS_5 \times S^5$. How can this be possible? The answer lies in the domain of applicability of the two descriptions of D3-branes. The supergravity solution (1.2) is only valid when $R \gg l_s$ i.e. when the curvature of the spacetime is much larger than the string length. This requires $g_s N_c \gg 1$. In the strict limit $g_s \to 0$ where we may neglect string loop corrections, we therefore require that $N_c \to \infty$ such that $\lambda \equiv 2\pi g_s N_c$ is non-zero, and then $\lambda \to \infty$ for the supergravity solution to be valid. In the gauge field theory description of D3-branes, $\lambda = g_{YM}^2 N_c$ is the 't Hooft coupling constant of the field theory.

And thus a statement of gauge/gravity duality can be made as follows [1]. Classical type IIB supergravity on $AdS_5 \times S^5$ is equivalent to $\mathcal{N} = 4$ $SU(N_c)$ supersymmetric Yang-Mills theory in (3+1)-dimensions with infinitely strong 't Hooft coupling and $N_c \to \infty$. Noting that finite λ corrections in the field theory correspond to non-zero l_s corrections to supergravity, it is claimed that the spacetime effective action of type IIB string theory on $AdS_5 \times S^5$, at leading order in g_s but including all α' corrections, is equivalent to $\mathcal{N} = 4$ $SU(N_c)$ supersymmetric Yang-Mills theory in (3+1)-dimensions with arbitrary coupling λ and $N_c \to \infty$. We emphasise at this point that this is a *conjecture* — the argument outlined above is a motivation for this conjecture rather than a proof. There is, however, a lot of evidence to support this claim and we will outline a small fraction of this in the following subsection.

The equivalence described above is the simplest example of gauge/gravity duality. Generically, gauge/gravity dualities claim that a certain gauge theory, involving a gauge group of large rank, is dual to (i.e. equivalent to) a certain gravitational theory, and that the couplings of the two theories are reciprocal. Other (conjectured) examples of such duality can be obtained by beginning with different configurations of D-branes (or M-branes) and finding two equivalent descriptions — one of which is

gravitational and one of which is field theoretic — with reciprocal coupling constants as above (see, for example, [22]). We will present some other examples in chapters 3 and 4.

1.2.2 The gauge/gravity dictionary

If a certain gauge theory really is equivalent to a gravitational theory, we should be able to determine (in principle) all of the properties of the gauge theory from its gravitational dual. In this subsection we will outline how this 'dictionary' between the theories works. For simplicity, we will focus on the particular case of the duality described in the previous subsection, noting along the way how it generalises to other cases.

Symmetries

The most basic entry in this dictionary involves the gravitational spacetime itself. Which properties of the field theory result in it taking the form $AdS_5 \times S^5$? The answer to this is found in the isometry groups of the two five-dimensional manifolds. The compact manifold S^5 has an isometry group SO(6) which is realised in the field theory as the bosonic R-symmetry group. In more general setups the isometry group of the compact manifold M is equivalent to a global symmetry of the field theory.

The non-compact AdS_5 manifold has an isometry group SO(4,2). This is identified not with the gauge group of the field theory but with the fact that the field theory is *conformal*. The conformal symmetry group in (3+1)-dimensions is SO(4,2) and is an extension of the Poincaré group that includes scale invariance. This scale invariance of the field theory is an invariance under

$$(t, x, y, z, E) \to (\Lambda t, \Lambda x, \Lambda y, \Lambda z, E/\Lambda)\,, \tag{1.4}$$

where E is the energy scale in the field theory. One of its consequences is that the

field theory coupling λ does not run. This scaling invariance (a subset of the full conformal invariance) is realised in the AdS_5 metric via the isometry

$$(t, x, y, z, r) \to (\Lambda t, \Lambda x, \Lambda y, \Lambda z, r/\Lambda)\,, \tag{1.5}$$

of the metric (1.3). The co-ordinate r labelling the non-compact extra dimension of AdS_5 which is not spanned by the field theory therefore has a clear meaning: it is a geometrisation of the energy scale of the field theory $r/R^2 \sim E$.

The identification of the isometries of AdS spacetime with the conformal group of a field theory in one lower spatial dimension is crucial. In general, the field theory dual to a gravitational theory on $AdS_{d+2} \times M$, for some compact manifold M, is a conformal field theory in $(d+1)$-dimensions. The class of gauge/gravity dualities which are of this form are often called AdS/CFT correspondences, and these are the best understood of such dualities.

How does this generalise to non-conformal field theories? In this thesis, we will be concerned with non-conformal field theories which arise due to simple deformations of conformal field theories such as turning on a temperature, a density or a mass.[2] In such theories, conformal invariance will be restored at high energies (i.e. where the energy is much greater than all other scales), and thus the non-compact part of the geometry of the dual theory will be AdS as $r \to \infty$. However, in the interior of such an 'asymptotically AdS' geometry this will not be the case and the isometries of the non-compact geometry over different values of r encode information about any spacetime, and/or scaling, symmetries of the dual field theory over the corresponding range of E.

[2]Everything we write henceforth should be taken to be true only for such theories, where the gauge/gravity dictionary is well-developed.

The field/operator dictionary

The next entry in the dictionary will also be the most useful for our purposes. It concerns how the properties of the field theory operators — in particular their correlation functions — are encoded in the gravity dual. To motivate this, let us return to our first description of the scenario of a stack of N_c coincident D3-branes in flat space. Before taking the low energy limit, the supersymmetric Yang-Mills degrees of freedom on these branes interact with fluctuations of the bulk fields in flat spacetime via an interaction Lagrangian $\mathcal{L}_{\text{int.}}$ of the form [18, 19]

$$\int d^4x \mathcal{L}_{\text{int.}}\left[\phi_0\right] = \frac{1}{8\pi^3 g_s \alpha'^2} \int d^4x \left[\text{Tr}\left(\frac{1}{4}\Phi_0 F_{\alpha\beta}F^{\alpha\beta}\right) + \frac{1}{2}h_0^{\alpha\beta}T_{\alpha\beta} + \ldots \right], \quad (1.6)$$

where $F_{\alpha\beta}$ is the $SU(N_c)$ gauge field strength on the brane, $T_{\alpha\beta}$ is the stress-energy tensor of the field theory on the brane, Φ_0 is the bulk dilaton, $h_0^{\alpha\beta}$ is the bulk graviton and ϕ_0 is shorthand for the set of bulk fields which are coupled to the brane. The subscript '0' indicates that these fields live in a (3+1)-dimensional Minkowski spacetime. Each bulk field in flat spacetime thus acts as a source for a specific gauge-invariant operator in the field theory.

In our second description of this scenario, valid for large λ, all of the gauge field degrees of freedom are replaced by supergravity fields in the $AdS_5 \times S^5$ geometry 'near' the D3-branes (i.e. in the $\rho \to 0$ limit of the geometry that they source). Before taking the low energy limit, these interact with the supergravity fields that live in the flat spacetime 'far' from the D3-branes (i.e. in the $\rho \to \infty$ limit of the geometry). From the point of view of the fields living in the $AdS_5 \times S^5$ geometry, their interaction with bulk supergravity fields in flat spacetime will arise when these fields propagate in from the $\rho \to \infty$ region of the D3-brane geometry and reach the boundary ($r \to \infty$) of the $AdS_5 \times S^5$ geometry. Thus the analogue of (1.6), in the

supergravity limit (i.e. when the gauge theory is strongly-coupled), is

$$\int d^4x \mathcal{L}_{\text{int.}}\left[\phi_0\right] = \int d^{10}x \mathcal{L}_{\text{SUGRA}}\left[\phi\left(r\to\infty\right)=\phi_0\right], \tag{1.7}$$

where ϕ denotes a generic bulk excitation, r is the radial co-ordinate of the $AdS_5\times S^5$ spacetime (1.3), ϕ_0 is a generic function of the (t,x,y,z) directions of (1.3) and it is understood that the supergravity Lagrangian is evaluated on-shell in an $AdS_5\times S^5$ background. The values of the fields at the conformally flat boundary of the $AdS_5\times S^5$ geometry, ϕ_0, are analogous to the fields $\Phi_0, h_0^{\alpha\beta}$ in (1.6) by the argument just outlined.

Noting, for example, that Φ_0 acts as a source for the field theory operator $\frac{1}{4}\text{Tr}\left(F_{\alpha\beta}F^{\alpha\beta}\right)$ in the weakly-coupled description, this analysis suggests that in our supergravity description of the strongly-coupled field theory we should identify $\Phi(r\to\infty)$ as the source term for $\frac{1}{4}\text{Tr}\left(F_{\alpha\beta}F^{\alpha\beta}\right)$. This is true for the other gauge-invariant operators shown in (1.6) also, and indeed is true in general in gauge/gravity duality. It is called the field/operator correspondence and asserts that each gauge-invariant operator $\mathcal{O}$ of the field theory is 'dual' to a bulk field ϕ, such that the boundary value of this field $\phi(r\to\infty)$ acts as the source term for $\mathcal{O}$. Mathematically, we may write [23, 24]

$$\left\langle \exp\left(\int d^dx \mathcal{O}(x)\phi_0(x)\right)\right\rangle_{\text{QFT}} = \exp\left(-\int d^dx dr \mathcal{L}^E_{\text{gravity}}\left[\phi\left(x,r\to\infty\right)=\phi_0\left(x\right)\right]\right), \tag{1.8}$$

where the Euclidean gravitational action is evaluated on-shell in the appropriate background (which will always be asymptotically AdS for our purposes, as mentioned earlier). On the right hand side it is implicit that we have integrated over any compact manifold present. Note that we have formulated the correspondence in Euclidean spacetime — the generalisation to Lorentzian spacetime will be described shortly.

As different field theories possess different sets of operators, the precise oper-

ator/field mapping depends upon which pair of dual theories one is considering.[3] We introduced this mapping via the method above for pedagogical purposes, as it motivates why such an assertion may be true. To make a more complete mapping, one can match a set of gauge-invariant operators in a given representation of the symmetry group of the field theory to a set of fields in the same representation of the symmetry group of the dual gravitational theory. Two generic kinds of mapping, which are important for our purposes, are that the stress energy tensor $T^{\alpha\beta}$ of the field theory is dual to the bulk graviton $h_{\alpha\beta}$ and that a global symmetry current J^{α} of the field theory is dual to a bulk gauge field A_{α}.

Field theory correlation functions

Equation (1.8) is, for our purposes, the key insight of gauge/gravity duality. It states that the generating function of a strongly-interacting quantum field theory can be written in terms of a gravitational theory. In the limit in which the coupling constant of this field theory is strictly infinite, the gravitational theory becomes purely classical.[4] In particular, equation (1.8) allows us to compute the correlation functions of operators in the strongly-interacting field theory simply by evaluating the on-shell action of the gravitational theory and taking functional derivatives with respect to the boundary value of the dual field.

Let us present a simple example of such a calculation in the canonical case of strongly-coupled $\mathcal{N} = 4$ supersymmetric Yang-Mills theory with gauge group $SU(N_c)$ and $N_c \to \infty$. We will compute the two-point function of $\frac{1}{4}\mathrm{Tr}\left(F_{\alpha\beta}F^{\alpha\beta}\right)$ in this theory [23]. As described above, to obtain this two-point function at infinitely strong coupling we must evaluate the on-shell action of type IIB classical supergravity on $AdS_5 \times S^5$ in terms of the boundary value of the dilaton fluctuation φ. We will perform this computation in Euclidean signature, and will discuss the equivalent computation in Lorentzian signature in the following subsection.

[3] See [22] for this mapping for some of the operators in $\mathcal{N} = 4$ supersymmetric Yang-Mills.
[4] Henceforth, we will focus only on this particular limit.

Expanding the action on the Euclidean $AdS_5 \times S^5$ background with $\Phi \to \Phi + \varphi(\tau, z, r)$ and then integrating over the S^5 yields

$$S_E = \frac{N_c^2}{16\pi^2 R^3} \int d^5x_E \sqrt{g} \left[g^{\mu\nu} \partial_\mu \varphi \partial_\nu \varphi + O\left(\varphi^3\right) \right], \tag{1.9}$$

where τ is the Euclidean time co-ordinate and we note that we have chosen momentum to flow along the z-direction of the field theory without loss of generality. To compute two-point correlation functions, we may neglect cubic (and higher order) terms as their contribution will vanish once one takes two functional derivatives of the action with respect to the sources and then sets the sources to zero. This yields the following equation of motion for the dilaton fluctuation

$$\partial_\mu \left[r^3 g^{\mu\nu} \partial_\nu \varphi(\tau, z, r)) \right] = 0. \tag{1.10}$$

In (Euclidean) Fourier space, this is an ordinary differential equation in r which therefore has a solution of the form

$$\tilde{\varphi}(r, k_E) \equiv f_{k_E}(r)\, \tilde{\varphi}_0(k_E). \tag{1.11}$$

Specifically,

$$f_{k_E}(r) = \frac{A}{r^2} I_2\left(\frac{k_E R^2}{r}\right) + \frac{B}{r^2} K_2\left(\frac{k_E R^2}{r}\right), \tag{1.12}$$

where $k_E = |\mathbf{k}_E|$ is the magnitude of the Euclidean four-wavevector and I_ν and K_ν denote the modified Bessel functions. We require a unique solution to this (as we must put the supergravity action on-shell) and thus we must impose two boundary conditions. Firstly, on physical grounds, we require that $\tilde{\varphi}(r, k_E)$ be regular throughout the spacetime. This requires us to discard the I_2 solution above, which diverges exponentially as $r \to 0$. The second boundary condition is simply that the field approaches its boundary value near the boundary of the spacetime: $\tilde{\varphi}(r \to \infty, k_E) = \tilde{\varphi}_0(k_E)$. To be more precise, one should regulate the spacetime

with a large-radius cutoff r_Λ and then impose the boundary condition

$$\tilde{\varphi}\left(r_\Lambda, k_E\right) = \tilde{\varphi}_0\left(k_E\right), \tag{1.13}$$

or equivalently

$$f_{k_E}\left(r_\Lambda\right) = 1. \tag{1.14}$$

Eventually the limit $r_\Lambda/R \to \infty$ will be taken, but it may be necessary to introduce counterterms to remove large r divergences first. Substituting this solution into (1.9), one finds the quadratic on-shell action

$$S_E^{\text{on-shell}} = \frac{N_c^2}{16\pi^2 R^3} \int \frac{d^4\mathbf{k}_E}{(2\pi)^4} \frac{d^4\mathbf{k}'_E}{(2\pi)^4} \frac{r_\Lambda^5}{R^5} f'_{k_E}\left(r_\Lambda\right) \tilde{\varphi}_0\left(k'_E\right) \tilde{\varphi}_0\left(k_E\right) (2\pi)^4 \delta^{(4)}\left(k_E + k'_E\right), \tag{1.15}$$

and then employing the gauge/gravity duality formula (1.8) and taking $r_\Lambda/R \to \infty$, the two-point function in the infinitely strongly-coupled field theory is obtained

$$\left\langle \mathcal{O}\left(k_E\right) \mathcal{O}\left(k'_E\right) \right\rangle = -\frac{N_c^2}{64\pi^2} k_E^4 \ln k_E^2 \, (2\pi)^4 \delta^{(4)}\left(k_E + k'_E\right) + \text{contact terms}, \tag{1.16}$$

where contact terms are terms which are analytic in k_E (and thus pointlike upon transforming back to real space). The contact terms are divergent but these divergences may be removed by adding local boundary counterterms to the action at $r = r_\Lambda$ in a procedure known as holographic renormalisation. We will not be concerned with contact terms in the rest of this thesis and thus we refer the interested reader to [25] for further details on this point. Fourier transforming the result (1.16), we find that the real-space two-point function is

$$\left\langle \mathcal{O}\left(x_E\right) \mathcal{O}\left(x'_E\right) \right\rangle = \frac{48 N_c^2}{\pi^2 \left|x_E - x'_E\right|^8}, \tag{1.17}$$

where x_E is a Euclidean position four-vector. This is a remarkable result — a derivation of a correlation function at infinitely strong coupling!

As the focus of this thesis is to use gauge/gravity duality to compute properties of strongly-coupled field theories, let us briefly indicate how the above calculation generalises for other field theory operators (and hence other bulk fields). Consider the fluctuation of a bulk field whose quadratic Euclidean action is that of a massive scalar φ in AdS_5 [23, 24]

$$S_E = N \int d^5 x_E \sqrt{g} \left[g^{\mu\nu} \partial_\mu \varphi \partial_\nu \varphi + m^2 \varphi^2 \right], \tag{1.18}$$

where N is an overall normalisation constant that arises from integrating over the compact manifold. After imposing the boundary conditions, the on-shell solution is

$$\tilde{\varphi}\left(r, k_E\right) = \frac{r_\Lambda^2 K_\nu \left(\frac{k_E R^2}{r}\right)}{r^2 K_\nu \left(\frac{k_E R^2}{r_\Lambda}\right)} \tilde{\varphi}_0\left(k_E\right), \tag{1.19}$$

where $\nu = \sqrt{4 + m^2 R^2}$. The naive two-point function of the dual operator, extracted from the leading non-analytic term in the on-shell action, is then[5]

$$\begin{aligned} \left\langle \mathcal{O}_\varphi\left(k_E\right) \mathcal{O}_\varphi\left(k'_E\right) \right\rangle = \lim_{\frac{r_\Lambda}{R} \to \infty} & \left[-N R^3 \frac{4\Gamma\left(1-\nu\right)}{\Gamma\left(\nu\right)} \left(2\pi\right)^4 \delta^{(4)}\left(k_E + k'_E\right) r_\Lambda^{-2\Delta_-} \left(\frac{k_E}{2}\right)^{2\nu} \right] \\ & + \text{contact terms}, \end{aligned} \tag{1.20}$$

where

$$\Delta_- \equiv \nu - 2 = \sqrt{4 + m^2 R^2} - 2. \tag{1.21}$$

The first important feature of this relation is that the leading term which is non-analytic in k depends on r_Λ, and in fact diverges when $\Delta_- < 0$. This can be remedied if we renormalise the source term

$$\tilde{\varphi}_0^{\text{ren.}}\left(k_E\right) = r_\Lambda^{-\Delta_-} \tilde{\varphi}_0\left(k_E\right). \tag{1.22}$$

[5]Note that this expression is only valid for non-integer ν. When ν is an integer, there are additional terms which are logarithmic in k_E.

Heuristically, this renormalisation gives an important clue to the meaning of Δ_-. As the coupling between a source and its operator at the boundary of AdS_5 produces a term in the action of the form

$$S_{\text{coupling}} = \int d^4x \left(\frac{r_\Lambda}{R}\right)^4 \tilde{\varphi}_0 \mathcal{O}_\varphi, \tag{1.23}$$

it implies that the dual operator must be renormalised also

$$\mathcal{O}_\varphi^{\text{ren.}} = r_\Lambda^{4+\Delta_-} \mathcal{O}_\varphi = r_\Lambda^{\Delta_+} \mathcal{O}_\varphi, \tag{1.24}$$

such that the boundary action is finite, where we have defined

$$\Delta_+ \equiv \Delta_- + 4 = \sqrt{4 + m^2 R^2} + 2. \tag{1.25}$$

Recalling that the radial direction r represents the energy scale of the field theory, the renormalised operator in the field theory then scales as $\mathcal{O}_\varphi^{\text{ren.}} \to \Lambda^{-\Delta_+} \mathcal{O}_\varphi^{\text{ren.}}$ under the scale transformation (1.4). This leads to the identification of Δ_+ with the scaling dimension of the dual operator.

The final result, upon Fourier transforming (1.20), is

$$\left\langle \mathcal{O}_\varphi^{\text{ren.}}(x_E)\, \mathcal{O}_\varphi^{\text{ren.}}(x'_E) \right\rangle \propto \frac{1}{|x_E - x'_E|^{2\Delta_+}}, \tag{1.26}$$

which has the expected functional dependence given our interpretation of Δ_+ as the scaling dimension of a scalar operator in a four-dimensional conformal field theory.

Although the argument above was in AdS_5, the method generalises to AdS_{d+1}, with (1.21) and (1.25) replaced by [24]

$$\Delta_\pm (\Delta_\pm - d) = m^2 R^2. \tag{1.27}$$

For higher spin fields in AdS_{d+1}, similar relations can be derived between the mass

of a bulk field and the scaling dimension of its dual operator. For example, for a 1-form field with mass m [24],

$$(\Delta_\pm + 1)(\Delta_\pm + 1 - d) = m^2 R^2, \tag{1.28}$$

and for the massless spin-2 graviton field,

$$(\Delta_\pm + 2)(\Delta_\pm + 2 - d) = 0. \tag{1.29}$$

We note that these relations imply that the operator dual to the graviton has the same scaling dimension as the energy-momentum tensor of a CFT and that the operator dual to a gauge field has the same scaling dimension as a conserved current of a CFT. This is consistent with the field/operator dictionary outlined in the previous subsection. Finally, we note that the requirement that these scaling dimensions be real imposes a lower bound on the allowed masses of fields in an AdS_{d+1} spacetime. For example, for scalar fields this bound is

$$m^2 R^2 \geq -\frac{d^2}{4}. \tag{1.30}$$

This is the Breitenlohner-Freedman bound [26] whose discovery predates the conjecture of the duality.

The arguments above also apply to gravitational theories in geometries that are only asymptotically AdS, which are dual to field theories that are conformal only at high energies as explained earlier. In these examples Δ_+, given by the mass term in the equation of motion at large r, is the scaling dimension of the dual operator in the UV conformal field theory.

This is where we conclude our brief introduction to the computation of two-point functions using gauge/gravity duality. We hope to have given the reader an indication of how one uses the gauge/gravity formula (1.8) in practice. To compute

the two-point functions in field theories at non-zero temperature and density, two further complications must be clarified. One of these — how to deal with bulk fields which are coupled at the quadratic level — is a practical complication that we will address in the next chapter. The second — how to compute the correlators in Lorentzian, rather than Euclidean, spacetime — requires a modification of the gauge/gravity formula (1.8) which we shall address in the following subsection.

1.2.3 States with non-zero temperature and density

As outlined in section 1.1, we are primarily interested in using gauge/gravity duality to study strongly-interacting field theories at non-zero temperature and density. How do these field theoretic features manifest themselves in the gravitational theory? We will again consider the $AdS_5 \times S^5$ example for definiteness, although many of the results are generic.

Non-zero temperature

Suppose we couple our strongly-interacting $SU(N_c)$ supersymmetric Yang Mills theory to a heat bath of temperature T. At energies $E \gg T$, we should not expect to see any effect on the theory's physical properties due to the non-zero T. Thus, using the relation between energy and bulk radial direction r, our gravitational theory should be unchanged at large r. However, at small values of r, it should be significantly altered. Such a 'local' alteration in the bulk can be obtained by changing the gravitational background (i.e. the metric and/or other bulk fields) in that region. There is one natural example of such an alteration which one may associate a temperature with: the introduction of a black hole [27]. This argument leads to the conjecture that $\mathcal{N} = 4$ supersymmetric Yang-Mills theory with gauge group $SU(N_c)$ and $N_c \to \infty$ at temperature T is equivalent to type IIB supergravity in the planar Schwarzschild-$AdS_5 \times S^5$ background with Hawking temperature T. This solution

has the form

$$\begin{aligned} ds^2 &= \frac{r^2}{R^2}\left(-f(r)dt^2 + dx^2 + dy^2 + dz^2\right) + \frac{R^2}{r^2 f(r)}dr^2 + R^2 d\Omega_5^2, \\ f(r) &= 1 - \left(\frac{r_H}{r}\right)^4, \end{aligned} \tag{1.31}$$

where the Hawking temperature of the planar horizon at $r = r_H$ is

$$T_{\text{Hawking}} = \frac{r_H}{\pi R^2}. \tag{1.32}$$

Note that this solution has the properties outlined above: when $r \gg r_H$ (i.e. $E \gg T$ in the field theory) it looks just like the $AdS_5 \times S^5$ solution dual to the $T = 0$ field theory, but when $r \sim r_H$ (i.e. $E \sim T$) it looks very different. This difference manifests itself in the expectation values of operators of the field theory. For example, using (1.8), one can compute the energy density

$$\frac{1}{V_3}\left\langle T^{tt}\right\rangle = \frac{3\pi^2}{8}N_c^2 T^4. \tag{1.33}$$

We pause here to note that our previous statement of this gauge/gravity duality — that strongly-interacting $\mathcal{N} = 4$ supersymmetric Yang-Mills theory with gauge group $SU(N_c)$ and $N_c \to \infty$ is equivalent to type IIB supergravity in $AdS_5 \times S^5$ — was slightly inaccurate. What we really meant was that the *vacuum* state of the field theory is dual to type IIB supergravity in this spacetime. In general, other states of the field theory (such as the thermal state described above) are dual to other solutions of the type IIB supergravity equations of motion (such as the planar black hole solution).

The argument above applies in general in gauge/gravity duality. The thermal state of a field theory (with temperature T) is dual to a gravitational solution with a horizon at Hawking temperature T.

Non-zero density

We now turn to the classical gravitational solution dual to a field theory state with a non-zero density of a conserved, global charge. For simplicity, we will consider a U(1) charge. To induce a state with non-zero charge density, one must source it in the field theory Lagrangian via a term

$$\mathcal{L}_{\text{density}} = A_t J^t = \mu J^t, \tag{1.34}$$

where J^t is the conserved charge and μ is called the chemical potential for that charge. From (1.8), this means that our gravitational solution must have a non-zero value for $A_t\left(x, r \to \infty\right)$ where $A_t\left(x, r\right)$ now denotes the U(1) *bulk gauge field* dual to the global U(1) charge operator J^t. Its boundary value gives the field theory chemical potential: $A_t\left(x, r \to \infty\right) = \mu$.

For definiteness, let us consider the $\mathcal{N} = 4$ supersymmetric Yang-Mills theory with gauge group $SU(N_c)$ and $N_c \to \infty$, and with a non-zero density of the diagonal $U(1)$ R-charge. Recall that this theory has an $SO(6)$ R-charge. This has a $U(1)^3$ Cartan subalgebra and we wish to turn on an equal charge for each of these $U(1)$ factors. After dimensionally reducing classical type IIB supergravity on the S^5 (which produces an $SO(6)$ gauge field dual to the R-charge current), the resulting action can be consistently truncated to that of Einstein-Maxwell gravity with a cosmological constant and a Chern-Simons term, after identifying each of the three $U(1) \subset SO(6)$ gauge fields $A_\mu\left(x, r\right)$ [28, 29]. This has a well-known solution with a non-zero $A_t(x, r \to \infty)$ called the planar Reissner-Nordström-AdS_5 black hole

$$\begin{aligned} ds^2 &= -\frac{r^2 f(r)}{R^2} dt^2 + \frac{r^2}{R^2}\left(dx^2 + dy^2 + dz^2\right) + \frac{R^2}{r^2 f(r)} dr^2, \qquad \mu = \frac{\sqrt{3} r_0 Q}{2L^2}, \\ f(r) &= 1 - \left(1 + Q^2\right)\frac{r_0^4}{r^4} + Q^2 \frac{r_0^6}{r^6}, \qquad T_{\text{Hawking}} = \mu \frac{2 - Q^2}{\sqrt{3}\pi Q}, \qquad A_t(r) = \mu\left(1 - \frac{r_0^2}{r^2}\right). \end{aligned} \tag{1.35}$$

This is the gravitational solution that is dual to the field theory state with tem-

perature $T_{\rm Hawking}$ and chemical potential μ. The dimensionless parameter Q, which takes values between 0 and $\sqrt{2}$, controls the ratio T/μ in the field theory. Note that the metric asymptotes to AdS_5 as $r \to \infty$ such that we reproduce the $\mu = T = 0$ results for $E \gg T, \mu$. A computation of the charge density of the dual field theory state yields [28]

$$\frac{1}{V_3}\left\langle J^t \right\rangle = \frac{4N_c^2\mu^3}{3\pi^2}\left(2 + \frac{3\pi^2T^2}{2\mu^2} - \frac{\sqrt{3}\pi T}{\mu}\sqrt{2 + \frac{3\pi^2T^2}{4\mu^2}}\right)^{-1}, \tag{1.36}$$

which is non-zero as advertised.

As indicated above, it is a generic feature of gauge/gravity duality that field theory states at non-zero density are dual to gravitational solutions with a non-vanishing temporal component of a gauge field near the boundary. This gauge field must be sourced somewhere within the interior of the spacetime. In the example above it was sourced by the black hole horizon but generically this is not the case. In fact, it is this richness in the variety of gravitational solutions dual to field theories at non-zero density that gives gauge/gravity duality the potential to be relevant for condensed matter physics. We will return to this topic in the next chapter.

We conclude our remarks on field theories at non-zero temperature and density by noting that field theory states at non-zero temperature and density are no longer supersymmetric or conformally invariant.

Correlators at non-zero temperature and density

The final property of gauge/gravity duality that we wish to address is how to compute the field theory two-point correlators in Lorentzian signature from its dual gravitational theory. This is most easily understood in terms of field theories in a thermal state, although it is applicable more generally, and thus we will consider such a theory here.[6]

[6] At $T = 0$, the argument below applies with the horizon $r = r_H$ replaced by the $r \to 0$ deep interior of the bulk geometry.

Attempting to directly apply the prescription of section 1.2.2, one encounters two problems:

- Both solutions to the classical equation of motion for the bulk field are regular in the interior of the geometry. One corresponds to waves travelling into the horizon, and one corresponds to wave coming out of the horizon.

- After selecting a boundary condition and using (1.8), the resulting correlator (in frequency space) is always real. In general, correlators in Lorentzian signature should be complex.

The first of these apparent problems is actually a virtue. In d-dimensional Lorentzian spacetime there are many possible two-point functions of an operator. For example, there is the retarded Green's function

$$G^R_{\mathcal{O}\mathcal{O}}(\omega, k) = -i \int d^d x e^{i\omega t - k\cdot x} \theta(t) \langle [\mathcal{O}(x), \mathcal{O}(0)] \rangle , \tag{1.37}$$

where $\theta(t)$ denotes the Heaviside step function and the advanced Green's function

$$G^A_{\mathcal{O}\mathcal{O}}(\omega, k) = i \int d^d x e^{i\omega t - k\cdot x} \theta(-t) \langle [\mathcal{O}(x), \mathcal{O}(0)] \rangle , \tag{1.38}$$

to name but two. The choice of boundary conditions on the bulk field at the horizon actually corresponds to choosing which two-point function one is computing [30,31]. Specifically, imposing ingoing boundary conditions on the bulk field at the horizon corresponds to computing the retarded Green's function, and imposing outgoing boundary conditions on the bulk field at the horizon corresponds to computing the advanced Green's function. This is easily understood in terms of causality: the retarded Green's function is always causal because it tells us the response of the system when a source is applied (this will be shown explicitly in the following chapter). Similarly, the ingoing boundary conditions are causal in classical gravity as nothing can come out of a black hole horizon. A similar argument applies to the acausal case

of the advanced Green's function and outgoing boundary conditions. Other Green's functions, such as the time-ordered Green's function, can be constructed from the retarded and advanced Green's functions.

The second problem, of the reality of the resulting two-point function, can be remedied by altering the prescription (1.8). Let us assume that the bulk field $\tilde{\varphi}(r,\omega,k) = f_{\omega,k}(r)\,\tilde{\varphi}_0(\omega,k)$ has been renormalised (as described in section 1.2.2) such that it asymptotes to a constant near the boundary of the asymptotically-AdS_{d+1} spacetime. The on-shell action then takes the form

$$S_{\text{on-shell}} = -\int \frac{d\omega d^{d-1}k}{(2\pi)^d}\tilde{\varphi}_0(-\omega,-k)\,\mathcal{F}(\omega,k,r)\,\tilde{\varphi}_0(\omega,k)\Big|_{r_H}^{r_\Lambda}, \tag{1.39}$$

where the form of the flux factor $\mathcal{F}(\omega,k,r)$ depends upon the specific bulk action under consideration. Instead of taking functional derivatives with respect to the source, the two point function in Lorentzian spacetime is given, up to contact terms, by

$$G^R_{\mathcal{O}\mathcal{O}}(\omega,k) = \lim_{\frac{r_\Lambda}{R}\to\infty}\left[-2\mathcal{F}(\omega,k,r_\Lambda)\right]. \tag{1.40}$$

This is *not* the result obtained by taking functional derivatives of (1.39), and it gives complex two-point functions with conjugation properties consistent with those of retarded and advanced Green's functions [30].

1.3 Landau Fermi liquid theory

After that brief introduction to gauge/gravity duality, and how it may be exploited to compute the properties of strongly-interacting field theories at non-zero temperature and density, we will now review a more conventional approach to studying systems at non-zero temperature and density. In fact, we will focus on one particular kind of system. This is the Landau Fermi liquid (LFL), which describes how a large density of interacting fermions may behave [32–35]. We will first outline

the basis of this theory and some of its predictions. We will then frame the theory in the context of the renormalisation group, which explains its usefulness but also highlights why new approaches are required to explain the properties of non-Landau Fermi liquids.

1.3.1 Landau's theory

Before addressing the problem of interacting fermions, let us review the non-interacting case: the free Fermi gas. If we have N non-interacting fermions of mass m in d spatial dimensions,[7] the ground state is constructed by filling the N lowest free fermion eigenstates in line with the Pauli exclusion principle. This ground state is characterised by the Fermi sphere in d-dimensional momentum space, where each state within the sphere is occupied by two fermions (one in each spin eigenstate), and each state outside is unoccupied. The radius of this sphere k_F defines the Fermi momentum and the chemical potential μ is the energy required to increase N by one

$$\mu = \varepsilon\left(k_F\right), \tag{1.41}$$

where $\varepsilon\left(k\right)$ is the dispersion relation of the fermions. The excited states are generated by moving individual fermions from a state inside the Fermi sphere to a state outside the Fermi sphere. This excitation can be viewed as the creation of a particle/hole pair, where the particle is created with momentum $|\mathbf{k}| > k_F$ and a hole is created with $|\mathbf{k}| < k_F$. This is shown schematically in figure 1.1.

How will this change if the fermions are interacting? In general, it can change dramatically. For example, an interaction could cause the fermions to pair up and form bosons, resulting in completely different behaviour. Landau's theory is based on the *assumption* that when one turns on an interaction between fermions, the resultant ground state is still a filled Fermi sphere in momentum space, but the sphere is filled with interacting fermionic 'quasiparticles' of mass m^* [32]. In other

[7] We are interested in the cases $d = 2$ and $d = 3$, both of which Landau's theory is valid for.

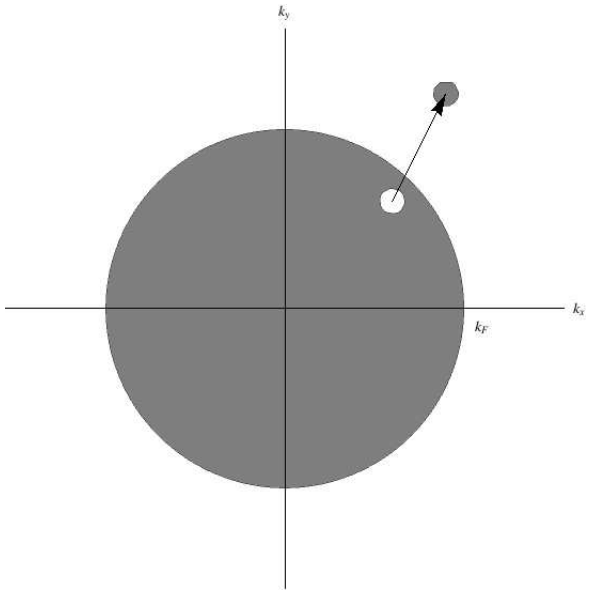

Figure 1.1: A sketch of an excited state of a (2+1)-dimensional ideal Fermi gas in momentum space. The grey regions denote the occupied states and the white regions denote the unoccupied states.

words, the effect of the interaction is to change the mass of the fermionic degrees of freedom and leave a residual interaction between them.

A generic state of the system may be characterised by the distribution of quasiparticles in momentum space $n_{\mathbf{k}}$. In equilibrium, at zero temperature, this distribution is simply the Fermi-Dirac distribution

$$n^0_{\mathbf{k}} = \begin{cases} 1, & |\mathbf{k}| < k_F, \\ 0, & |\mathbf{k}| > k_F. \end{cases} \tag{1.42}$$

Consider a small excitation around the ground state. This has energy

$$E[n_{\mathbf{k}}] - E[n^0_{\mathbf{k}}] = \sum_{\mathbf{k}} \frac{\delta E\left[n_{\mathbf{k}}\right]}{\delta n_{\mathbf{k}}} \delta n_{\mathbf{k}} + O\left(\delta n^2_{\mathbf{k}}\right) \equiv \sum_{\mathbf{k}} \epsilon_{\mathbf{k}} \delta n_{\mathbf{k}} + O\left(\delta n^2_{\mathbf{k}}\right), \tag{1.43}$$

where $E[n^0_{\mathbf{k}}]$ is the ground state energy. This defines the *quasiparticle energy* as the functional derivative

$$\epsilon_{\mathbf{k}} \equiv \frac{\delta E\left[n_{\mathbf{k}}\right]}{\delta n_{\mathbf{k}}}. \tag{1.44}$$

It is important to note firstly that the quasiparticle energy is only a useful concept when $\delta n_{\mathbf{k}}$ is sufficiently small, and secondly that it depends explicitly upon the distribution of quasiparticles $n_{\mathbf{k}}$ in the rest of the system. The free energy F of such an excitation is

$$\begin{aligned} F\left[n_{\mathbf{k}}\right] - F[n_{\mathbf{k}}^0] &= E[n_{\mathbf{k}}] - E[n_{\mathbf{k}}^0] - \mu \sum_{\mathbf{k}} \left(n_{\mathbf{k}} - n_{\mathbf{k}}^0\right) \\ &= \sum_{\mathbf{k}} \left(\epsilon_{\mathbf{k}} - \mu\right) \delta n_{\mathbf{k}} + O\left(\delta n_{\mathbf{k}}^2\right), \end{aligned} \tag{1.45}$$

where the chemical potential is simply the energy required to add a quasiparticle on the surface of the Fermi sphere (on the 'Fermi surface'): $\mu = \epsilon_{\mathbf{k}_F}$.

We are primarily interested in small fluctuations around equilibrium. Such excitations involve changing the occupation number $\delta n_{\mathbf{k}} = \pm 1$ in a narrow band of energies close to the Fermi surface $\epsilon_{\mathbf{k}} \sim \mu$. For these fluctuations, the leading term in the expansion (1.45) is really quadratic in small numbers and thus for consistency we must augment it to include all second order terms

$$F\left[n_{\mathbf{k}}\right] - F[n_{\mathbf{k}}^0] = \sum_{\mathbf{k}} \left(\epsilon_{\mathbf{k}} - \mu\right) \delta n_{\mathbf{k}} + \frac{1}{2} \sum_{\mathbf{k},\mathbf{k}'} f_{\mathbf{k}\mathbf{k}'} \delta n_{\mathbf{k}} \delta n_{\mathbf{k}'} + O\left(\delta n_{\mathbf{k}}^3\right), \tag{1.46}$$

where

$$f_{\mathbf{k}\mathbf{k}'} = \frac{\delta^2 E[n_{\mathbf{k}}]}{\delta n_{\mathbf{k}} \delta n_{\mathbf{k}'}}, \tag{1.47}$$

accounts for the interaction between quasiparticles. The inclusion of this term is of critical importance and results in interesting new phenomena, as we will show shortly. It is useful to define the free energy due to adding an additional quasiparticle as

$$\bar{\epsilon}_{\mathbf{k}} - \mu = \left(\epsilon_{\mathbf{k}} - \mu\right) + \sum_{\mathbf{k}'} f_{\mathbf{k}\mathbf{k}'} \delta n_{\mathbf{k}'}, \tag{1.48}$$

which now has an explicit contribution due to interactions of the quasiparticle with other excited quasiparticles.

Before discussing the phenomenological features of this theory, we pause to discuss the range of validity of the theory. Let us denote the energy and magnitude of momentum of an excited state, relative to the ground state, as ω and q respectively. Then the restriction described above of considering only excitations near the Fermi surface translates to

$$\omega, q \ll \mu. \tag{1.49}$$

A second restriction arises when we consider a non-zero temperature T. A non-zero temperature alters the equilibrium distribution (1.42) by thermally exciting quasiparticles within a range $\omega, q \lesssim T$ of the Fermi surface

$$n^0_{\mathbf{k}}(T) = \frac{1}{1 + \exp\left[\left(\bar{\epsilon}_{\mathbf{k}} - \mu\right)/T\right]}. \tag{1.50}$$

Landau's theory is explicitly constructed in terms of excitations around a Fermi surface and thus it is only valid when

$$T \ll \mu. \tag{1.51}$$

Outside this range, the thermal excitations are sufficiently important that the equilibrium state can no longer be approximated by a Fermi sphere. We note that the Landau Fermi liquid is referred to as a *quantum liquid*. This is because it is inherently quantum due to the explicit role played by the Pauli exclusion principle in its construction.

Heat capacity

Having outlined the assumptions of Landau's theory and its range of validity above, we may now compute its physical implications. We begin by considering the heat

capacity at constant particle number and low temperature

$$C_V = \left(\frac{\partial E}{\partial T}\right)_N. \tag{1.52}$$

Explicitly

$$E = \int_0^\infty \frac{\bar{\epsilon}_{\mathbf{k}} g\left(\epsilon_{\mathbf{k}}\right)}{1 + \exp\left[\left(\bar{\epsilon}_{\mathbf{k}} - \mu\right)/T\right]} d\epsilon_{\mathbf{k}}, \tag{1.53}$$

where $g\left(\epsilon_{\mathbf{k}}\right)$ is the total degeneracy of states and

$$\bar{\epsilon}_{\mathbf{k}} = \epsilon_{\mathbf{k}} + \sum_{\mathbf{k},\mathbf{k}'} f_{\mathbf{k}\mathbf{k}'} \delta n_{\mathbf{k}'} = \epsilon + \int_0^\infty g\left(\epsilon'\right) f\left(\epsilon, \epsilon'\right) \left[\frac{1}{1 + \exp\left[\left(\epsilon' - \mu\right)/T\right]} - \theta\left(\mu - \epsilon'\right)\right] d\epsilon', \tag{1.54}$$

to lowest order in $\delta n_{\mathbf{k}}$ where θ denotes the Heaviside step function and we have suppressed the momentum indices. Expanding in a power series in $\left(\epsilon' - \mu\right)/T$, with $T \ll \mu$, and assuming that $g\left(\epsilon'\right)$ and $f\left(\epsilon, \epsilon'\right)$ are analytic near $\epsilon' = \mu$, it can be shown that [34]

$$\bar{\epsilon}_{\mathbf{k}} = \epsilon_{\mathbf{k}} + O\left(T^2\right). \tag{1.55}$$

That is, the lowest-order correction to the energy of a quasiparticle due to the interactions scales like T^2 at low temperatures. Thus the corrections to (1.53) due to the interaction term are subleading in T and hence the leading term in C_V is unchanged from the result for the Fermi gas, except for the renormalisation of mass $m \to m^*$. The heat capacity is therefore $C_V \propto T$ for a Landau Fermi liquid. This is just one example of a property of a Landau Fermi liquid which is qualitatively the same as that of a free Fermi gas. There are many such examples. In the next subsection we will describe something quite different: a property of Landau Fermi liquids which is exclusively due to quasiparticle interactions and thus is not present in the free Fermi gas.

1.3.2 Excitations of Landau's theory

One of the most striking features of Landau's theory of Fermi liquids is the prediction of a new type of long-lived excitation, not present in the free Fermi gas. This 'zero sound' excitation, which we will describe shortly, arises due to the coherent interaction between a large number of quasiparticles and was subsequently observed experimentally in liquid ^{3}He, the prototypical example of a Landau Fermi liquid.

Let us consider an inhomogeneous perturbation of the ground state. We will pursue a semi-classical treatment in which quasiparticle excitations near the Fermi surface are long-lived and thus we may treat them classically (within the range of parameters given earlier in (1.49) and (1.51)). The inhomogeneous state may be characterised by the distribution function $n_{\mathbf{k}}(\mathbf{x}, t)$, where $n_{\mathbf{k}}(\mathbf{x}, t)\, d^d\mathbf{x} d^d\mathbf{k}$ is the number of quasiparticles in volume element $d^d\mathbf{x}$ and with momentum in the range $d^d\mathbf{k}$ at time t. Quasiparticles may be scattered in or out of this element of phase space via collisions

$$\frac{d}{dt} n_{\mathbf{k}}(\mathbf{x}, t) = I(n_{\mathbf{k}}), \tag{1.56}$$

where $I(n_{\mathbf{k}})$, the collision integral, represents such scatterings. In the absence of external forces, this becomes

$$\frac{\partial n_{\mathbf{k}}}{\partial t} + (\nabla_{\mathbf{k}} \bar{\epsilon}_{\mathbf{k}}) \cdot \partial_{\mathbf{x}} n_{\mathbf{k}} - (\nabla_{\mathbf{x}} \bar{\epsilon}_{\mathbf{k}}) \cdot \partial_{\mathbf{k}} n_{\mathbf{k}} = I(n_{\mathbf{k}}), \tag{1.57}$$

where it is implicit that $n_{\mathbf{k}}$ depends upon the spacetime co-ordinates. This is the Boltzmann equation for a Landau Fermi liquid. As we are only interested in small fluctuations around the equilibrium state, we write

$$n_{\mathbf{k}}(\mathbf{x}, t) = n^0_{\mathbf{k}} + \delta n_{\mathbf{k}}(\mathbf{x}, t). \tag{1.58}$$

Expanding the Boltzmann equation (1.57) to linear order in fluctuations, one obtains

$$\frac{\partial \delta n_{\mathbf{k}}(\mathbf{x},t)}{\partial t} + \mathbf{v}_{\mathbf{k}} \cdot \left(\partial_{\mathbf{x}} \delta n_{\mathbf{k}}(\mathbf{x},t)\right) - \left(\partial_{\mathbf{k}} n^0_{\mathbf{k}}\right) \cdot \sum_{\mathbf{k}'} f_{\mathbf{k}\mathbf{k}'} \left(\nabla_{\mathbf{x}} \delta n_{\mathbf{k}'}(\mathbf{x},t)\right) = I\left(\delta n_{\mathbf{k}}(\mathbf{x},t)\right), \tag{1.59}$$

where $\mathbf{v}_{\mathbf{k}} = \nabla_{\mathbf{k}} \epsilon_{\mathbf{k}}$. For plane wave fluctuations $\delta n_{\mathbf{k}}(\mathbf{x},t) = \delta n_{\mathbf{k}}(\mathbf{q},\omega)\, e^{-i\omega t + i\mathbf{q}\cdot\mathbf{x}}$, this equation becomes

$$\left(\mathbf{q}\cdot\mathbf{v}_{\mathbf{k}} - \omega\right) \delta n_{\mathbf{k}} - \mathbf{q}\cdot\mathbf{v}_{\mathbf{k}} \frac{\partial n^0_{\mathbf{k}}}{\partial \epsilon_{\mathbf{k}}} \sum_{\mathbf{k}'} f_{\mathbf{k}\mathbf{k}'} \delta n_{\mathbf{k}'} = I\left(\delta n_{\mathbf{k}}\right). \tag{1.60}$$

This is the transport equation for a Landau Fermi liquid in the absence of external forces. Solutions to this equation correspond to long-lived excitations of a Landau Fermi liquid, of which there are two classes. For now, let us consider the case where there are no collisions and thus $I\left(\delta n_{\mathbf{k}}\right) = 0$. We will consider the effect of collisions shortly.

The first class of excitation is the localised quasiparticle excitation, where a single quasiparticle with momentum $\mathbf{k}_0$ is added. This has the form

$$\delta n_{\mathbf{k}} = \delta_{\mathbf{k},\mathbf{k}_0} + \xi_{\mathbf{k}}. \tag{1.61}$$

It differs from the corresponding single particle excitation in a free Fermi gas by the term $\xi_{\mathbf{k}}$, which encodes the 'polarisation' effect on the other quasiparticles in the system due to their interaction with the excited one. We note that one may formally solve the transport equation (1.60) for $\xi_{\mathbf{k}}$, but we will not do this here. Instead let us consider the second class of excitation, which has no analogue in the free Fermi gas.

Collisionless zero sound

The second class of excitations is the collective excitations which arise due to a coherent response of the system as a whole. This is possible in a Landau Fermi

liquid, but not in a free Fermi gas, due to the interaction between the quasiparticles. Explicitly, these coherent excitations correspond to oscillations of the Fermi surface, which may be sustained if the quasiparticle interaction is short-ranged, repulsive, and suitably strong. For definiteness, let us consider a (3+1)-dimensional liquid from now on, although the results are qualitatively the same for a (2+1)-dimensional liquid also.

Consider a coherent excitation of the quasiparticles on the Fermi surface such that the Fermi surface is normally-displaced by an amount $u_{\mathbf{k}}$. This excitation has the form

$$\delta n_{\mathbf{k}} = \delta\left(\epsilon_{\mathbf{k}} - \mu\right) v_F u_{\mathbf{k}}, \tag{1.62}$$

where the displacement of the Fermi surface satisfies the transport equation (from (1.60))

$$\left(\mathbf{q}\cdot\mathbf{v}_{\mathbf{k}} - \omega\right) u_{\mathbf{k}} + \mathbf{q}\cdot\mathbf{v}_{\mathbf{k}} \sum_{\mathbf{k}'} f_{\mathbf{k}\mathbf{k}'}\delta\left(\epsilon_{\mathbf{k}} - \mu\right) u_{\mathbf{k}'} = 0, \tag{1.63}$$

if we again neglect collisions. In general, we may decompose the Fermi surface displacement $u_{\mathbf{k}}$ as a sum of spherical harmonics $Y_{lm}(\theta,\phi)$, where each harmonic is the linear sum of two terms: one where the two spin eigenstates move in phase (spin-symmetric), and one where they move out of phase (spin-antisymmetric). Depending on the properties of the quasiparticle interaction $f_{\mathbf{k}\mathbf{k}'}$, this can lead to a whole spectrum of non-trivial collective excitations in a Landau Fermi liquid.

Let us concentrate on the most basic of these — the spin-symmetric longitudinal excitation (i.e. the $m = 0$ harmonics). This mode satisfies the equation

$$\left(\cos\theta - \frac{\omega}{q v_F}\right) u(\theta) + \frac{1}{2}\cos\theta \int_0^{\pi} d\theta' \sin\theta' F\left(\theta - \theta'\right) u\left(\theta'\right) = 0, \tag{1.64}$$

where θ is the polar angle around the $\mathbf{q}$ axis, and the spin-symmetric dimensionless

interaction strength F in the integral is given by

$$f_{\mathbf{k}\mathbf{k}'} = \frac{\pi^2}{V_3 m^* \mu} F = \sum_{l=0}^{\infty} \frac{\pi^2}{V_3 m^* \mu} F_l P_l \left(\cos\left(\theta - \theta'\right)\right), \tag{1.65}$$

where P_l are the Legendre polynomials and V_3 is the three-dimensional spatial volume of the liquid.

For simplicity, let us consider the case where the interaction $f_{\mathbf{k}\mathbf{k}'}$ is constant and thus only F_0 is non-vanishing. Then one finds a solution to equation (1.64) of the form

$$u\left(\theta\right) \propto \frac{q v_F \cos\theta}{\omega - q v_F \cos\theta}, \tag{1.66}$$

with a dispersion relation given implicitly by

$$\frac{\omega}{2 q v_F} \log\left[\frac{\omega + q v_F}{\omega - q v_F}\right] - 1 = \frac{1}{F_0}. \tag{1.67}$$

Thus for $F_0 > 0$, one finds a propagating density wave in the liquid which is called 'zero sound'. For a strongly-interacting liquid ($F_0 \gg 1$), this has a solution

$$\omega \approx \sqrt{\frac{F_0}{3}} v_F q, \tag{1.68}$$

in contrast to the corresponding dispersion relation of hydrodynamic sound in a strongly-interacting Fermi liquid

$$\omega \approx \sqrt{\frac{1 + F_0}{3}} v_F q. \tag{1.69}$$

Note that the speeds of the two kinds of sound mode are equal in the limit of infinitely strong interactions $F_0 \to \infty$. The zero sound mode is a key prediction of Landau's theory and is due to coherent oscillations of the Fermi surface caused by the quasiparticle interaction. The 'sound' part of its name is simply because it is a propagating density wave, and 'zero' refers to the fact that *it exists even*

at zero temperature. This is the critical difference between zero sound and the usual hydrodynamic sound. Hydrodynamic sound is sustained by thermal collisions between the constituents of a system and thus requires a significant temperature to propagate. Zero sound, on the other hand, is sustained by the *quantum interactions* of the quasiparticles of a Landau Fermi liquid and hence propagates even in the absence of thermal collisions. Let us now address the collision integral that we disregarded previously.

Collisions and zero sound

Thus far we have neglected the collision integral $I(\delta n_{\mathbf{k}})$ in the transport equation (1.60). This can be done only if we are considering fluctuations with a frequency $\omega \gg \nu$ where ν is the frequency of collisions. The collision frequency for a quasiparticle may be computed via Fermi's Golden Rule and has the schematic form

$$\nu \sim W \frac{(\pi T)^2 + (\epsilon_{\mathbf{k}} - \mu)^2}{1 + \exp\left[-(\epsilon_{\mathbf{k}} - \mu)/T\right]}, \tag{1.70}$$

where W is proportional to the squared matrix element for 2 particle $\to$ 2 particle scattering and, to leading order, is independent of T and $(\epsilon_{\mathbf{k}} - \mu)$ [34, 36]. The important feature of the expression (1.70) for the collision frequency is that it is quadratic both in the temperature and in the energy of the quasiparticle relative to the Fermi surface. This dependence is purely kinematic and arises due to integration over the phase space of possible final states, weighted by the Fermi-Dirac distribution for each quasiparticle (1.50). Note that n particle $\to$ n particle scattering events contribute terms to this expression which are higher order in both T and $(\epsilon_{\mathbf{k}} - \mu)$ and are neglected here.

Consider a sound wave of fixed frequency ω travelling along the x^1-axis. The amplitude of this wave will decay like $e^{-\Gamma_q x^1}$ due to collisions with other quasiparticles near the Fermi surface, where $\Gamma_q \sim \nu$ [33]. At $T = 0$, the amplitude attenuation

coefficient Γ_q is

$$\Gamma_q \sim \left(\frac{\epsilon_{\mathbf{k}} - \mu}{\mu}\right)^2 \sim \left(\frac{\omega}{\mu}\right)^2, \tag{1.71}$$

which is small in the approximation where Landau's theory is valid. This justifies our earlier assertion that the zero sound mode propagates at zero temperature. As the temperature is increased, the decay rate of the zero sound mode changes and can fall into one of three regimes

- When $\omega/\mu \gg T/\mu \gg (T/\mu)^2$, thermal excitations are very rare and thus the decay rate is $\Gamma_q \sim \omega^2$, essentially unchanged from the $T = 0$ case. This is called the 'quantum collisionless regime' due to the lack of thermal collisions.

- When $T/\mu \gg \omega/\mu \gg (T/\mu)^2$, thermal excitations become important and they have a significant effect upon the decay rate of the zero sound mode, resulting in $\Gamma_q \sim T^2$. This is called the 'thermal collisionless regime' as there are thermal collisions but they are not frequent enough to destroy the zero sound mode.

- When $T/\mu \gg (T/\mu)^2 \gg \omega/\mu$, the thermal collision frequency is much larger than the frequency of the mode itself. In this regime, the zero sound mode becomes extremely short-lived as almost all of the quasiparticles are scattered before the Fermi surface can complete a coherent oscillation. However, in this 'hydrodynamic regime' there is local thermodynamic equilibrium due to the frequent thermal collisions and normal hydrodynamic behaviour is found, including long-lived charge diffusion and hydrodynamic sound modes.

A sketch of these three regimes as a function of frequency is shown in figure 1.2, and a sketch of the temperature dependence of Γ_q in each regime is shown in figure 1.3.

We conclude our discussion of the zero sound mode here. In summary, Landau's theory predicts the existence of this non-trivial mode at zero temperature as well as how its behaviour changes as the temperature is increased.

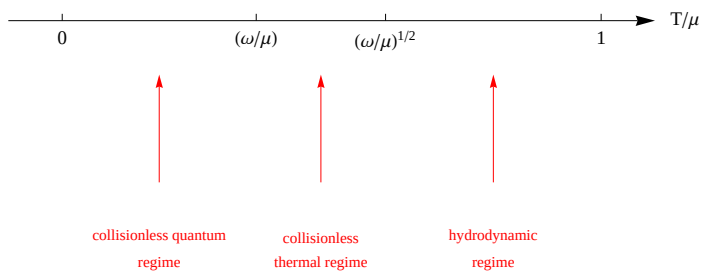

Figure 1.2: Relative scales in the hydrodynamic, collisionless thermal and collisionless quantum regimes of a Landau Fermi liquid.

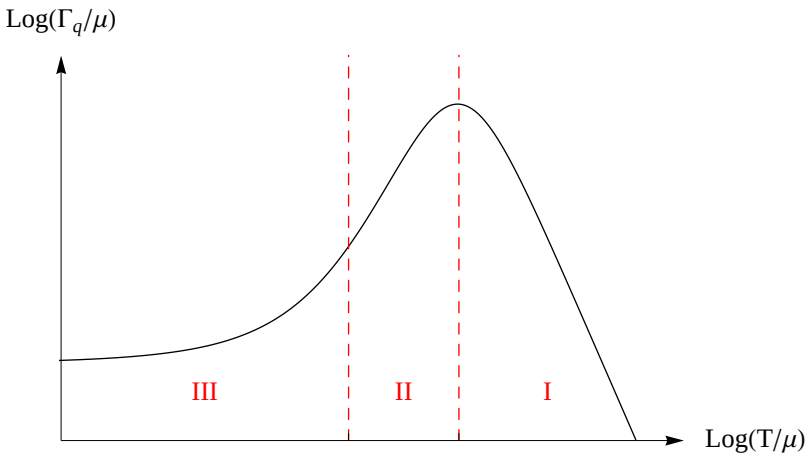

Figure 1.3: The temperature dependence of the sound attenuation coefficient Γ_q in the hydrodynamic (I), collisionless thermal (II) and collisionless quantum (III) regimes. of a Landau Fermi liquid at fixed ω.

A real Landau Fermi liquid: ^{3}He

Landau's theory was based on the assumption that the ground state of the system is a Fermi sphere filled with interacting quasiparticles. From this assumption, the phenomenological theory was constructed largely using Landau's intuition to give detailed predictions such as the prediction of the zero sound mode and how its properties vary with temperature. We will see in the following section why the subsequent development of the theory of the renormalisation group shed much light upon the usefulness of Landau's theory, but let us first justify its usefulness by comparisons with experimental data.

Figure 1.4 shows the experimentally-observed sound speed and sound attenuation

in liquid ^{3}He as a function of temperature [37]. The sound speed and attenuation show a clear transition as the temperature is raised. At very low temperatures, sound travels at a well-defined speed and with an attenuation that rises as T^2. This is the zero sound mode predicted by Landau in the collisionless thermal regime (the collisionless quantum regime, expected at even lower temperatures, has not been accessed experimentally). As the temperature is increased, there is a crossover to a sound mode propagating with a different sound speed, and with an attenuation that now begins to drop as T^{-2}. This is the collisionless/hydrodynamic crossover described above. The observed behaviour of the sound mode in ^{3}He is consistent with the predictions of Landau's theory (as shown in figure 1.3), which are that the speed of hydrodynamic sound is different from that of zero sound (except in the limit of infinitely strong interactions $F_0 \to \infty$), and that the attenuation of hydrodynamic sound is proportional to T^{-2}.

Although we will not describe the results here, it is possible to extract values for the quantities m^*, F_0 etc. for ^{3}He from such experiments [34, 38]. Instead, we just wish to emphasise that Landau's theory *is* realised in nature. The clearest example is liquid ^{3}He, while various enhancements of Landau's theory underpin our understanding of other materials. For example, the theory of a charged Landau Fermi liquid coupled to a lattice is used to explain the properties of most metals.

1.3.3 Fermi liquids and non-Fermi liquids

Landau's theory of Fermi liquids is a somewhat phenomenological theory whose existence was motivated in part by Landau's intuition. One can place this intuition on a more solid footing using renormalisation group arguments which were unknown (at least formally) to Landau and his colleagues [39, 40]. These arguments also give insight into why such a simple theory provides a good description of the low energy properties of a huge number of different materials.

Suppose one begins with a UV Lagrangian for interacting fermions at a scale

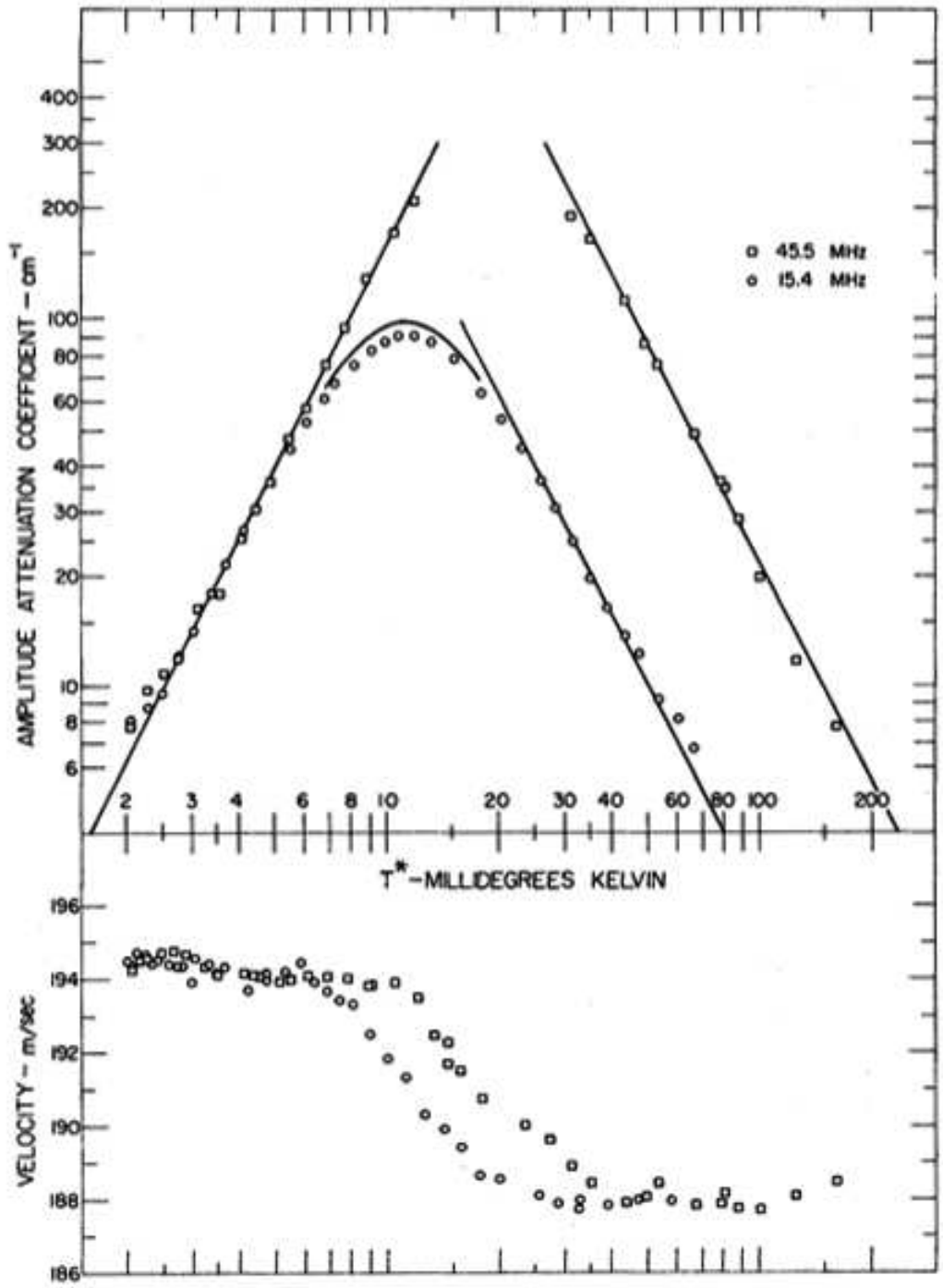

Figure 1.4: Temperature dependence of the acoustic speed and attenuation in liquid ^{3}He at P=32 kPa measured at both 15.4 MHz (◯) and 45.5 MHz (□). The lines through the data correspond to $\log \Gamma_q \sim 2 \log T$ and $\log \Gamma_q \sim -2 \log T$ in the collisionless thermal and hydrodynamic regimes, respectively, in agreement with Table 3.1. Reprinted with permission from Abel *et al.* [37]. Copyright (1966) by the American Physical Society.

Λ_{UV} and then integrates out modes with momenta between Λ_{UV} and k_F. Recall that for relativistic fermions at zero chemical potential, the four-point interaction is irrelevant. However, due to the special kinematics of the Fermi surface, this is not the case when $\mu \neq 0$. The four-point couplings which scatter fermions on the Fermi surface fall into two classes. These are denoted V for the scattering of two fermions whose momenta sum to zero, and F for the scattering of two fermions whose momenta do not sum to zero. All other couplings are irrelevant.

If V is positive (i.e. repulsive) then it is marginally irrelevant at low energies and if it is negative (i.e. attractive) then it is marginally relevant and flows to strong coupling. This second case corresponds to the BCS instability and leads to spontaneous breaking of a U(1) symmetry and a superfluid (or superconducting) state. Let us follow Landau in assuming that no such symmetry breaking occurs (i.e. that the ground state is still the filled Fermi sphere). Then we find that, at very low energies $\omega, q \ll k_F$, there is a fixed point theory described by states on a Fermi sphere interacting via the marginal coupling F. This theory corresponds precisely to Landau's theory. The quasiparticles of Landau's theory are simply excitations of the renormalised fermionic fields and their interaction $f_{\mathbf{k}\mathbf{k}'}$ corresponds to F. There is a quantitative agreement between these two approaches — for example, one may derive the dispersion relation of zero sound (1.68) from the pole in the four-point function (at low energy and momentum), which is given by resumming an infinite series of four-point diagrams with the appropriate coupling F into a geometric series.

As discussed in section 1.3.2, Helium-3 is well described by this theory. To describe metals, one must include two new effects. Firstly, the quasiparticles now carry an electromagnetic charge which can destroy the zero sound mode, producing instead a plasmon (i.e. a plasma oscillation). Secondly, the quasiparticles no longer move through free space but through a positively charged ionic lattice. The quasiparticles can interact with the oscillating modes of this lattice which are named phonons. One may integrate out these phonons (at energies $E \ll M_{\text{ion}}$ where M_{ion}

is the ionic mass), which simply renormalises the coupling V at the scale $E = M_{\text{ion}}$, typically making it more likely to be attractive [39]. The properties of most metallic substances can be understood in this way.

The great success of these renormalisation group arguments — that, under a very limited number of assumptions, they explain the inevitability of Landau's theory — has an accompanying dark side. How can one understand the properties of materials which differ from those predicted by Landau? Such 'strange metal' phases have been observed experimentally in many materials (see, for example, [41–45]). A characteristic property of these strange metals is that the electronic contribution to their resistivity is proportional to T, whereas for an ordinary metal this contribution is proportional to T^2 at leading order.[8] This property is ill-understood, and is often accompanied in the phase diagram of these strange metals by other ill-understood features such as quantum criticality and high-temperature superconductivity. We note here that due to their structure, some of these materials are expected to be understood in terms of theories with less than three spatial dimensions (for example, if the relevant electrons are restricted to moving in a plane).

A different effective theory is clearly governing the low energy properties of these materials, but this theory is unknown. The robustness of the renormalisation group arguments above indicate that it is not simply a matter of tweaking coupling constants or including extra interaction terms, but that something quite different is required. We will not review the various proposals here, but simply note that some of these proposals involve coupling the fermions to other low energy degrees of freedom such as gauge fields.[9] The holographic quantum liquids we will study in the rest of this thesis provide another class of examples where one would not expect the low energy theory to be simply Landau's theory of Fermi liquids. These theories typically involve infinitely-strongly interacting gauge fields, fermions and scalars

[8] Note that for many metals the T^2 term has a small coefficient and thus it is the higher-order T^5 term, due to electrons scattering from the lattice, which is measured experimentally (see e.g. [46]).

[9] These are not the fundamental gauge fields of the standard model but emergent gauge fields which are postulated to arise in the low energy effective theories. For one example, see [47].

and, as we shall see, have properties quite different to those of LFLs. As the investigation of holographic quantum liquids is still in its infancy, the question of whether these theories have any relevance for real materials is still unknown and we will not address this question in the remainder of this thesis.

Chapter 2

Holographic quantum liquids

In the previous chapter, we introduced gauge/gravity duality and described how it can be exploited to compute properties of strongly-interacting field theories. From now on we will concentrate on a particular class of field theories — holographic quantum liquids. These are low-temperature, strongly-interacting field theories with a large density of matter, which have a classical gravitational dual. They are strongly-coupled analogues of conventional quantum liquids, such as the Landau Fermi liquid of the previous chapter.

In this chapter, we will expand upon the gauge/gravity dictionary given in section 1.2, focusing on how to compute, and interpret, properties of these liquids which are relevant for comparison with conventional theories and experiments.[1] These include, for example, the thermodynamic properties of a liquid and its low-energy excitation spectrum. In the subsequent chapters we will describe the results of these calculations for certain holographic quantum liquids.

2.1 Equilibrium properties

We begin by considering equilibrium properties of holographic quantum liquids. Firstly we will discuss the generic form of the classical gravitational theories dual

[1] See [16, 48–52] for introductory lecture notes on this topic.

to holographic quantum liquids, before describing how one computes the thermodynamic properties of these liquids using gauge/gravity duality.

2.1.1 Gravitational duals of holographic quantum liquids

The key feature of a holographic quantum liquid is the non-zero density of matter present. As was described in section 1.2.3, this requires the dual gravitational theory to contain a $U(1)$ gauge field. The relevant solutions of this theory are those with a non-zero value for the temporal component of this gauge field A_t at the boundary of the spacetime, corresponding to a non-zero chemical potential in the field theory. For consistency of the bulk theory, this gauge field at the boundary must be sourced by some charge within the interior of the spacetime. There are a large variety of possible sources of bulk charge including scalar fields, fermions, p-form fields and black hole horizons.

Typically, the form of the bulk charge carriers play a major role in determining the properties of the dual field theory state. For example, suppose the charge is sourced by a bulk scalar field in the interior of the geometry. In other words, this scalar field vanishes near the boundary of the spacetime but becomes non-zero as one moves inward. Using the gauge/gravity duality dictionary, this means that the field theory has a scalar operator, charged under a global $U(1)$ symmetry, which is not sourced in the Lagrangian but which has a non-zero expectation value nonetheless. In other words, the field theory state is one in which the $U(1)$ global symmetry has been spontaneously broken by a scalar operator. This is precisely an s-wave superfluid state (the analogous s-wave superconductor state is obtained if the broken $U(1)$ is a local gauge symmetry). Holographic quantum liquids of this type are generically called holographic superconductors [50, 53–55].

In this thesis, we will focus on a different class of holographic quantum liquids — those in which the global $U(1)$ symmetry is *unbroken*. These are the strongly-coupled analogues of Landau Fermi liquids. As the $U(1)$ symmetry is global in holographic

quantum liquids, these bear more of a resemblance to ^{3}He than to metallic materials in which the $U(1)$ symmetry (electromagnetism) is gauged.

Generically, a given gravitational theory will contain numerous charged (and uncharged) matter fields and will have various different solutions to its equations of motion, with the bulk charge sourced in different ways. Each of these solutions corresponds to a different equilibrium field theory state. One determines the preferred state of the system by examining thermodynamic properties of the field theory, as will be described in the following subsection. The preferred state typically depends upon the parameters of the system such as the chemical potential and the temperature. By altering these quantities, one can induce phase transitions between different field theory states. For example, suppose one begins at $T = 0$ with a scalar field sourcing the bulk charge. It is typically found that as the temperature is raised, it becomes thermodynamically favourable for the charge to fall inside a black hole horizon until the scalar field vanishes at a temperature T_c. In the field theory, this is a superfluid phase transition with critical temperature T_c.

On a practical level, it is very difficult to perform an analysis of a higher-dimensional gravitational theory including all of its fields. Thus it is very common to instead study consistent truncations of these theories to a more manageable number of fields. However, one should bear in mind that more complex phase diagrams can be engineered by considering a more general truncation of the theory that includes more fields.[2] This is desirable if one is to make contact with real strange metal phases which typically appear as part of a complex phase diagram.

Before we discuss how to compute thermodynamic quantities, let us recall we are interested in the parameter range $T \ll \mu$ of our field theories. When $T = 0$, this corresponds to a horizonless bulk geometry whereas at non-zero temperatures a horizon will be present. This does not restrict the bulk charge carriers - it is perfectly possible to have bulk matter carrying charge even in the presence of a horizon.

[2]Provided, of course, that consistent theories of gravity exist which have the required phase structure. We will not address this issue here.

2.1.2 Thermodynamic properties of holographic quantum liquids

To compute the thermodynamic properties of a quantum field theory, one compactifies the time co-ordinate t to Euclidean time $\tau = -it$ with a period $\beta = 1/T$. This turns the field theory path integral into the partition function Z of the field theory at temperature T. The free energy F is then related to the partition function Z via

$$Z = e^{-\beta F}. \tag{2.1}$$

Using the gauge-gravity duality formula (1.8), one finds that the free energy of the field theory at infinitely strong coupling may be computed from the value of the on-shell action

$$F = \frac{1}{\beta} S^E, \tag{2.2}$$

where S^E is the on-shell Euclidean action for the dual classical gravitational theory with a compactified time co-ordinate with period β. Note that one must include the relevant counterterms, mentioned in section 1.2.2, when doing this computation.

Having determined the free energy, it is simple to compute the thermodynamic properties of the field theory state such as the entropy density and the heat capacity. Additionally, one can determine which phase is thermodynamically stable at a given (T, μ) by determining which has the lowest free energy.

2.2 Low energy excitations

In addition to the equilibrium thermodynamic properties of holographic quantum liquids, we are interested in their low energy excitations. In this section we will describe how to compute the bosonic excitation spectrum from the dual gravitational theory.

2.2.1 Quasinormal modes and collective excitations

The bosonic excitation spectrum of a field theory is encoded in the Green's functions of its bosonic operators. As described in section 1.2.3, it is the retarded Green's function (1.37) which is the natural object to compute in holographic theories. It is very instructive to give a concrete physical meaning to this object. Suppose we have a system with Hamiltonian $\hat{H}_0$ which is in a state with density matrix $\hat{\rho}_0(x)$ until it is perturbed at time t_0 to have a Hamiltonian

$$\hat{H}(t) = \hat{H}_0 + \delta\hat{H}(t), \tag{2.3}$$

where

$$\delta\hat{H}(t) = \int dx \hat{\mathcal{O}}(x)\,\phi(x,t), \tag{2.4}$$

i.e. $\phi(x,t)$ is the time-dependent source for the perturbing operator $\hat{\mathcal{O}}(x)$. Utilising the interaction picture, the expectation value of the operator $\hat{\mathcal{O}}$ is

$$\begin{aligned}\langle\hat{\mathcal{O}}(x,t)\rangle &\equiv \mathrm{Tr}\left(\hat{\rho}(x,t)\,\hat{\mathcal{O}}(x,t)\right)\\ &= \mathrm{Tr}\left(\hat{\rho}_0(x)\,\hat{\mathcal{O}}(x,t)\right) - i\mathrm{Tr}\left(\hat{\rho}_0(x)\int_{t_0}^{t} dt'\left[\hat{\mathcal{O}}(x,t), \delta\hat{H}(t')\right]\right),\end{aligned} \tag{2.5}$$

to first order in the perturbation $\delta\hat{H}$. Writing $\langle\hat{\mathcal{O}}(x,t)\rangle \equiv \langle\hat{\mathcal{O}}(x,0)\rangle + \delta\langle\hat{\mathcal{O}}(x,t)\rangle$, the change in expectation value of $\hat{\mathcal{O}}$ due to the source is

$$\begin{aligned}\delta\langle\hat{\mathcal{O}}(x,t)\rangle &= -i\mathrm{Tr}\left(\hat{\rho}_0(x)\int_{-\infty}^{t} dt'dx'\left[\hat{\mathcal{O}}(x,t), \hat{\mathcal{O}}(x',t')\right]\phi(x',t')\right)\\ &= -i\int_{-\infty}^{\infty} dt'dx'\theta(t-t')\left\langle\left[\hat{\mathcal{O}}(x,t), \hat{\mathcal{O}}(x',t')\right]\right\rangle\phi(x',t'),\end{aligned} \tag{2.6}$$

where the angled brackets on the right hand side denote a trace over states of our system with density matrix $\hat{\rho}_0$. Defining the real-space retarded Green's function by

$$\delta\langle\hat{\mathcal{O}}(x,t)\rangle \equiv \int_{-\infty}^{\infty} dt'dx' G^R(x,x';t,t')\,\phi(x',t'), \tag{2.7}$$

we find that the retarded Green's function is

$$G^R\left(x,x';t,t'\right)=-i\theta\left(t-t'\right)\left\langle\left[\hat{\mathcal{O}}\left(x,t\right),\hat{\mathcal{O}}\left(x',t'\right)\right]\right\rangle. \tag{2.8}$$

That is, it tells us the change in the expectation value of an operator when the system is perturbed by a source for that operator. It is causal, because it vanishes for $t<t'$ i.e. before the source is applied. For a translationally invariant theory, $G^R\left(x,x';t,t'\right)=G^R\left(x-x';t-t'\right)$ and we may then Fourier transform to obtain the retarded Green's function in frequency space (1.37), where ω and k are the Fourier conjugate variables of $t-t'$ and $x-x'$ respectively. Fourier transforming both sides of (2.7), we find that in frequency and momentum space, the Green's function is

$$G^R_{\mathcal{O}\mathcal{O}}\left(\omega,k\right)=\left.\frac{\delta\left\langle\mathcal{O}\left(\omega,k\right)\right\rangle}{\delta\phi_0\left(\omega,k\right)}\right|_{\delta\phi_0\to 0}, \tag{2.9}$$

where ϕ_0 is a source for the operator $\mathcal{O}$. That is, it tells us how the expectation value of an operator changes when a small source is applied to it at a given ω and k.

The excitations of the field theory correspond to the poles of the retarded Green's function. In Fourier space, each pole will have a dispersion relation $\omega\left(k\right)$. This definition of an excitation is natural from (2.9) — a small source applied at an excitation frequency $\omega\left(k\right)$ will produce an enormous response in the expectation value. The dispersion relation $\omega\left(k\right)$ will have both real and imaginary parts

$$\omega\left(k\right)=\omega_*\left(k\right)-i\Gamma\left(k\right). \tag{2.10}$$

Fourier transforming to real spacetime, one finds that for an on-shell excitation,

$$G^R\left(t,x\right)\sim e^{-\Gamma t}\exp\left(-i\omega_* t+ikx\right). \tag{2.11}$$

Thus the real part of the dispersion relation $\omega_*(k)$ gives the propagating frequency of the excitation, and the imaginary part $\Gamma(k)$ is the decay rate. Furthermore, this analysis demonstrates that the excitations must have a negative imaginary part. A positive imaginary part leads to an exponential growth in time of the expectation value which triggers a continuous phase transition. Thus a phase which has a pole of any retarded Green's function with positive imaginary part is unstable. We are particularly interested in the low energy excitations of holographic quantum liquids — these are the poles which have a small imaginary part and thus which dominate the long-time dynamics of the field theory.

To determine the excitation spectrum of the field theory, we must compute the poles of the retarded Green's functions. The procedure for calculating the retarded Green's function of an operator $\mathcal{O}_\varphi$ using holography was outlined in section 1.2.3. One has to excite the dual field $\varphi \to \varphi + \delta\varphi(r,\omega,k)\,\varphi_0(\omega,k)$, solve the equation of motion for $\delta\varphi(r,\omega,k)$ subject to ingoing boundary conditions at the horizon and $\delta\varphi(r_\Lambda,\omega,k) = 1$, and then compute the on-shell action for $\delta\varphi(r,\omega,k)$ to quadratic order. Near the boundary, the solution takes the form[3]

$$\delta\varphi(r,\omega,k) = \frac{A(\omega,k)\,r^{-\Delta_-}[1+\ldots] + B(\omega,k)\,r^{-\Delta_+}[1+\ldots]}{A(\omega,k)\,r_\Lambda^{-\Delta_-}[1+\ldots] + B(\omega,k)\,r_\Lambda^{-\Delta_+}[1+\ldots]}, \tag{2.12}$$

where $A(\omega,k)$ and $B(\omega,k)$ are analytic in ω and k, and $\ldots$ denote higher order terms in r in an expansion around r_Λ. The on-shell action generically takes the form (1.39) with

$$\mathcal{F}(r,\omega,k) = \varphi(r,-\omega,-k)\,\mathcal{A}(r,\omega,k)\,\partial_r\varphi(r,\omega,k), \tag{2.13}$$

where $\mathcal{A}(r,\omega,k)$ is analytic in ω and k. After renormalising the source term (as

[3]This is simply the general solution of the equation of motion near the boundary of an AdS spacetime, as can be seen, for the example of a scalar field, by expanding (1.19) at large r.

described in section 1.2.2), one applies the prescription of section 1.2.3 to find that

$$G^R_{\mathcal{O}_\varphi\mathcal{O}_\varphi} = 2\left(\Delta_+ - \Delta_-\right)\mathcal{A}\left(r_\Lambda, \omega, k\right)\frac{B\left(\omega,k\right)}{A\left(\omega,k\right)} r_\Lambda^{-\Delta_+ + \Delta_- - 1} + \ldots, \tag{2.14}$$

where the ellipsis represents higher-order terms in the expansion around r_Λ, in addition to contact terms. This demonstrates that poles of the retarded Green's functions (i.e. when $A\left(\omega,k\right) = 0$) have frequencies $\omega\left(k\right)$ equivalent to the *quasinormal frequencies* of the dual gravitational theory [30]. That is, they correspond to the frequencies of the modes of the gravitational background whose leading term vanishes at the boundary of the spacetime and which are purely ingoing at the horizon.

2.2.2 Spectral functions

Whilst the poles of the retarded Green's functions contain a lot of information about the excitations of the field theory, they do not tell one everything. The residue at each of these poles is also important. This information is encoded in the *spectral functions* of the theory

$$\chi_{\mathcal{O}\mathcal{O}}\left(\omega,k\right) \equiv -2\mathrm{Im}G^R_{\mathcal{O}\mathcal{O}}\left(\omega,k\right), \tag{2.15}$$

which measure the time average (over a cycle) of the rate of work done on the system by applying a small source for the operator $\mathcal{O}$ with frequency ω and momentum k [49]. Stability of the state requires that $\omega\chi_{\mathcal{O}\mathcal{O}}\left(\omega,k\right) \geq 0$.

The spectral function is computed from the dual gravitational theory simply by taking the imaginary part of the retarded Green's function, computed via the method described in section 1.2.3. We note here that the counterterms required to regularise the action give a purely real contribution to the retarded Green's function for every example in this thesis, and so do not affect the spectral function. There is clearly a very close connection between the poles of the retarded Green's function and the spectral function. A simple pole of the form (2.10) will give rise to a peak

in the spectral function of the form,

$$\chi\left(\omega \sim \omega_*\right) = \frac{\mathrm{Im}\left(\mathcal{R}\right)\left(\omega-\omega_*\right) - \mathrm{Re}\left(\mathcal{R}\right)\Gamma}{\left(\omega-\omega_*\right)^2+\Gamma^2} + \text{terms analytic in } \left(\omega-\omega_*\right), \quad (2.16)$$

where $\mathcal{R}$ is the residue at the pole. By locating the maximum of a spectral function of the form (2.16), one can see that the exact location of the peak depends upon $\mathcal{R}$ but in all the examples we will encounter it will be at approximately $\omega = \omega_*$ with a width that increases with Γ. The residue at a pole is clearly important for another reason also — if it is very small then it tells us that despite the presence of an excitation, the excitation couples very weakly to an external source.

2.3 Coupled operators

We have restricted our discussion so far to field theory operators $\mathcal{O}$ whose two-point functions are determined solely by the behaviour of their dual gravitational field φ. However, we expect that the operators will generically not behave completely independently. One example is in a holographic quantum liquid where one would naturally expect a fluctuation in the $U(1)$ charge density to result in a fluctuation of the energy density, since the matter carrying this charge will also carry some energy. This dependence manifests itself in the gravitational description of the theory via coupling between the dual classical fields. In this section we will describe how to compute the two-point functions of coupled operators, and indicate how the Ward identities relating such two-point functions can be made manifest in the gravitational description.

2.3.1 Solving coupled gravitational equations

Suppose we have M gravitational fields whose fluctuations $\Phi^I\left(r,\omega,k\right) = F^I_J\left(r,\omega,k\right)\Phi^J_0\left(\omega,k\right)$, around some solution to the background equations of motion, obey a coupled system of M equations of motion. This indicates that the two-point functions of their

dual operators $\mathcal{O}_I$ around the equilibrium field theory state are also coupled. Let us assume that the fields Φ_I have been renormalised as outlined in section 1.2.2 such that they asymptote to a constant near the asymptotically-AdS boundary of the spacetime. To quadratic order in such fluctuations, the action may be written in the general form

$$\begin{aligned} S = \int dr \frac{d\omega d^{d-1}k}{(2\pi)^d} \Big[& \partial_r \Phi^I (r,-\omega,-k) A_{IJ} (r,\omega,k) \partial_r \Phi^J (r,\omega,k) \\ & + \Phi^I (r,-\omega,-k) B_{IJ} (r,\omega,k) \partial_r \Phi^J (r,\omega,k) \\ & + \Phi^I (r,-\omega,-k) C_{IJ} (r,\omega,k) \Phi^J (r,\omega,k) \Big], \end{aligned} \tag{2.17}$$

Analogously to the $M = 1$ case presented in section 1.2.3, one can write the on-shell action in the form

$$S = \int_{\omega>0} \frac{d\omega d^{d-1}k}{(2\pi)^d} \Phi_0^I (-\omega,-k) \mathcal{F}_{IJ} (r,\omega,k) \Phi_0^J (\omega,k) \Big|_{r_H}^{r_\Lambda}, \tag{2.18}$$

where the flux factor

$$\mathcal{F} (r,\omega,k) = 2F^\dagger (r,\omega,k) A^H (r,\omega,k) \partial_r F (r,\omega,k) + F^\dagger (r,\omega,k) B^\dagger (r,\omega,k) F (r,\omega,k), \tag{2.19}$$

is now an $M \times M$ matrix, with A^H denoting the Hermitian part of the matrix A, and the integral is only over modes with $\omega > 0$.[4] Note that the flux factor does not depend upon the coefficients $C_{IJ} (r,\omega,k)$ as these non-derivative terms vanish when the action is put on-shell. The procedure to determine the retarded Green's functions is a simple generalisation of the $M = 1$ case. The retarded Green's functions are given by the flux factor [56]

$$G^R_{\mathcal{O}_I \mathcal{O}_J} (\omega,k) = \lim_{\frac{r_\Lambda}{R} \to \infty} \left[-\mathcal{F}_{IJ} (r_\Lambda,\omega,k) \right], \tag{2.20}$$

[4]This is valid provided that $A_{IJ} (r,-\omega,-k) = A^*_{IJ} (r,\omega,k)$ and similarly for B_{IJ} and C_{IJ}, as is the case for the theories discussed in chapters 3 and 4. We assume this property from now on.

evaluated on the solution with the following boundary conditions. At the horizon, all M fields must be purely ingoing and at the asymptotically-AdS boundary, they must obey

$$F_J^I\left(r_\Lambda, \omega, k\right) = \delta_J^I, \tag{2.21}$$

which ensures that the boundary value of Φ^I acts as the source for the dual operator $\mathcal{O}_I$.

Analogously to the uncoupled case, the poles of $G^R_{\mathcal{O}_I\mathcal{O}_J}$ exist for certain $\omega\left(k\right)$ where the source terms (i.e. the terms constant in r near the boundary of the spacetime) of Φ^I and Φ^J vanish with respect to the expectation value terms (i.e. the subleading terms near the boundary). Since this means that the source terms of all of the coupled fields are vanishing near the boundary, it's clear that all of the coupled operators share a common set of poles of their two-point functions. However, the residue at each pole will differ between the two-point functions of different coupled operators.

One may define an $M \times M$ anti-Hermitian matrix of spectral functions for a set of coupled operators

$$\chi_{IJ}\left(\omega, k\right) \equiv i\left(G^R_{\mathcal{O}_I\mathcal{O}_J}\left(\omega, k\right) - G^R_{\mathcal{O}_J\mathcal{O}_I}\left(\omega, k\right)^*\right). \tag{2.22}$$

As before, a diagonal component $\mathcal{O}_{II}\left(\omega, k\right)$ (no sum) of this matrix measures the average rate of work done on the system when a small source for $\mathcal{O}_I\left(\omega, k\right)$ is applied. Hence an excitation which couples strongly to an external source for a particular operator $\mathcal{O}_I$ will be visible as a large peak in χ_{II} near the propagating frequency ω_* of that mode.

Numerical implementation

Although simple in principle, the determination of the two-point functions is often complicated in practice due to the complexity of the gravitational equations of mo-

tion. Thus a numerical solution to these is often required. For the majority of the results in this thesis, this can be done by imposing boundary conditions at the horizon and numerically integrating outwards to the boundary of the spacetime. When there are coupled fields, this procedure is complicated by the fact that one must apply the correct boundary conditions at the horizon, to ensure that the conditions (2.21) are satisfied near the boundary.[5] Simply demanding ingoing conditions is not enough — these fix only M of the $2M$ boundary conditions of the system of differential equations.

There is a systematic procedure [56] to construct the solutions for coupled Φ^I which obey the required boundary conditions at the horizon and boundary. At the horizon one performs a Frobenius expansion of the fields, allowing one to write the solution as the product of an oscillating, ingoing piece and a regular power series

$$\Phi^I(r,\omega,k) = \varphi_{\text{in}}(r,\omega)\left(\varphi_0^I + \varphi_1^I(r-r_H) + \ldots\right), \tag{2.23}$$

where $\varphi_{\text{in}}(r,\omega)$ is typically of the form

$$\varphi_{\text{in}} = (r-r_H)^{-i\omega/4\pi T}, \tag{2.24}$$

and r_H is the horizon radius.[6] The M remaining boundary conditions correspond to the coefficients φ_0^I, and we wish to choose these such that the fields satisfy (2.21) near the asymptotically-AdS boundary. Initially, one should generate M linearly independent solutions labelled $\Phi_J = \{\Phi_J^1, \Phi_J^2, \ldots, \Phi_J^M\}$ by choosing, for example

$$\left(\varphi_0^I\right)_J = \delta_J^I, \tag{2.25}$$

where δ_J^I is the usual Kronecker delta. Although generically none of these solutions

[5]Note that for a single field this is trivial — one can simply rescale the field by dividing by its boundary value, ensuring that this rescaled field will tend towards 1 near the boundary.

[6]Note that such a Frobenius expansion is not possible around an extremal horizon, where r_H is an irregular singular point of the differential equations.

satisfy the required boundary conditions (2.21) near the boundary of the spacetime, one can use the linearity of the differential equations to construct a linear combination of Φ_J that do satisfy this. This linear combination is given by the matrix product

$$F\left(r,\omega,k\right)=H\left(r,\omega,k\right)\cdot H\left(r_{\Lambda},\omega,k\right)^{-1}, \tag{2.26}$$

where the $M\times M$ matrix H has elements

$$\left[H\left(r,\omega,k\right)\right]_{J}^{I}=\Phi_{J}^{I}\left(r,\omega,k\right), \tag{2.27}$$

i.e. the Jth column of H contains the fields satisfying the near-horizon boundary conditions (2.25). By construction, this matrix F_J^I is a set of solutions to the coupled differential equations which obey ingoing boundary conditions at the horizon and the boundary conditions (2.21) near the boundary of the AdS spacetime.

Poles of the Green's functions arise when there is a pole of the flux factor (2.19). This requires that the matrix

$$F'\left(r_{\Lambda},\omega,k\right)=H'\left(r_{\Lambda},\omega,k\right)\cdot H\left(r_{\Lambda},\omega,k\right)^{-1}, \tag{2.28}$$

has a pole (where the prime denotes a derivative with respect to r). As the solutions $\Phi_J^I\left(r,\omega,k\right)$ are smooth, this means that a pole can only exist when

$$\det\left[H\left(r_{\Lambda},\omega,k\right)\right]=0. \tag{2.29}$$

Thus, by computing this determinant as a function of ω and k, one can locate the corresponding poles of the Green's functions of the dual theory. It is clear from this formulation that all operators in the field theory will share a common set of Green's function poles.

We note that as mentioned previously, numerically integrating outward from the horizon is, a priori, unreliable for extremal black holes. In section 4.A.2, we

will discuss an alternative numerical approach which works for some extremal black holes.

Numerical check

To verify the accuracy of the numerical solutions obtained, it is advisable to perform consistency checks on the results obtained. For the coupled set of differential equations described above, a strong consistency check is possible. The off-shell action (2.17), which may be written

$$S = \int_{\omega>0} \frac{d\omega d^{d-1}k}{(2\pi)^d} dr \left(\Phi^I_{\omega,k}\right)^* \left[2\partial_r F^\dagger A^H \partial_r F + F^\dagger B \partial_r F + \partial_r F^\dagger B^\dagger F + 2F^\dagger C^H F\right]_{IJ} \Phi^J_{\omega,k}, \tag{2.30}$$

is invariant under the global transformation

$$F^I_J(r,\omega,k) \to e^{i\alpha_{IJ}} F^I_J(r,\omega,k), \tag{2.31}$$

since it is quadratic in the fields. Using this, we can construct an $M \times M$ matrix of Noether currents [56]

$$\mathcal{J}_{IJ}(r,\omega,k) = -i\left(\mathcal{F} - \mathcal{F}^\dagger\right)_{IJ}, \tag{2.32}$$

which is invariant under translations in r. Thus for a given set of solutions to the differential equations, one can construct the Noether current (2.32) and ensure this is invariant in r. If not, it indicates that the numerical solutions obtained cannot be trusted. All of the numerical results presented in this thesis have passed this check.

2.3.2 Ward identities and gauge-invariant variables

In the preceding subsection we have described the procedure for determining the Green's functions of a set of coupled operators from the dual gravitational theory. However, it is often the case that the relation between these Green's functions is very simple and determined by a Ward identity. For such operators, the machinery of the

previous subsection may be avoided by working in gauge-invariant variables, which 'decouple' certain subsets of the bulk fields and explicitly encode the aforementioned Ward identities.

Suppose we are considering a gauge theory with a conserved global $U(1)$ current J^α. Using the gauge/gravity duality dictionary of section 1.2, we know that the dual gravitational theory will contain a $U(1)$ gauge field A_μ. The components of the fluctuations of this gauge field a_μ will generically couple to one another and thus the complicated procedure above must be followed to determine the Green's functions of J^α. However, assuming that we are considering a field theory state in which this symmetry is not spontaneously broken, we know that these Green's functions are interrelated in a very simple way via Ward identities. Specifically, if we label the direction in which momentum flows in the field theory x^1, the Ward identities require that

$$G^R_{J^t J^t}(\omega,k) = \frac{k}{\omega} G^R_{J^t J^{x^1}}(\omega,k) \qquad \text{and} \qquad G^R_{J^t J^t}(\omega,k) = \frac{k^2}{\omega^2} G^R_{J^{x^1} J^{x^1}}(\omega,k)\,, \tag{2.33}$$

where the equalities should be understood to hold up to contact terms (i.e. terms analytic in ω and k).

These Ward identities may be made manifest in the bulk theory by working directly in gauge-invariant variables. The gauge field fluctuations transform as

$$a_\mu \to a_\mu - \partial_\mu \Lambda, \tag{2.34}$$

under a $U(1)$ gauge transformation and we may therefore define a gauge-invariant field

$$Z(r,\omega,k) \equiv \omega a_{x^1}(r,\omega,k) + k a_t(r,\omega,k)\,. \tag{2.35}$$

As the bulk theory is gauge-invariant, its equations of motion, on-shell action etc. may be written entirely in terms of Z, rather than a_t and a_{x^1}. Practically, this

is important as it reduces the number of independent variables which are coupled. With the on-shell action in the form

$$S_{\text{on-shell}} = \int \frac{d\omega d^{d-1}k}{(2\pi)^d} Z\left(r,-\omega,-k\right) \mathcal{A}\left(r,\omega,k\right) \partial_r Z\left(r,\omega,k\right)\Big|_{r_H}^{r_\Lambda} + \text{non-derivative terms}, \tag{2.36}$$

we may factor out the source term

$$Z\left(r,\omega,k\right) \equiv f_Z\left(r,\omega,k\right) Z^0\left(\omega,k\right) = f_Z\left(r,\omega,k\right)\left[\omega a^0_{x^1}\left(\omega,k\right) + k a^0_t\left(\omega,k\right)\right], \tag{2.37}$$

where $f_Z\left(r_\Lambda,\omega,k\right) = 1$. Substituting this into the on-shell action, we find

$$\begin{aligned} S_{\text{on-shell}} = -\int \frac{d\omega d^{d-1}k}{(2\pi)^d} \mathcal{A}\left(r,\omega,k\right) \partial_r f_Z\left(r,\omega,k\right) \Bigg[& k^2 a^0_t\left(-\omega,-k\right) a^0_t\left(\omega,k\right) \\ & + \omega k \Big\{ a^0_{x^1}\left(-\omega,-k\right) a^0_t\left(\omega,k\right) + a^0_t\left(-\omega,-k\right) a^0_{x^1}\left(\omega,k\right) \Big\} \\ & + \omega^2 a^0_{x^1}\left(-\omega,-k\right) a^0_{x^1}\left(\omega,k\right) \Bigg]\Bigg|_{r_H}^{r_\Lambda} + \text{non-derivative terms}. \end{aligned} \tag{2.38}$$

Computing the correlators via the procedure of section 1.2.3, one finds that

$$G^R_{J^t J^t}\left(\omega,k\right) = -2k^2 \mathcal{A}\left(r_\Lambda,\omega,k\right) \partial_r f_Z\left(r_\Lambda,\omega,k\right) + \text{contact terms}, \tag{2.39}$$

where $f_Z\left(r,\omega,k\right)$ obeys the ingoing boundary condition at the horizon in addition to the boundary condition at r_Λ given above. Because of the structure of the action (2.38), the other J^t and J^{x^1} correlators are explicitly related to $G^R_{J^t J^t}$ by the Ward identities (2.33) [57]. Thus, in addition to reducing the complexity of the equations of motion, gauge-invariant variables explicitly encode the field theory Ward identities. Note that the non-derivative terms contribute only contact terms to the correlators.

As our dual theories always involve gravitational degrees of freedom, there is a diffeomorphism symmetry transformation associated to all fields. This can be understood easily as follows. Under a diffeomorphism transformation $x^\mu \to \xi^\mu\left(x^\mu\right)$,

the background metrics $g_{\mu\nu}$ and $g_{\mu\nu}-\bar{\nabla}_\mu\xi_\nu-\bar{\nabla}_\nu\xi_\mu$ are equivalent to linear order in ξ^μ, where $\bar{\nabla}$ is the covariant derivative with respect to the metric $g_{\mu\nu}$ [58]. The metric fluctuations around these two equivalent parameterisations of the same solution are

$$\begin{aligned} &g_{\mu\nu} \to g_{\mu\nu} + h_{\mu\nu}, \\ &g_{\mu\nu} \to \left(g_{\mu\nu} - \bar{\nabla}_\mu\xi_\nu - \bar{\nabla}_\nu\xi_\mu\right) + h_{\mu\nu}, \end{aligned} \tag{2.40}$$

to linear order in $h_{\mu\nu}$. As the background has been fixed, the two fluctuations

$$h_{\mu\nu} \quad \text{and} \quad h_{\mu\nu} - \bar{\nabla}_\mu\xi_\nu - \bar{\nabla}_\nu\xi_\mu, \tag{2.41}$$

are physically equivalent to first order in $h_{\mu\nu}$. This gives the first order diffeomorphism symmetry transformation

$$\delta h_{\mu\nu} = -\bar{\nabla}_\mu\xi_\nu - \bar{\nabla}_\nu\xi_\mu, \tag{2.42}$$

of the metric fluctuations. The transformation laws of other fields under such diffeomorphisms may also be obtained.

As in the example of a $U(1)$ symmetry above, one can again construct combinations of the metric fields which are invariant under these transformations and write the equations of motion solely in terms of these gauge-invariant variables (see section 4.2.4 for such variables in a specific case). This significantly reduces the overall number of equations of motion and enforces the Ward identities of the field theory Green's functions required by conservation of the stress-energy tensor [57]. This happens because the derivative terms in the quadratic on-shell action of the fluctuations (2.36) may be written solely in terms of the gauge-invariant variables. Whilst the non-derivative terms in (2.36) may not be written in terms of these variables, these do not affect the Ward identities as they contribute only counterterms to the field theory Green's functions. Finally, we note that the fact that the non-derivative

terms in the on-shell action cannot be written in terms of variables invariant under the transformation (2.42) does not mean that the theory is not diffeomorphism-invariant. It is simply that the transformation (2.42) is valid only to linear order in fluctuations, while the on-shell action is quadratic in fluctuations.

We close this subsection with some remarks on the easiest practical implementation of the gauge-invariant approach described above. Consider first the case of a $U(1)$ gauge symmetry transformation (2.34). The simplest way to obtain the equation of motion for the gauge-invariant variable (2.35) is to write the equations for the fundamental fluctuations in a non-gauge-fixed form (i.e. do *not* set $a_r = 0$ as is often done in holographic computations), and then algebraically solve the equation of motion coming from varying the action with respect to a_r for the field a_r. This solution for a_r may then be substituted into all other equations of motion, after which one will find that a_{x^1} and a_t appear everywhere in the combination (2.35). Furthermore, after this substitution one will find that many of the original equations of motion are no longer linearly-independent and thus the total number of linearly-independent equations of motion has been reduced in line with the reduction of the total number of independent variables of the system. Performing a similar procedure with the action (on-shell or off-shell) yields the action in terms of the gauge-invariant variables. For diffeomorphism transformations of the metric fluctuation (2.42), the approach is similar. However, one should now algebraically solve a subset of the equations of motion of the metric fluctuations for the fields $h_{r\mu}$.

In general, a theory will have numerous gauge symmetries. One should construct a set of linearly-independent variables which are invariant under *all* symmetry transformations. This may be done by identifying the subset of fields which can be solved for algebraically and substituting these solutions back into the remaining equations of motion, and then identifying those resultant equations of motion which are linearly-independent. These equations are naturally expressed in terms of the gauge-invariant variables.

Chapter 3

Collective excitations in the D3/D7 theory

3.1 Introduction

Using the methods described in the previous two chapters, we can now calculate the properties of certain holographic quantum liquids from their classical duals. In this chapter, based on the paper [59], we investigate the behaviour of the collective modes of the $\mathcal{N} = 4$ $SU(N_c)$ supersymmetric Yang-Mills theory coupled to N_f $\mathcal{N} = 2$ fundamental hypermultiplets at infinitely large 't Hooft coupling $\lambda = g^2_{YM}N_c$ in the limit $N_c \gg 1$, $N_c \gg N_f$ and at non-zero temperature T and at large density of the fundamental matter d. The holographic dual of this theory is provided by embedding N_f D7-branes in the gravitational background created by N_c D3-branes and treating the D7-branes as probes [60]. Although a seemingly elaborate construction, this is one of the simplest known finite-density field theories for which an explicit dual is known, and it has some interesting properties.

At strictly zero temperature and zero hypermultiplet mass, the theory supports a collective excitation which appears as a pole in the density-density correlator [61]. Such an excitation, found in [61] using the dual gravity methods and thus

referred to here as the "holographic zero sound", is reminiscent of the zero sound mode predicted to exist by Landau in a class of Fermi liquid systems [32] (see also [33–35,62,63]) and subsequently observed in liquid Helium-3 [37,38]. In Landau Fermi liquids (LFLs), the zero sound mode arises due to (non-thermal) interactions between the constituent fermions which result in oscillations of the Fermi surface, as we reviewed in section 1.3. The holographic zero sound mode in the D3/D7 system at zero temperature has a speed equal to that of the ordinary (first) sound and an attentuation proportional to the square of the momentum. This is identical to what one finds in the Fermi liquid models where the interaction strength (parameterised by the Fermi liquid coefficient F_0) approaches infinity [34]. At the same time, the heat capacity of the D3/D7 system is proportional to T^6 at low temperatures whereas in normal Fermi liquids it is proportional to T.

Similar investigations have been made in other string-theoretic constructions — in [64] it was shown that the holographic zero sound mode persists at $T = 0$ when the hypermultiplet is given a finite mass, in [65] a similar mode was found in the $T = 0$ D4/D8/$\overline{\text{D8}}$ theory at finite density, in [66] a "zero sound" mode was reported to exist in the (1+1)-dimensional theory on the D3/D3 intersection and in [67] a low temperature zero sound mode was found in the theory on the (2+1)-dimensional D3/D7 brane intersection. In the D4/D8/$\overline{\text{D8}}$ case — where the only fundamental matter present is fermions — the heat capacity is proportional to T as expected for a Landau Fermi liquid. However, the imaginary part of the zero sound mode in this case has an unconventional q^3 dependence, which is at odds with the predictions of LFL theory. Holographic zero sound modes have also been discovered in theories consisting of probe DBI actions embedded in Lifshitz (i.e. non-relativistic) spacetimes [68, 69]. Such modes have a density-dependent speed, and their properties depend upon the critical exponent of the spacetime. In addition to these, the field theory dual to (3+1)-dimensional Einstein-Maxwell gravity with a cosmological constant was found to support a long-lived sound mode at zero temperature [70].

A natural question to ask is what happens to the holographic zero sound mode when the temperature is turned on. In [71], it was argued that at any infinitesimal temperature the zero sound mode of the D3/D7 theory is no longer dominant and instead density transport occurs mainly via diffusion. In this chapter we show that this is not the case — at low temperatures, the holographic zero sound mode still dominates the density-density correlator with a dispersion relation very similar to that at $T = 0$. Furthermore, we show (numerically) that the real part of this mode is independent of temperature whereas its imaginary part receives corrections proportional to T^2. At a sufficiently high temperature, there is a crossover to a hydrodynamic regime where the diffusion mode of [71] dominates (such crossovers are common — see [56, 72–76] for other holographic examples of this). This behaviour is familiar as it is the same as that predicted by Landau's theory of Fermi liquids, to which we now turn to help clarify these results and to identify the relevant scales involved.

In Fermi liquids, the zero sound mode is a longitudinal, gapless, collective excitation corresponding to oscillations of the Fermi surface around its equilibrium shape at zero temperature. Its dispersion relation $\omega(q) = v_s\, q - i\Gamma_\omega$ contains a non-zero damping due to the mode's decay into quasiparticle-quasihole pairs. It is often more convenient to work with real frequency and complex wave vector: $q(\omega) = \omega/v_s + i\Gamma_q$. The damping rate is conveniently characterised by considering the argument of q, $\arg q(\omega) = \mathrm{Im}\, q/\mathrm{Re}\, q$, as a function of the frequency.

The zero sound mode persists at small, non-zero temperatures as well, but its properties are altered by the thermal collisions of the quasiparticles. As we reviewed in section 1.3.2, one can distinguish three regimes: the hydrodynamic regime, when $\omega \ll T^2/\mu, T$, the collisionless thermal (classical) regime when $T^2/\mu \ll \omega \ll T$, and the collisionless quantum regime when $T^2/\mu, T \ll \omega$. The zero temperature zero sound mode persists essentially unaltered in the collisionless quantum regime, where thermal excitations are too weak and infrequent to influence it. In this regime, one

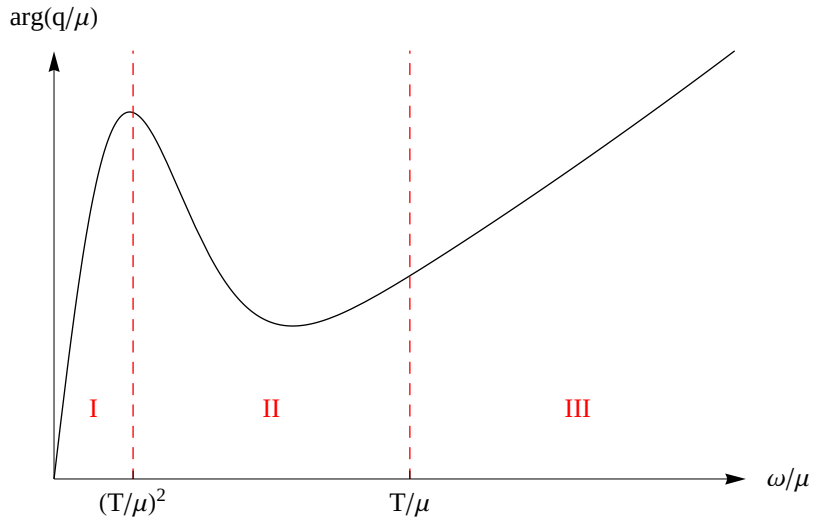

Figure 3.1: A sketch of the dependence of the argument of the zero sound mode dispersion relation on frequency in the hydrodynamic (I), collisionless thermal (II) and collisionless quantum (III) regimes of a Landau Fermi liquid. First sound propagates in region I while the zero sound mode exists in regions II and III.

has $\Gamma_q \sim \omega^2/\mu$ and $\arg q(\omega) \sim \omega/\mu$. As the temperature is increased, however, thermal excitations change the attenuation of the zero sound mode such that $\Gamma_q \sim T^2/\mu$ and $\arg q(\omega) \sim (T/\mu)^2\mu/\omega$ in the thermal collisionless regime. In the hydrodynamic regime, thermal excitations destroy the zero sound mode completely. However, these excitations support the ordinary hydrodynamic sound mode with viscous damping, and the thermal diffusion mode. The attenuation of hydrodynamic (first) sound is determined by the viscosity and is proportional to ω^2/T^2 [34, 62, 63].

The three regimes observed as one changes T at fixed ω were shown in figure 1.2. The sound attenuation constants in various regimes are shown in table 3.1 and figures 1.3 and 3.1. We shall use this information as a suggestive guide in our investigation of the holographic zero sound at finite temperature.

Table 3.1: Sound attenuation coefficients in a Landau Fermi liquid

	Γ_ω	Γ_q	$\mathrm{Arg}\, q$
Hydrodynamic regime	$\left(\frac{\mu}{T}\right)^2 \frac{q^2}{\mu}$	$\frac{\mu\omega^2}{T^2}$	$\left(\frac{\mu}{T}\right)^2 \frac{\omega}{\mu}$
Collisionless thermal regime	$\frac{T^2}{\mu}$	$\frac{T^2}{\mu}$	$\left(\frac{T}{\mu}\right)^2 \frac{\mu}{\omega}$
Collisionless quantum regime	$\frac{q^2}{\mu}$	$\frac{\omega^2}{\mu}$	$\frac{\omega}{\mu}$

In the massless D3/D7 system at low temperature, the chemical potential is proportional to the cubic root of the volume density d of the $U(1)$ "baryon" charge[1] [61]

$$\mu = \alpha\, d^{1/3} \left(1 + O\left(\frac{T}{d^{1/3}}\right)\right) , \tag{3.1}$$

where α can be expressed using the Euler beta-function, $\alpha = B(1/3, 7/6)/2 \approx 1.402$. We shall study the D3/D7 theory in the limit $T \ll d^{1/3}$, $\omega \ll d^{1/3}$ formally corresponding to the applicability regime (1.49) and (1.51) of Landau Fermi liquid theory. The appropriate dimensionless variables are

$$\bar{\omega} = \frac{\omega}{d^{1/3}} , \qquad \bar{q} = \frac{q}{d^{1/3}} , \qquad \tilde{d} = \frac{d}{(\pi T)^3} . \tag{3.2}$$

A priori, we do not expect to find agreement with the LFL results outlined above since the D3/D7 system appears to be microscopically rather different, with no obviously detectable Fermi surface or long-lived quasiparticles in its vicinity. Nevertheless, we do find that the behaviour of the zero sound mode at finite temperature is qualitatively similar to the one predicted (and observed) in a Landau Fermi liquid:

i) The three regimes (hydrodynamic, collisionless thermal and collisionless quantum) are readily identified by analysing the behaviour of the lowest quasinormal frequencies and the spectral function of the charge density correlator. The hydrodynamic/collisionless thermal transition occurs at $\bar{\omega}\, \tilde{d}^{2/3} \sim 1$ and is most spectacularly manifested in the motion of the zero sound poles in the complex frequency plane: as the temperature is increased, the two poles (corresponding to zero sound propagation with velocities $+v_s$ and $-v_s$ in the field theory) recede into the complex plane, approximately tracing a circle, until they collide on the imaginary axis and form two poles with zero real part — one of these new poles recedes even deeper into the complex plane while the other approaches the origin. The latter pole is the charge density diffusion mode (with the diffusion constant computed in [71, 78])

[1] An explicit expression for the charge density operator involving fundamental fermions and scalars of the $\mathcal{N} = 2$ hypermultiplet is given in Appendix A of [77].

characteristic of the hydrodynamic regime. Such behaviour was previously observed in [56] and also in a (2+1)-dimensional holographic field theory in [67], where it was correctly identified as the hydrodynamic/collisionless transition involving the zero sound mode. A similar transition between propagating and diffusive modes has been seen in a model of a holographic superconductor [76]. The second transition, between the collisionless thermal and the collisionless quantum regimes, is observed at $\bar{\omega}\,\tilde{d}^{1/3} \sim 1$.

As our investigation is limited to the current-current correlators, we are not able to follow the emergence of first sound in the hydrodynamic regime — this should appear as a pole in the energy-momentum tensor correlators of the field theory which are decoupled from the current-current correlators in the probe brane limit. Accordingly, we do not expect the details of the hydrodynamic/collisionless thermal transition described above to survive beyond the probe brane approximation: it seems more likely that the acoustic poles, rather than colliding on the imaginary axis as the temperature is raised, will recede deeper into the complex plane, reflecting the behavior of the attenuation curve in figure 1.3, and then come back close to the real axis again as the hydrodynamic sound poles.

ii) The D3/D7 zero sound attenuation coefficients exhibit the momentum, temperature and density dependence typical of a Landau Fermi liquid as shown in Table 3.1. We find that the dependence of the acoustic damping upon frequency and temperature is qualitatively the same as shown in figures 1.3 and 3.1 in regions II and III.

iii) These results remain valid in the case of a non-vanishing hypermultiplet mass.[2]

The structure of this chapter is as follows. In section 3.2, we give a brief description of the D3/D7 field theory and its gravitational dual, in addition to some of the relevant properties of its Green's functions and spectral functions. In section 3.3

[2]Within the region of thermodynamic stability of the theory.

we present our numerical results for the density-density spectral function (and the dominant pole of the corresponding Green's function) when $T \ll d^{\frac{1}{3}}$. We identify the three regimes similar to those of a Landau Fermi liquid, and describe in detail the behaviour of the collective modes as the temperature of the system is varied. We summarize our results and discuss how they may generalize to other holographic finite density systems in section 3.4. Some details relevant for the case of a massive hypermultiplet are relegated to appendices: Appendix 3.A.1 contains the action and equations of motion for the fluctuations, and Appendix 3.A.2 provides a derivation of the holographic zero sound attenuation constant at zero temperature.

3.2 The D3/D7 holographic quantum liquid

The specific field theory whose elementary excitations at non-zero temperature and large density we wish to investigate is (3+1)-dimensional $\mathcal{N} = 4$ $SU(N_c)$ supersymmetric Yang-Mills theory coupled to N_f $\mathcal{N} = 2$ fundamental hypermultiplets with a global $U(N_f)$ flavour symmetry. It arises as the low-energy theory on the worldvolume of a set of N_c D3-branes and N_f D7-branes intersecting along the (3+1)-dimensions of the D3-brane worldvolume. The resulting theory has $\mathcal{N} = 2$ supersymmetry and is no longer a conformal field theory, but has a non-zero beta function $\beta_\lambda \propto N_f/N_c$ [79]. The Lagrangian of the theory is given in appendix A of [80].

To obtain the holographic dual of this theory, we can use a similar argument to that of section 1.2.1. Beginning with a flat (9+1)-dimensional spacetime containing N_c D3-branes and N_f D7-branes intersecting along the D3-brane worldvolume, one can take the low energy limit at small λ to obtain the field theory described above. The fundamental degrees of freedom in this theory arise from strings stretched between the D3- and D7-branes, with a mass proportional to the inverse brane separation.

To find the dual gravitational description, valid when $\lambda \gg 1$, one wishes to find the supergravity solution sourced by these objects. This solution is unknown. However, in the 'probe limit' $N_f \ll N_c$, the energy-momentum tensor of the D3-branes is vastly bigger than that of the D7-branes and will dominate the geometry sourced by the brane configuration. In the strict limit $N_f/N_c \to 0$, the near-horizon supergravity solution is simply $AdS_5 \times S^5$. That is, the corrections to the background geometry due to the D7-branes are negligible. However the D7-branes also source bulk fields which the D3-branes do not and thus in the probe limit, the D7-brane action for these fields is still important.

Thus by taking $N_c \to \infty$ with both $\lambda = g_{YM}^2 N_c$ and N_f/N_c fixed, and subsequently taking $N_f/N_c \to 0$ and $\lambda \to \infty$, we obtain the classical gravitational dual to this field theory [60, 81]:

$$\begin{aligned} S &= S_{\text{adjoint}} + S_{\text{fundamental}}, \\ &= S_{\text{adjoint}} - N_f T_{D7} \int d^8\xi \sqrt{-\det\left(g_{ab} + F_{ab}\right)}, \end{aligned} \tag{3.3}$$

where S_{adjoint} is the ten-dimensional supergravity action and T_{D7} is the tension of a D7-brane. In this probe brane limit, the metric is fixed and it is $S_{\text{fundamental}}$ which contains the dynamical information. For a zero temperature field theory, the contribution of the fundamental matter is the DBI action of N_f probe D7-branes extended along an $AdS_5 \times S^3$ section of the (fixed) $AdS_5 \times S^5$ background spacetime (1.3) generated by the D3-branes.[3] In equation (3.3), g_{ab} denotes the induced worldvolume metric on the D7-brane and F_{ab} is the field strength of a worldvolume $U(1) \subset U(N_f)$ gauge field.

When the field theory is at a non-zero temperature, the background spacetime is that of an AdS-Schwarzschild black brane (1.31). The D7-brane wraps an asymptotically $AdS_5 \times S^3$ section of the metric, with the horizon radius of the background

[3]The Wess-Zumino term in the D7-brane action is not important for the properties studied here.

related to the temperature of the field theory via $T = r_H/\pi R^2$.

In terms of the dimensionless radial coordinate $u = r_H^2/r^2$, the metric (1.31) can be written as

$$ds_{10}^2 = \frac{(\pi T R)^2}{u}\left(-f dt^2 + d\vec{x}^2\right) + \frac{R^2}{4u^2 f}du^2 + R^2\left(d\theta^2 + \sin^2\theta ds_{S^1}^2 + \cos^2\theta ds_{S^3}^2\right), \tag{3.4}$$

where $f(u) = 1 - u^2$. In these coordinates, the horizon is located at $u = 1$ and the boundary at $u = 0$. In equilibrium, the D7-brane embedding can be characterised by a single embedding coordinate $\theta(u)$ (which determines which S^3 section of the background S^5 it wraps). The gauge field on the brane is dual to a global flavour current in the field theory and thus turning on the time component of a $U(1) \subset U(N_f)$ gauge field $A_t(u)$ on the brane corresponds to introducing a finite density d of the $U(1)$ "baryon" charge in the field theory. In this case, it corresponds to a net density of fundamental fermions and scalars.

The equations of motion for the background fields are obtained from the DBI action

$$S_{\text{fundamental}} = -\frac{N r_H^4}{2}\int_0^1 du d^4x \frac{\cos^3\theta}{u^3}\sqrt{1 + 4u^2 f\theta'^2 - 4\frac{u^3}{r_H^2}A_t'^2}\,, \tag{3.5}$$

where $N = N_f T_{D7} V_{S^3}$ is a normalisation constant determined by the gauge-gravity duality dictionary [77] and primes denote derivatives with respect to u. One of the equations of motion derived from the action (3.5) reduces to

$$A_t'(u) = -\frac{r_H \tilde{d}}{2}\sqrt{\frac{1 + 4u^2 f(u)\theta'(u)^2}{\cos^6\theta(u) + \tilde{d}^2 u^3}}\,, \tag{3.6}$$

where $\tilde{d} \equiv dR^6/r_H^3 = d/(\pi T)^3$ is a dimensionless parameter of the field theory

related to the net number density of "quarks" n_q in the field theory[4] via

$$\tilde{d} = \frac{2^{5/2} n_q}{\sqrt{\lambda} N_f N_c T^3} \,. \tag{3.7}$$

For a given density $\tilde{d}$, there is a corresponding dimensionless chemical potential given by

$$\tilde{\mu} = \frac{\tilde{d}}{2} \int_0^1 du \sqrt{\frac{1 + 4 f(u) u^2 \theta'(u)^2}{\cos^6 \theta(u) + \tilde{d}^2 u^3}} \,, \tag{3.8}$$

which is related to the field theory chemical potential μ_{FT} by $\tilde{\mu} \equiv \mu/\pi T = \sqrt{\frac{2}{\lambda}} \frac{\mu_{FT}}{T}$. In the massless case, the integral in equation (3.8) can be computed exactly [61]: it reduces to (3.1) in the low temperature limit. The important scaling (not entirely obvious from (3.8) and generically accompanied by mass and temperature corrections [61, 82]) to emphasize is

$$\frac{\mu}{T} \sim \tilde{\mu} \sim \tilde{d}^{1/3} \,. \tag{3.9}$$

The equation of motion for the embedding coordinate is

$$\frac{d}{du} \left(\frac{f(u) \cos^3 \theta(u) \theta'(u)}{u \sqrt{G(u)}} \right) + \frac{3 \cos^2 \theta(u) \sin \theta(u) \sqrt{G(u)}}{4 u^3} = 0 \,, \tag{3.10}$$

where

$$G(u) = \cos^6 \theta(u) \frac{1 + 4 u^2 f(u) \theta'(u)^2}{\cos^6 \theta(u) + u^3 \tilde{d}^2} \,.$$

Equation (3.10) has no known generic analytic solution and must be solved numerically[5]. Near the boundary, the solution has the form

$$\theta(u) = \frac{\tilde{m}}{\sqrt{2}} \sqrt{u} + \ldots \,, \tag{3.11}$$

[4]Note that our normalisation of d is different from the one used in [77]: in [77], $d \sim n_q$ whereas in our case $d \sim n_q/\sqrt{\lambda} N_c N_f$.

[5]A method to approximate the solution in the low temperature limit has been proposed in [83].

where $\tilde{m}$ is related to the bare mass[6] of the fundamental matter in units of temperature via [84]

$$\tilde{m} = \frac{2}{\sqrt{\lambda}} \frac{M_q}{T}. \tag{3.12}$$

To study the temperature dependence of the theory at finite density, it will be more convenient to use the field theory mass normalised with respect to density rather than temperature:

$$\bar{m} = \frac{\tilde{m}}{\tilde{d}^{\frac{1}{3}}} = \frac{2\pi}{\sqrt{\lambda}} \frac{M_q}{d^{\frac{1}{3}}} \,. \tag{3.13}$$

Note that $\theta(u) = 0$ for a massless hypermultiplet, and thus the dual description greatly simplifies in this case — there is only one non-trivial background field $A_t(u)$ which has the simple equation of motion

$$A_t'(u) = -\frac{r_H \tilde{d}}{2} \left(1 + \tilde{d}^2 u^3\right)^{-1/2} \,. \tag{3.14}$$

The thermodynamics of the system can be determined by computing the on-shell action as described in section 2.1.2. In the massless case, the specific heat schematically has the following temperature dependence [61]:

$$c_V \sim N_c^2 T^3 + \cdots + \lambda N_f N_c T^6/d + \cdots \,, \tag{3.15}$$

where the first term comes from the adjoint $\mathcal{N} = 4$ SYM degrees of freedom. The pressure P, the entropy density s and the energy density ε can be computed from the thermodynamic potential $\Omega(\mu, T)$ given explicitly in [61]: the entropy density is finite in the $T \to 0$ limit, $s \sim \mu^3$, and the equation of state is $\varepsilon = 3P$ for all T and μ (and thus the speed of first sound is $v_s = 1/\sqrt{3}$). In certain regimes, the system becomes thermodynamically unstable: there appears to be an instability at low density $\tilde{d} < \tilde{d}_c \approx 0.00315$ [75, 77], and at high density and large mass $\bar{m} \gg 1, \tilde{d} \gg 1$ [83]. In addition, when $d \neq 0$ and $m \neq 0$ there is a lower limit on the possible

[6]The explicit field theory "quark" mass operator is given in Appendix A of [77].

value of μ, below which there is a phase transition to a Minkowski embedding with $d = 0$ [82, 85–88]. The values of the parameters considered in this paper are outside of these regimes.

To determine the field theory excitations, one considers fluctuations of the background bulk fields

$$\begin{aligned} \theta(u) &\to \theta(u) + \phi(u, z, t)\,, \\ A_t(u) &\to A_t(u) + a_t(u, z, t)\,, \\ A_i(u) &\to a_i(u, z, t)\,, \end{aligned} \tag{3.16}$$

$i = x, y, z$, where we have chosen the fluctuations to depend on time, the radial coordinate and one of the spatial coordinates (z) only (the latter is possible due to the isotropy of the theory). Introducing Fourier components for the embedding fluctuation

$$\phi(u, z, t) = \int \frac{d\omega\, dq}{(2\pi)^2} e^{-i\omega t + iqz}\, \tilde{\phi}\,(u, \omega, q)\,, \tag{3.17}$$

and similarly for $a_\mu(u, z, t)$, and expanding the DBI action (3.5) to quadratic order in fluctuations, one finds the resulting action and the corresponding equations of motion. The transverse modes $\tilde{a}_x$, $\tilde{a}_y$ decouple from the longitudinal modes $\tilde{a}_t$, $\tilde{a}_z$ and $\tilde{\phi}$. In the following, we shall focus on the longitudinal modes as they are the ones that support the holographic zero sound mode.

For a non-zero hypermultiplet mass, the equations of motion lead to a pair of coupled differential equations for the embedding fluctuation $\tilde{\phi}\,(u, \bar{\omega}, \bar{q})$ and the $U(1)$ gauge-invariant combination

$$\bar{Z}(u, \bar{\omega}, \bar{q}) = \bar{\omega}\, \tilde{a}_z(u, \bar{\omega}, \bar{q}) + \bar{q}\, \tilde{a}_t(u, \bar{\omega}, \bar{q})\,, \tag{3.18}$$

where the dimensionless variables $\bar{\omega}$ and $\bar{q}$ were introduced in equation (3.2). The equations of motion and the action for the longitudinal fluctuations are given in Appendix 3.A.1.

In the zero mass limit, the equations for these two modes decouple and the

gauge-invariant combination (3.18) obeys the equation of motion

$$\frac{d}{du}\left[\frac{f(u)\,\bar{Z}'}{\sqrt{g(u)}\,(\bar{\omega}^2-\bar{q}^2 f g)}\right]+\frac{\tilde{d}^{\frac{2}{3}}\bar{Z}}{4u\sqrt{g(u)}f(u)}=0, \tag{3.19}$$

where $g(u)=(1+\tilde{d}^2u^3)^{-1}$. In this limit, the longitudinal part of the on-shell action is

$$S^{(2)}_{\text{long.}}=Nr_H^2\int\frac{d\omega dq}{(2\pi)^2}\frac{f\,\bar{Z}(u,-\bar{\omega},-\bar{q})\bar{Z}'(u,\bar{\omega},\bar{q})}{\sqrt{g}\,(\bar{\omega}^2-\bar{q}^2 f g)}\Bigg|_{u_H}^{u_B}. \tag{3.20}$$

In this massless case, we obtain the longitudinal retarded Green's functions from the gravitational fields via the procedure described in section 2.3.2

$$G^R_{J^zJ^z}(\bar{\omega},\bar{q})=-\lim_{\epsilon\to 0}2Nr_H^2\frac{\bar{\omega}^2}{\bar{\omega}^2-\bar{q}^2}\,\frac{\bar{Z}'(\epsilon,\bar{\omega},\bar{q})}{\bar{Z}(\epsilon,\bar{\omega},\bar{q})}\,, \tag{3.21}$$

where the $-\bar{\omega}^2$ factor comes from the definition (3.18), and $\bar{Z}(u,\bar{\omega},\bar{q})$ is the solution obeying ingoing boundary conditions at the horizon: $\bar{Z}(u,\bar{\omega},\bar{q})\sim(1-u)^\gamma$ as $u\to 1$, where $\gamma=-i\bar{\omega}\tilde{d}^{1/3}/4$. Poles of the retarded Green's function are, as described in section 2.2.1, determined by the values of $\bar{\omega}\,(\bar{q})$ for which the solution obeying the ingoing condition at the horizon vanishes at the boundary. The density-density correlation function follows trivially in these gauge-invariant variables $G^R_{J^tJ^t}(\bar{\omega},\bar{q})=\bar{q}^2\,G^R_{J^zJ^z}/\bar{\omega}^2$ and has the same poles as the longitudinal Green's function (3.21). The spectral functions of these operators are then obtained by taking the imaginary part:

$$\chi_{zz}(\bar{\omega},\bar{q})=-2\,\text{Im}\left[G^R_{J^zJ^z}(\bar{\omega},\bar{q})\right]\,,\qquad \chi_{tt}(\bar{\omega},\bar{q})=-2\,\text{Im}\left[G^R_{J^tJ^t}(\bar{\omega},\bar{q})\right]\,, \tag{3.22}$$

with $\chi_{tt}=\bar{q}^2\,\chi_{zz}/\bar{\omega}^2$. At zero temperature and density, the form of the longitudinal spectral function is known analytically [89]:

$$\chi_{zz}(\omega,q)=\frac{N_fN_c}{4\pi}\,\left(\omega^2-q^2\right)\,\Theta\left(\omega^2-q^2\right)\text{sgn}\,\omega\,, \tag{3.23}$$

where Θ is the Heaviside step function.

In the $\bar{m} \neq 0$ case, the coupled equations of motion for bulk fluctuations imply that the dual field theory operators mix and the method to determine the retarded Green's functions is more involved (see Appendix 3.A.1 for the details).

At zero mass, high densities $\omega, q \ll d^{\frac{1}{3}}$ and strictly zero temperature, the dominant pole of the correlators $G^R_{J^t J^t}$ and $G^R_{J^z J^z}$ has the dispersion relation [61, 90]

$$\bar{\omega} = \pm\frac{\bar{q}}{\sqrt{3}} - i\frac{\Gamma\left(\frac{1}{2}\right)}{\Gamma\left(\frac{1}{6}\right)\Gamma\left(\frac{1}{3}\right)}\bar{q}^2 + O\left(\bar{q}^3\right). \tag{3.24}$$

This corresponds to a collective excitation of the system — the holographic zero sound mode. Its speed is equal to that of hydrodynamic sound, and it has an imaginary part $\propto q^2$. In the hydrodynamic limit $\omega, q \ll T$ the dominant pole is a purely imaginary pole with the Fickian diffusion dispersion relation

$$\bar{\omega} = -iD\,\bar{q}^2 + O(\bar{q}^3), \tag{3.25}$$

where the diffusion constant is given by [71, 78]

$$D(\tilde{d}) = \frac{\tilde{d}^{\frac{1}{3}}}{2}\sqrt{1+\tilde{d}^2}\;{}_2F_1\left[\frac{3}{2}, \frac{1}{3}; \frac{4}{3}; -\tilde{d}^2\right]. \tag{3.26}$$

Between these two extreme temperature limits, the poles of the Green's functions are not known analytically.

These results were generalized to the case of a massive hypermultiplet in [64, 78]. The zero sound mode (3.24) persists when the hypermultiplet has a finite mass m, although the dispersion relation is altered to

$$\bar{\omega} = \pm\frac{1}{\sqrt{3}}\left(\frac{1-\mathfrak{m}^2}{1-\mathfrak{m}^2/3}\right)^{1/2}\bar{q} - i\,\frac{\Gamma\left(\frac{1}{2}\right)}{\Gamma\left(\frac{1}{3}\right)\Gamma\left(\frac{1}{6}\right)}\,\frac{(1-\mathfrak{m}^2)^{4/3}}{(1-\mathfrak{m}^2/3)^2}\,\bar{q}^2 + O\left(\bar{q}^3\right), \tag{3.27}$$

where $\mathfrak{m} = \tilde{m}/\sqrt{2}\tilde{\mu} = M_q/\mu$. The real part of the dispersion relation (3.27) was obtained in [64] and the attenuation is derived in Appendix 3.A.2. In the hydrody-

namic limit, there is again a diffusion pole (3.25) whose diffusion constant can be derived via an Einstein relation [78]

$$D(\tilde{d}) = \frac{\tilde{d}^{\frac{1}{3}}}{2}\sqrt{\tilde{d}^2+\cos^6\theta(1)}\int_0^1 du \frac{G(u)^{\frac{3}{2}}}{\cos^3\theta(u)H(u)}\Bigg[1+\tilde{d}\Bigg(\frac{4f(u)u^2\theta'(u)}{G(u)\cos\theta(u)}\frac{\partial}{\partial\tilde{d}}\left[\cos\theta(u)\theta'(u)\right] + \frac{\sin\theta(u)}{\cos^2\theta(u)}\left(3+\frac{4f(u)u^2\theta'(u)^2}{G(u)}\right)\frac{\partial}{\partial\tilde{d}}\sin\theta(u)\Bigg)\Bigg], \tag{3.28}$$

where $G(u)$ and $H(u)$ are defined in Appendix 3.A.1.

At finite hypermultiplet mass, the D3/D7 system has non-trivial bound states analogous to mesons [81]. These bound states are visible as peaks of the spectral function. When $d = 0$, such modes exist only for large enough values of $\tilde{m} \propto M_q/T$ [84, 89, 91–93]. When $d \neq 0$, it seems that necessary conditions for their existence are large values of $\tilde{m}$ and small enough values of q/T and $d^{\frac{1}{3}}/T$ [56, 75, 94–96]. This is outside of the regime of our current interest. A full numerical analysis of the quasinormal modes of the theory when $T = 0$ is given in [97].

3.3 The high density regimes of D3/D7 fundamental matter

In this section, we explore the behavior of the collective modes of the D3/D7 system in the low temperature regime $\tilde{d} \gg 1$ ($T \ll \mu$). Anticipating behavior similar to that observed in a Landau Fermi liquid, we expect the system to exhibit the three regimes shown in figure 1.2, and indeed we do find them. We investigate this by computing numerically the spectral functions and the poles of the Green's functions. We always plot the normalized spectral functions such as $\chi_{zz}\left(\bar{\omega},\bar{q}\right)/2N_fN_cT^2\bar{\omega}^2$: dividing by $\bar{\omega}^2$ has the advantage of reducing the high frequency asymptotics (3.23) to a constant. This normalised quantity is proportional to the density-density spectral function $\chi_{tt}\left(\bar{\omega},\bar{q}\right)/N_fN_cT^2$.

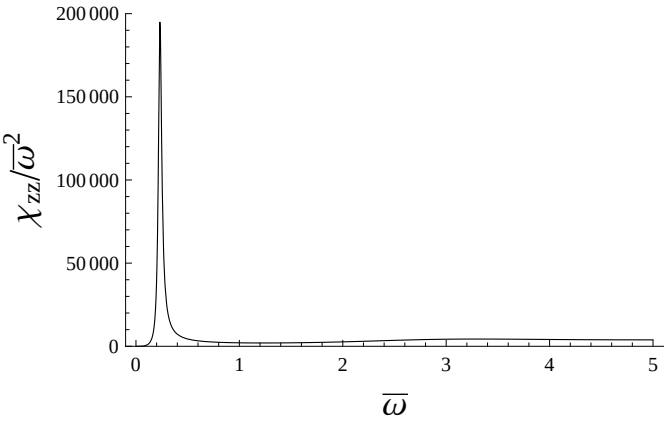

Figure 3.2: The holographic zero sound peak in the collisionless quantum regime. The longitudinal spectral function is shown at $\bar{m} = 0$, $\tilde{d} = 10^6$, $\bar{q} = 0.4$.

3.3.1 The collisionless quantum regime

The collisionless quantum regime corresponds to $\bar{\omega}$ and $\bar{q}$ being in the interval

$$\tilde{d}^{-1/3} \ll \bar{\omega}, \bar{q} \ll 1\,, \tag{3.29}$$

see equation (3.9) and figure 1.2. We start by fixing a large value of $\tilde{d}$, for example $\tilde{d} = 10^6$, and computing the longitudinal spectral function at a fixed momentum $\bar{q}$ in the interval (3.29), e.g. $\bar{q} = 0.4$. An isolated peak corresponding to the holographic zero sound mode in this low temperature regime is clearly visible in figure 3.2. Thus the zero sound mode persists at low but non-zero temperatures — contrary to the assertion in [71] that an infinitesimal temperature in the field theory will lead to diffusive transport.

By varying $\bar{q}$ (while keeping $\tilde{d}^{\frac{1}{3}}$ fixed), we can determine the dispersion relation of this collective mode at low temperature. Figure 3.3 shows the real and imaginary parts of the zero sound dispersion relation $\bar{\omega} = \bar{\omega}(\bar{q})$ at $\bar{m} = 0$, $\tilde{d} = 10^6$. Our numerical results are shown as dots and the solid lines correspond to the zero-temperature dispersion relation (3.24). We observe that in the collisionless quantum regime (3.29) the real part of the zero sound dispersion relation shows no noticeable deviation from the zero-temperature result (3.24). The imaginary part shows a close

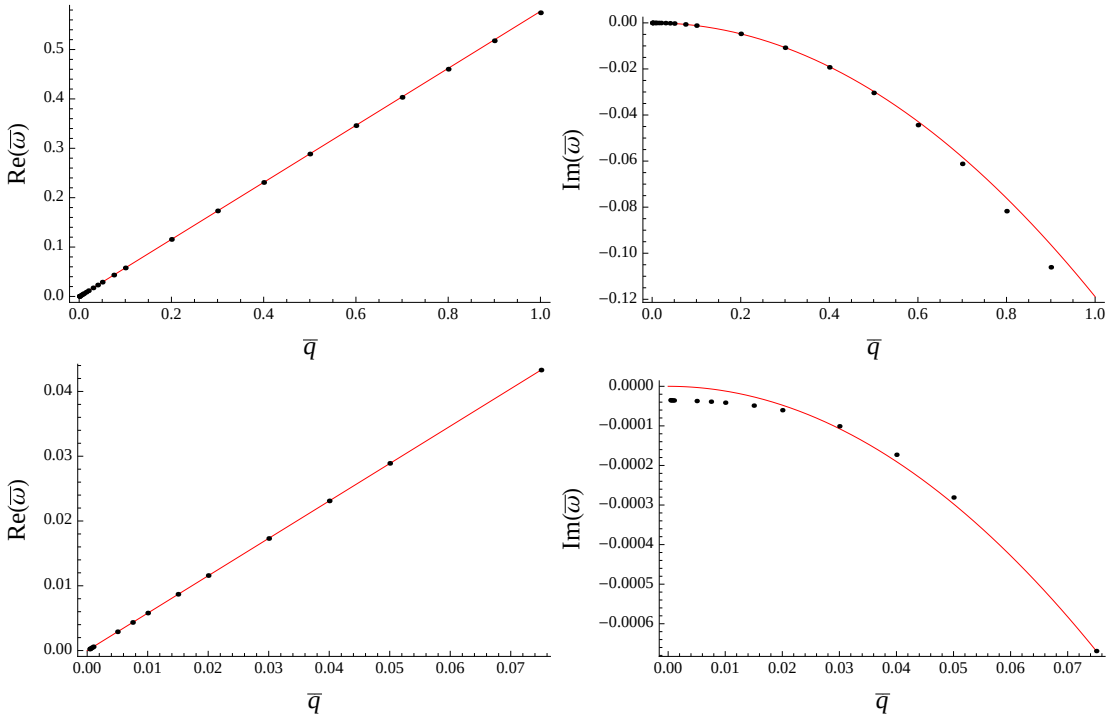

Figure 3.3: The dispersion relation of the dominant pole at $\bar{m} = 0$, $\tilde{d} = 10^6$. Dots show numerical results at low T and the solid lines are the analytic result (3.24) at $T = 0$.

agreement with the zero-temperature result over the parameter range (3.29). Visible deviations from the zero-temperature result are apparent at very small ($\bar{q} \lesssim 0.02 \sim \tilde{d}^{-1/3}$) and very large ($\bar{q} \gtrsim 0.7$) momenta close to the boundaries of the interval (3.29). Note that although the imaginary part appears to be tending to a constant at small $\bar{q}$, this is only true up until the crossover to the hydrodynamic regime occurs, after which we obtain a diffusive mode. This crossover will be discussed in detail later in this section. At large momentum, the system is entering the low temperature, low density regime $\tilde{d}^{-1/3} \ll 1 \ll \bar{\omega}, \bar{q}$ (i.e. $\omega, q \gg d^{\frac{1}{3}} \gg T$), where the zero sound mode becomes very short-lived as the corresponding pole recedes deep into the complex plane. As shown in figure 3.4, the zero sound peak in the spectral function gradually disappears in this regime, and the spectral function approaches the $d = 0$, $T = 0$ result (3.23).

At finite hypermultiplet mass, the results are qualitatively similar.[7] The lon-

[7]Technically, the massive case is more complicated as it involves solving a pair of coupled differential equations, with coefficients that depend upon the numerically-computed embedding

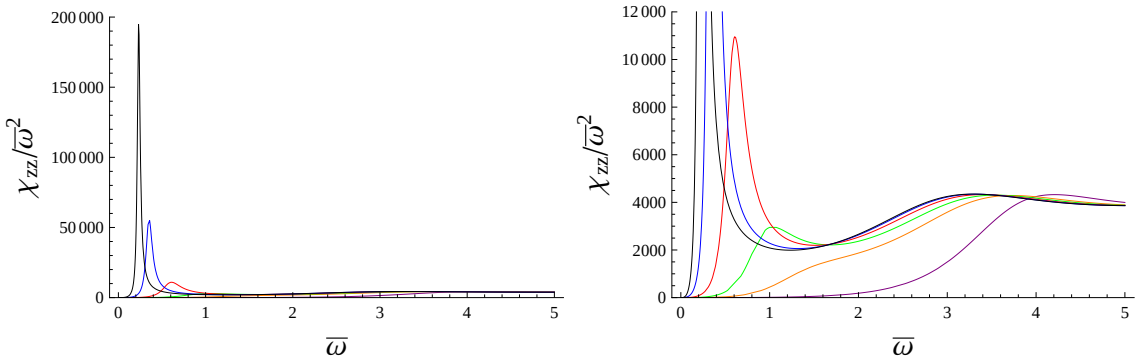

Figure 3.4: The longitudinal spectral function at $\bar{m} = 0$, $\tilde{d} = 10^6$. Moving from left to right corresponds to increasing momentum: $\bar{q} = 0.4$ (black), 0.6 (blue), 1.0 (red), 1.5 (green), 2.0 (orange), 3.0 (purple).

gitudinal spectral functions show a lone peak[8] (similar to the one shown in figure 3.2) for values of $\bar{\omega}$ in the range (3.29). As shown in figure 3.5, the real part of the dispersion relation is essentially identical to the zero-temperature result (3.27), and the imaginary part deviates from the zero-temperature dependence given in (3.27) only at the boundaries of the interval (3.29).

It is interesting to note that the zero sound mode exists for all (numerically accessible) values of $\bar{m}$, including those for which $\tilde{m} \propto M_q/T \ll 1$. Thus the high density and low temperature interval in which the $T = 0$ zero sound mode persists is the same as in the massless case (given by the inequality (3.29)), i.e. we do not have to take the limit $M_q/T \to \infty$ which would be the genuine zero temperature limit of the entire system.

3.3.2 The collisionless thermal regime

Having established the existence of a holographic zero sound mode at finite temperature, we now investigate the dependence of its velocity and attenuation on temperature, density, momentum and mass. The collisionless thermal regime corresponds

function. Due to numerical instability, we were not able to obtain accurate results for $\tilde{d} > 10^5$ and masses ouside the interval $0.002 \lesssim \bar{m} \lesssim 1.68$ (at $\tilde{d} = 10^5$). We believe this limitation demonstrates the lack of our numerical skills rather than an effect of any physical significance.

[8]Peaks corresponding to "meson" bound states may exist for higher values of $\bar{\omega}$. We have not investigated this issue.

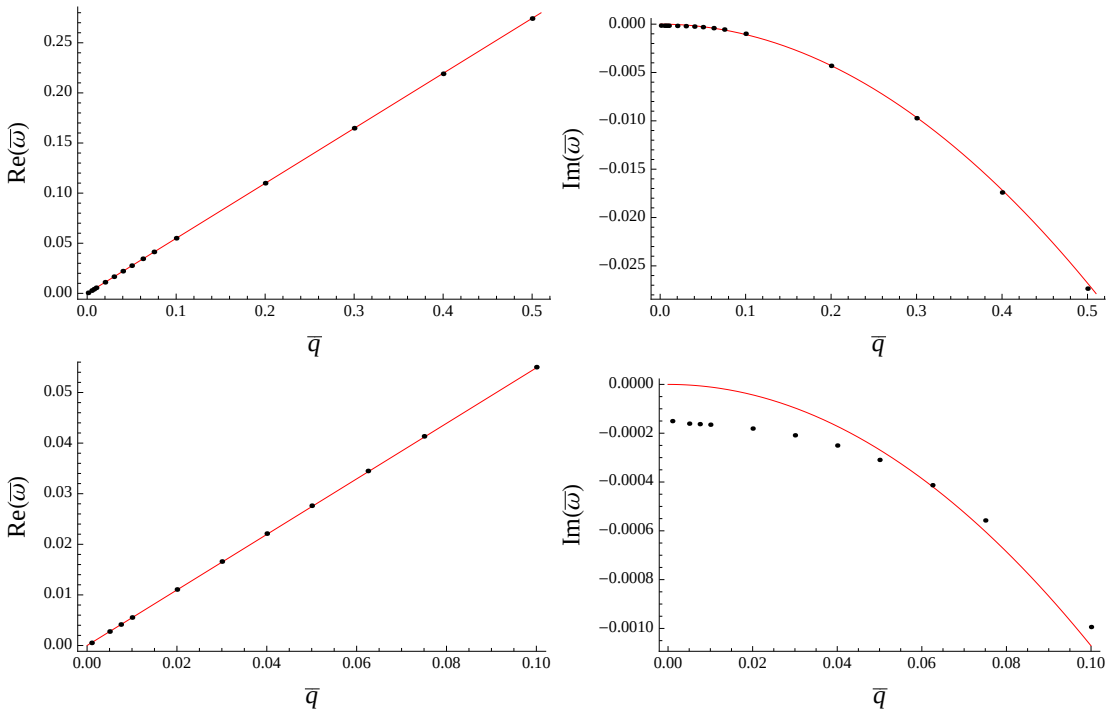

Figure 3.5: The holographic zero sound dispersion relation for $\bar{m} = 0.76$, $\tilde{d} = 10^5$. Dots show numerical results at low T and the solid lines show the analytic result (3.27) at $T = 0$.

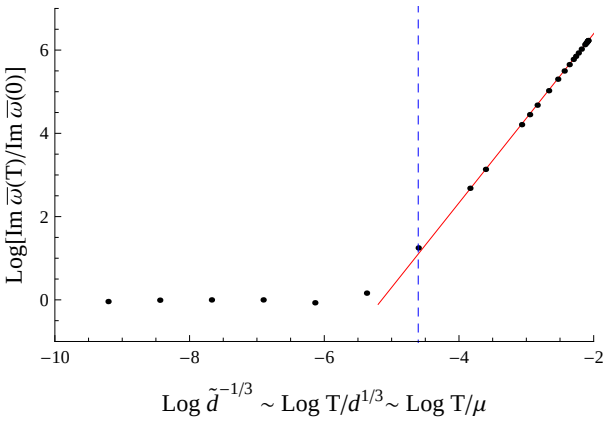

Figure 3.6: The imaginary part of the holographic zero sound dispersion relation at low temperatures showing the transition between the collisionless quantum (left) and collisionless thermal (right) regimes. The points are the numerical data, the dashed line denotes $\bar{q} = \tilde{d}^{-1/3} \sim T/\mu$ and the solid line is the best-fit straight line for the $T/\mu \gtrsim \bar{q} = 0.01$ points showing the $\sim T^2$ scaling of the attenuation in the collisionless thermal regime. The region corresponding to the hydrodynamic regime at even higher temperature $T/\mu \gg \sqrt{\bar{q}} = 0.1$ is not shown in the figure.

to excitations with $\bar{\omega}$ and $\bar{q}$ in the interval

$$\tilde{d}^{-2/3} \ll \bar{\omega}, \bar{q} \ll \tilde{d}^{-1/3} \,. \tag{3.30}$$

As discussed in section 3.3.1, the imaginary part of the dispersion relation $\bar{\omega} = \bar{\omega}(\bar{q})$ for the zero sound shows significant deviations from the zero temperature $\sim \bar{q}^2$ behavior in the region $\bar{q} \lesssim \tilde{d}^{-1/3}$. Investigating this further, one can see that in the interval $\tilde{d}^{-2/3} \lesssim \bar{q} \lesssim \tilde{d}^{-1/3}$ the imaginary part $\mathrm{Im}\,\bar{\omega}$ is essentially independent of $\bar{q}$. This is the characteristic behavior of the sound attenuation coefficient of a Landau Fermi liquid in the collisionless thermal regime (see Table 3.1). To determine the temperature dependence of the attenuation in this regime, in figure 3.6 we plot the logarithm of the ratio $\mathrm{Im}\,\bar{\omega}(T)/\mathrm{Im}\,\bar{\omega}(0)$ versus the logarithm of $\tilde{d}^{-1/3} \sim T/\mu$ at fixed $\bar{q} = 0.01$. In the collisionless quantum regime, the attenuation is essentially temperature-independent, whereas in the collisionless thermal regime it scales as $\sim T^2$. The transition occurs at $\bar{q} \sim \tilde{d}^{-1/3}$. This is fully compatible with LFL behavior (see Table 3.1 and figure 1.3). Figure 3.6 should be compared to the transition between regions III and II in figure 1.3.

At non-zero hypermultiplet mass the results are qualitatively the same and the plots for $\bar{m} = 0.76, 1.68$ are similar to figure 3.6. We do not show these plots for conciseness.

Another comparison with Landau Fermi liquid theory can be made by plotting the attenuation as a function of (real) frequency. As shown in figure 3.1 and Table 3.1, in the frequency dependence of the acoustic attenuation, the transition from the collisionless thermal regime to the collisionless quantum regime is characterized by a change of scaling from $\arg(q) \propto 1/\omega$ to $\arg(q) \propto \omega$ at $\bar{\omega} \sim T/\mu$. We can study this region in the D3/D7 system by fixing the temperature (at e.g. $\tilde{d} = 10^4$) and tracing the Green's function's pole in the complex momentum plane while varying the real frequency $\bar{\omega}$. The results are shown in figure 3.7 for the massless case. In

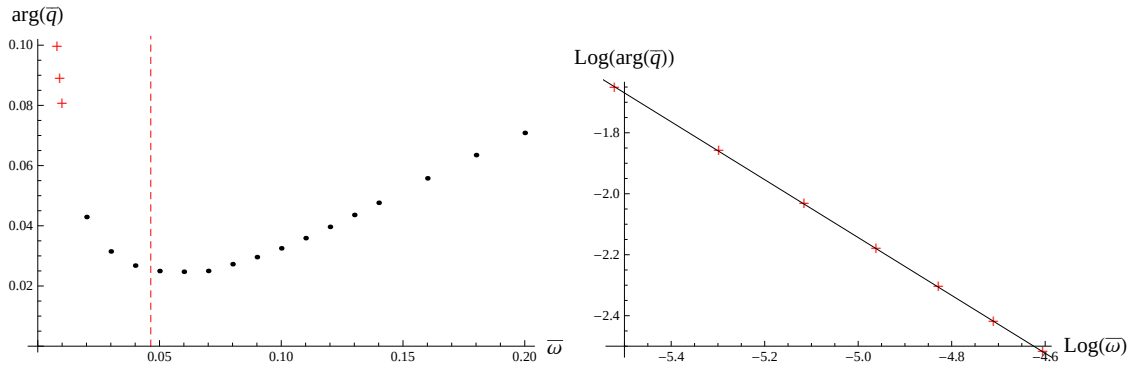

Figure 3.7: The frequency dependence of the D3/D7 acoustic mode when $\bar{m} = 0$, $\tilde{d} = 10^4$ in the collisionless regimes. The dots and crosses are our numerical results, the dashed line is $\bar{\omega} = \pi T/d^{1/3} \sim T/\mu$, and the solid line shows the best-fit straight line with gradient $\alpha \approx -0.95$. The points on the left of the left hand plot correspond to the rightmost points on the right hand plot.

the collisionless quantum regime, the points follow a straight line with gradient 1. In the collisionless thermal regime, for a region where there is a power law dependence $\arg(\bar{q}) \propto \bar{\omega}^{\alpha}$, the best fit value of α turns out to be $\alpha \approx -0.95$, which is sufficiently close to the LFL value of -1. Figure 3.7 can be compared to regions II and III in figure 3.1. As we approach the hydrodynamic regime, the power law dependence is lost as expected. We are not able to explore the acoustic mode in region I due to limitations of the probe brane approximation, as explained in the introduction. The best-fit gradients are the same for non-zero masses $\bar{m} = 0.76, 1.68$ and so they are not shown here for brevity.

3.3.3 The collisionless-hydrodynamic crossover

As the temperature is increased further, the zero sound mode becomes less stable, and the system enters the hydrodynamic regime characterized by

$$0 \leq \bar{\omega}, \bar{q} \ll \tilde{d}^{-2/3} \,. \tag{3.31}$$

The zero sound peak in the spectral function broadens and moves to the origin (see figure 3.8). The real and imaginary parts of the collective mode's dispersion relation

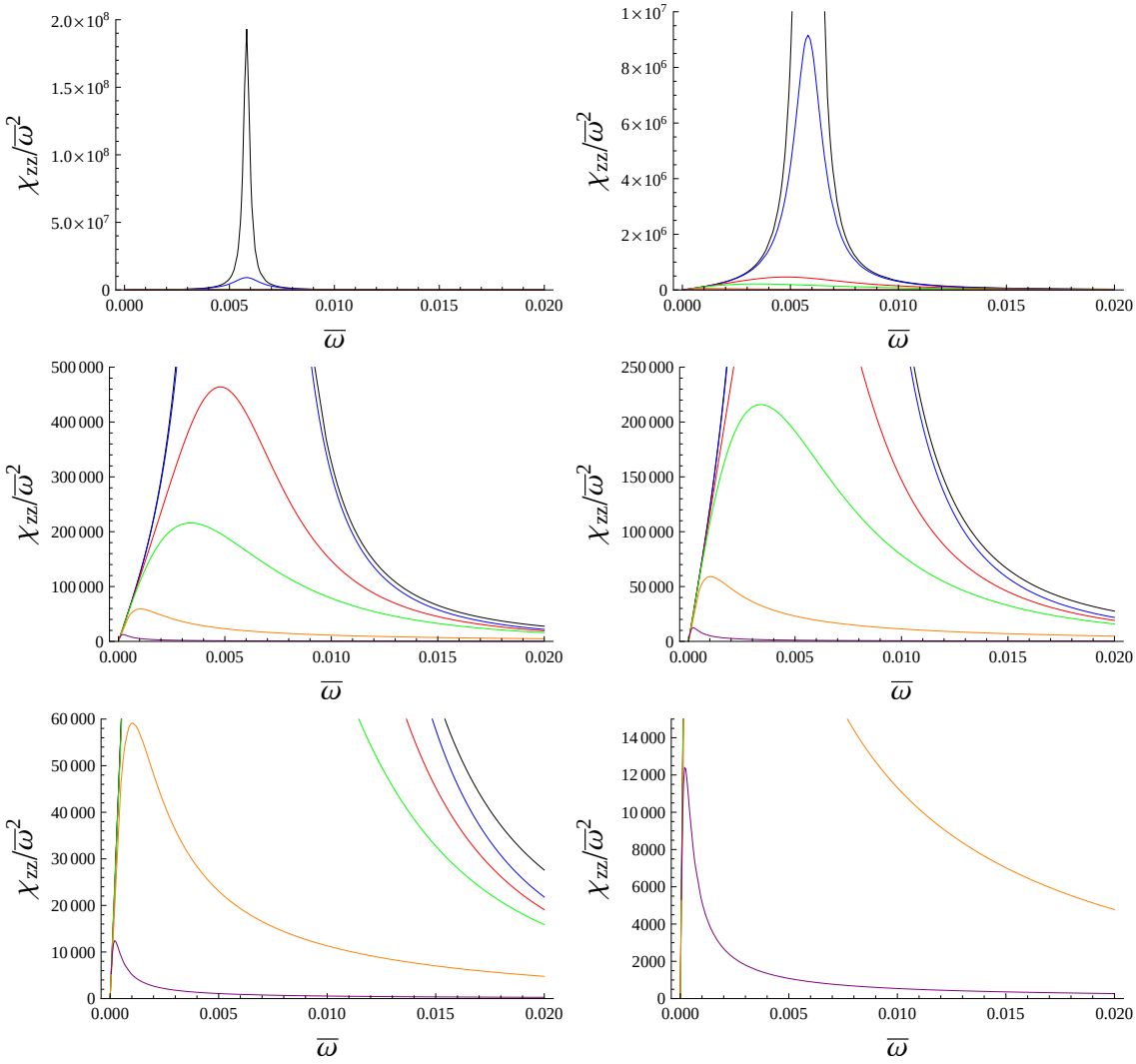

Figure 3.8: The longitudinal spectral functions for $\bar{m} = 0$, $\bar{q} = 0.01$. Moving from the top left corner to the bottom right corner: each subsequent figure zooms into the area of detail in the previous one (note the different scales on the vertical axes). In each figure, moving from the tallest peak to the smallest peak corresponds to raising the temperature: $\tilde{d} = 10^5$ (black), 10^4 (blue), 10^3 (red), 500 (green), 100 (orange), 10 (purple).

as functions of temperature are shown in figure 3.9 for massless and massive hypermultiplets. The real part decreases with increasing temperature until it becomes exactly zero at $T = T_{cross}$, and the mode ceases to propagate. The magnitude of the imaginary part increases until $T = T_{cross}$, then decreases again. For $T > T_{cross}$, the mode is purely diffusive, approaching at high temperatures the known analytic result (3.25) for the hydrodynamic charge density diffusion mode. The transition occurs at $\bar{q} \sim \tilde{d}^{-2/3}$, as we will shortly show.

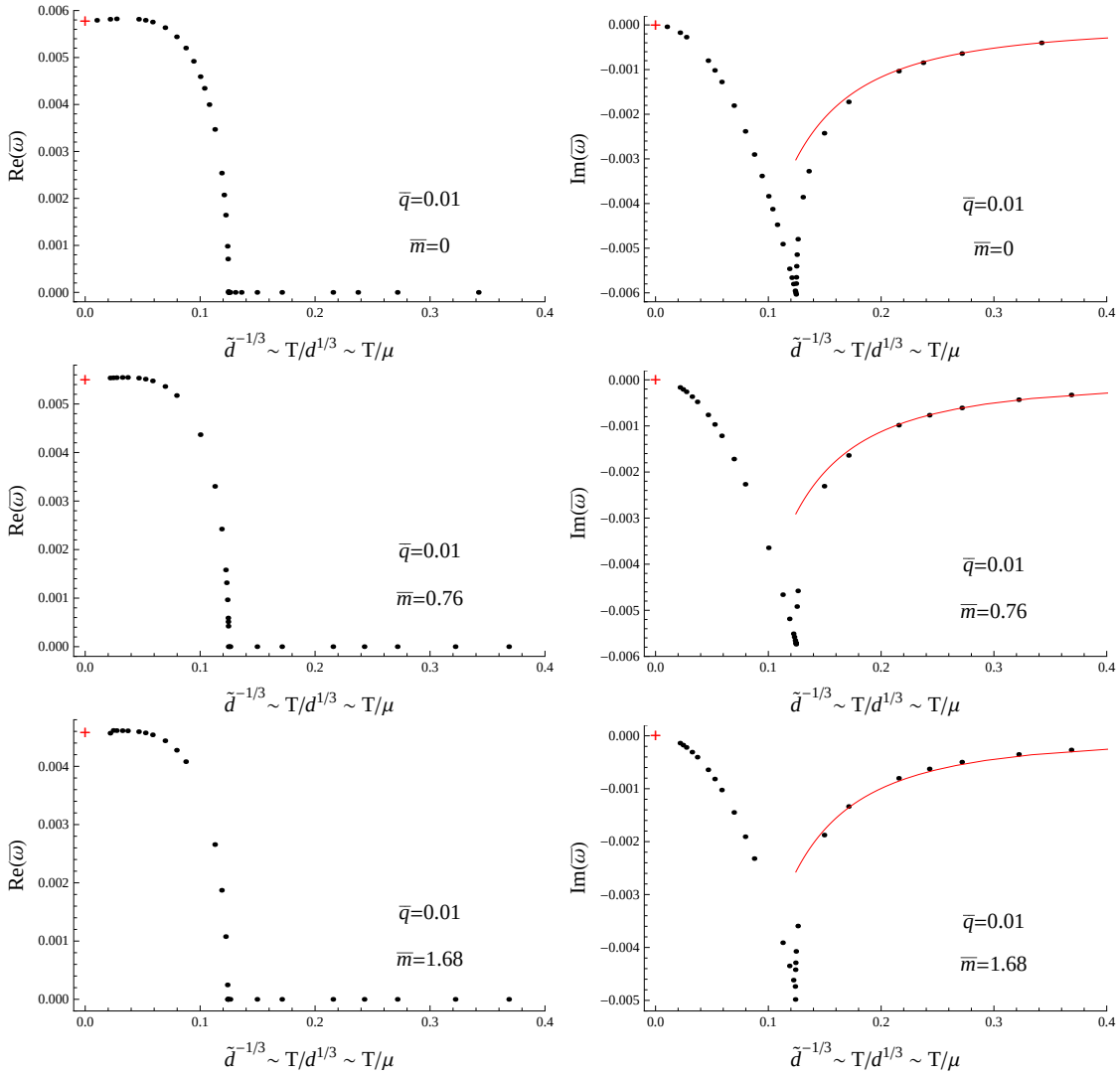

Figure 3.9: The temperature dependence of the real and imaginary parts of the dominant collective mode's dispersion relation at $\bar{q} = 0.01$ and $\bar{m} = 0; 0.76; 1.68$. Dots show the numerical results at low T, the crosses show the $T = 0$ zero sound results (3.24) and (3.27), and the solid lines show the analytic diffusion result (3.25).

The dynamics of this collisionless/hydrodynamic transition are best exhibited by the motion of the relevant poles in the complex frequency plane (see figure 3.10). As the temperature is raised, the two zero sound poles (corresponding to $\mathrm{Re}\,\bar{\omega} = \pm v_s \bar{q}$) move deeper into the complex plane, approximately along the circle $|\bar{\omega}| = \bar{q}/\sqrt{3}$, until they collide on the imaginary axis and form two purely imaginary poles. (For the parameters used in figure 3.10, this happens at $\tilde{d} = \tilde{d}_{cross} \approx 519$, i.e. in the region $\bar{q} \sim \tilde{d}^{-2/3}$.) One of these new poles recedes quickly into the complex plane as the temperature is raised further, while the other approaches the real axis and becomes the hydrodynamic diffusion mode (3.25) at high temperatures. This explains the temperature dependence of the collective mode dispersion relation in figure 3.9 and the behavior of the density-density spectral function in figure 3.8. At non-zero hypermultiplet mass, the transition is qualitatively similar, although the transition temperature decreases slightly with increasing mass ($\tilde{d}_{cross} \approx 520, 530$ for $\bar{m} = 0.76, 1.68$, respectively).

The phenomenon in which two poles on the imaginary axis collide and generate two propagating modes persists at lower densities as well (in fact, it was first observed in figure 3(c) of [56] for $\tilde{d} = 2$ which is the highest value of $\tilde{d}$ studied in that paper), although in the low density regime the pole collision occurs deep in the complex plane and the propagating mode is short-lived. The pole merger has also been recently observed and correctly identified as the hydrodynamic/collisionless transition involving the zero sound in a 2+1-dimensional theory in [67].

In Landau Fermi liquid theory, the collisionless-hydrodynamic transition occurs when $\omega\,\tau \sim 1$ and $q\,l_{\mathrm{mfp}} \sim 1$, where τ and l_{mfp} are the mean free time and mean free path, respectively, of the quasiparticles in the vicinity of the Fermi surface supporting the collective mode. Defining the collisionless/hydrodynamic transition in the D3/D7 holographic model as the event in which the two poles in figure 3.10 merge, we can cast the corresponding parameters in the familiar language of the Landau theory by introducing an effective $\tau = 1/|\omega_{\mathrm{cross}}|$ and $l_{\mathrm{mfp}} = 1/q_{\mathrm{cross}}$, and

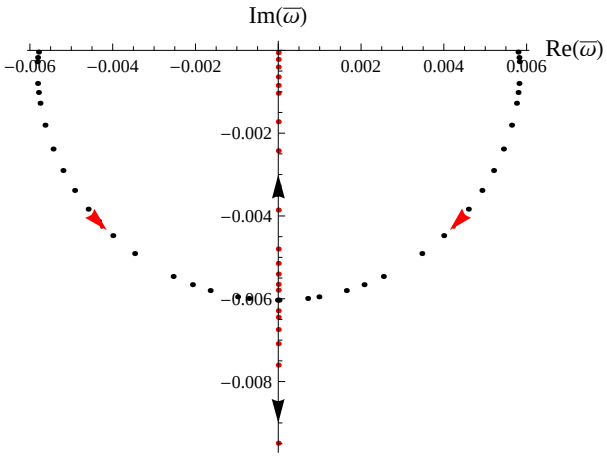

Figure 3.10: The positions of the dominant poles of the density-density correlator in the complex frequency plane at $\bar{m} = 0$, $\bar{q} = 0.01$ as the temperature is changed. The low temperature limit corresponds to the points furthest from the imaginary axis. As the temperature is increased, the points move inwards towards the imaginary axis where they collide to form two poles that move up and down the imaginary axis respectively. An animated version of this figure, and the corresponding animations for $\bar{m} = 0.76, 1.68$, are available at `http://www.physics.ox.ac.uk/users/Davison/D3D7animations.html`.

computing their temperature dependence. Assuming a simple power-dependence of the form

$$l_{\text{mfp}} \sim \tau \propto d^{-1/3} \left(\frac{T}{d^{1/3}} \right)^{\alpha}, \tag{3.32}$$

we expect a plot of $\log(\bar{q}_{cross})$ or $\log(|\bar{\omega}_{cross}|)$ versus $\log(\tilde{d}^{1/3}_{cross})$ to yield a straight line of gradient α. These plots are shown in figure 3.11 for the massless case. The numerical results are clearly consistent with a simple power law dependence. The

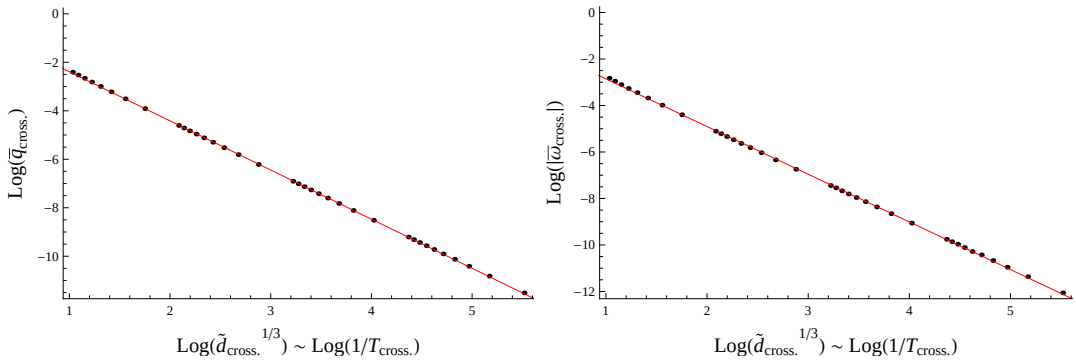

Figure 3.11: The temperature dependence of the collisionless-hydrodynamic crossover value of frequency and momentum for $\bar{m} = 0$. The points are our numerical results and the solid lines are the best-fit straight lines which both have gradient -2.0.

slope of the best-fit straight line is -2.0 in each case, which leads to the result

$$l_{\rm mfp} \sim \tau \sim d^{1/3}\, T^{-2} \sim \mu\, T^{-2}, \tag{3.33}$$

as in a Landau Fermi liquid [34]. For non-zero masses $\bar{m} = 0.76, 1.68$, the best-fit slopes are unchanged and so we do not show the results for brevity.

3.4 Summary and discussion

In this chapter, we have investigated the properties of the holographic zero sound mode and the fundamental matter diffusion mode in the D3/D7 system at non-zero temperature and high density. Similarly to the case of an ordinary Landau Fermi liquid, three regimes corresponding to different powers of the parameter $T/\mu \ll 1$ can be identified, with the modes having a distinctively different temperature and momentum dependence in each regime. In the collisionless quantum regime, the zero sound attenuation is essentially temperature-independent and proportional to the square of the momentum whereas in the collisionless thermal regime, the attenuation is momentum-independent and scales as the square of the temperature (see Table 3.1, figures 1.3 and 3.1, and the corresponding D3/D7 results in figures 3.6 and 3.7). The crossover transition between the two regimes is clearly visible in figures 3.6 and 3.7. In the hydrodynamic regime of a Landau Fermi liquid, the acoustic attenuation is proportional to the square of the momentum and scales as $\sim 1/T^2$. Restricted by the probe brane approximation, we are unable to study the acoustic collisionless-hydrodynamic crossover transition in the D3/D7 theory directly.[9] However, we do observe this transition in the density-density correlator as the motion of the lowest-lying poles in the complex frequency plane leads from the zero sound-dominated regime to the diffusion-dominated one as the parameter T/μ is increased (figure 3.10). The transition occurs at $\omega, q \sim T^2/\mu$, as if it were supported by Landau

[9] See [98] for some work on going beyond the probe approximation.

Fermi liquid quasiparticles with a lifetime $\sim 1/T^2$. These results do not qualitatively change as the mass of the fundamental matter in the field theory is varied, at least in the range $0 \leq \bar{m} \leq 1.68$ which we have studied numerically.

The main conclusion of our study is that the holographic zero sound of the D3/D7 system at finite temperature behaves exactly as the usual Landau zero sound. This is rather difficult to reconcile, at least within the standard Landau Fermi liquid paradigm, with two other properties of the system: the atypical temperature dependence of the specific heat ($c_V \propto T^6/d$ instead of $c_V \propto Td^{2/3}$) and the apparent absence of a singularity when $|\vec{q}| = 2q_F$ at zero frequency in the density-density correlator at zero temperature. One may add to these apparent discrepancies a finite zero-temperature limit of the entropy density [61]. Resolution of the above mentioned puzzles may involve modifications of the gravitational background considered, possibly in the spirit of [99]. On the other hand, the absence of the singularity in the zero frequency density-density correlator at $2k_F$ may have a simpler explanation[10]: assuming the validity of the Luttinger theorem[11], $n_q \sim k_F^3$, and therefore $q \sim 2k_F \sim n_q^{1/3} \sim d^{1/3}\lambda^{1/6}$, since $d \sim n_q/\sqrt{\lambda}$. This means that the corresponding $\bar{q}$ is large, $\bar{q} \sim \lambda^{1/6}$, and is not visible in the correlators in the probe brane limit. It is also possible that the $\sim T^6$ behavior of the specific heat is a genuine property of the considered microscopic model in the approximation described by the probe brane limit, there is no Fermi surface, and we are dealing with a new type of quantum liquid. This point of view, initially advocated in [61], is not in contradiction with the findings presented in this chapter.

We note that the effect of a magnetic field on the holographic zero sound mode of the D3/D7 theory at $T = 0$ has recently been studied [102]. One finds that the mode is gapped by the magnetic field, in accordance with Kohn's theorem for non-relativistic, interacting fermions [102, 103]. All known properties of the excitation

[10] We are indebted to Andrei Parnachev and Pavel Kovtun for valuable discussions on this issue.

[11] We note that recent work suggests that the Luttinger theorem may be violated in some theories where the bulk electric field is sourced by a black hole horizon, as is the case here [100, 101].

spectrum of this theory may be described by an LFL with infinitely large interaction terms [102].

There are other examples of theories with a dual holographic description which support a sound mode at $T = 0$. It would be interesting to determine whether the results presented here hold (qualitatively) in those cases also. The first class of such theories are probe brane theories [65–69]. Of particular interest are the D4/D8/$\overline{\text{D8}}$ theory, whose sound mode has a different dispersion relation from Landau Fermi liquid theory at $T = 0$, and the D3/D3 theory which is (1+1)-dimensional and hence to which Landau Fermi liquid theory does not apply. A qualitatively different holographic theory is the AdS_4 Einstein-Maxwell theory at finite density [70, 104–108]. In this theory, non-trivial density-dependent physics is possible via the strong coupling of the charge density to the energy density of the field theory. This is in contrast to probe theories, where the DBI coupling between the charge density gives rise to interesting density-dependent physics, despite the fact that the coupling of this sector to the overall energy density is suppressed via the probe limit. These are very different mechanisms and hence it would be very interesting to see if the low temperature sound mode in the Einstein-Maxwell theory behaves similarly to the corresponding sound mode in the D3/D7 theory. This theory will be studied in the following chapter.

Finally, it would be very interesting to generalise the approach to zero sound proposed in [90] to non-zero temperatures. In this approach, which provides an alternative way to derive the zero sound dispersion relation (3.24), one writes a low-energy, semi-holographic effective action for the zero sound mode in which its dissipative part is governed by the coupling to a one dimensional CFT. This is motivated by the observation that when $T = 0$, near the horizon of the bulk spacetime (i.e. at low energies in the field theory, according to the discussion in section 1.2.2) the equation of motion of the gauge-invariant, longitudinal mode reduces to that of a scalar in AdS_2. A similar result has subsequently been found for other probe brane

fields in this theory [97]. This suggests that at low energies there is a locally conformal theory governing the dynamics of the holographic quantum liquid (see [102] for further evidence for this coming from studying the correlators of the transverse current). This is quite different from Fermi liquid theory.

3.A Appendices

3.A.1 Fluctuation equations when $m \neq 0$

When the hypermultiplet has a non-zero mass, the bulk fluctuations of the embedding scalar and the longitudinal gauge field components are coupled and their solutions are no longer independent. In the field theory, this corresponds to mixing of the dual operators. An appropriate systematic formalism which we follow here was introduced in section 2.3. It will be convenient to work with the gauge-invariant variables

$$\varphi\left(u,\bar{\omega}\right)=r_H\tilde{\phi}\left(u,\bar{\omega}\right)\,,\qquad \bar{E}\left(u,\bar{\omega}\right)=-i\left[\bar{\omega}\tilde{a}_z(u,\bar{\omega})+\bar{q}\tilde{a}_t(u,\bar{\omega})\right]. \tag{3.34}$$

Note that the definition of $\bar{E}$ differs from the massless case (3.18) by a factor of $-i$. The coupled system of equations of motion for the variables $\bar{E}$ and φ is

$$\begin{aligned}
&\frac{d}{du}\left(\frac{f(u)\cos^3\theta}{\sqrt{G(u)}D(u,\bar{\omega})}\left[H(u)\bar{E}'(u,\bar{\omega})+4i\bar{q}f(u)u^2\theta'(u)A(u)\varphi'(u,\bar{\omega})\right.\right. \\
+\;& \left.\left.3i\bar{q}\tan\theta A(u)G(u)\varphi(u,\bar{\omega})\right]\right)+\frac{\tilde{d}^{\frac{2}{3}}\cos^3\theta H(u)}{4uf(u)\sqrt{G(u)}}\bar{E}(u,\bar{\omega}) \\
+\;& \frac{\tilde{d}^{\frac{2}{3}}\cos^3\theta uA(u)\theta'(u)}{\sqrt{G(u)}}i\bar{q}\varphi(u,\bar{\omega})=0,
\end{aligned} \tag{3.35}$$

and

$$
\begin{aligned}
&\frac{d}{du}\Bigg(\frac{f(u)\cos^3\theta}{u\sqrt{G(u)}D(u,\bar\omega)}\Big[\left(\bar\omega^2-\bar q^2 f(u)B(u)\right)\varphi'(u,\bar\omega) \qquad (3.36)\\
-\;& 4i\bar q f(u)u^3\theta'(u)A(u)\bar E'(u,\bar\omega)-3\tan\theta\theta'(u)G(u)\left(\bar\omega^2-\bar q^2 f(u)\right)\varphi(u,\bar\omega)\Big]\Bigg)\\
+\;& \frac{3\cos^2\theta\sin\theta f(u)A(u)\sqrt{G(u)}}{D(u,\bar\omega)}i\bar q\bar E'(u,\bar\omega)\\
-\;& \frac{\cos^3\theta u A(u)\theta'(u)\tilde{d^{\frac{2}{3}}}}{\sqrt{G(u)}}i\bar q\bar E(u,\bar\omega)+\frac{3\cos^2\theta\sin\theta f(u)\theta'(u)\sqrt{G(u)}\left(\bar\omega^2-\bar q^2 f(u)\right)}{uD(u,\bar\omega)}\varphi'(u,\bar\omega)\\
+\;& \frac{\cos^3\theta\tilde{d^{\frac{2}{3}}}\left(\bar\omega^2-\bar q^2 f(u)B(u)\right)}{4u^2 f(u)\sqrt{G(u)}}\varphi(u,\bar\omega)-\frac{9\cos\theta\sin^2\theta A(u)^2\sqrt{G(u)}\bar\omega^2}{D(u,\bar\omega)}\varphi(u,\bar\omega)\\
+\;& \frac{3\left(3\cos^3\theta-2\cos\theta\right)\sqrt{G(u)}}{4u^3}\varphi(u,\bar\omega)=0,
\end{aligned}
$$

where the coefficients are given by

$$
\begin{aligned}
&A(u)=\frac{A_t'(u)}{r_H}\,,\qquad B(u)=1-4u^3A(u)^2\,,\qquad G(u)=1+4u^2f(u)\theta'(u)^2-4u^3A(u)^2,\\
&H(u)=1+4f(u)u^2\theta'(u)^2\,,\qquad D(u,\bar\omega)=\bar\omega^2H(u)-\bar q^2f(u)G(u),
\end{aligned}
$$

and primes denote derivatives with respect to u.

The relevant part of the off-shell action quadratic in longitudinal fluctuations is

$$
\begin{aligned}
S^{(2)}_{\text{long.}} \;=\;& -Nr_H^2\int_0^1 du\frac{d\omega dq}{(2\pi)^2}\Bigg\{-\frac{\cos^3\theta f(u)H(u)}{\sqrt{G(u)}D(u,\bar\omega)}\,\bar E'(u,-\bar\omega)\,\bar E'(u,\bar\omega) \qquad (3.37)\\
&-\frac{8\cos^3\theta f(u)^2u^2\theta'(u)A(u)}{\sqrt{G(u)}D(u,\bar\omega)}i\bar q\,\bar E'(u,-\bar\omega)\,\varphi'(u,\bar\omega)\\
&-\frac{\cos^3\theta f(u)\left(\bar\omega^2-\bar q^2f(u)B(u)\right)}{u\sqrt{G(u)}D(u,\bar\omega)}\,\varphi'(u,-\bar\omega)\,\varphi'(u,\bar\omega)\\
&+\frac{6\cos^2\theta\sin\theta f(u)A(u)\sqrt{G(u)}}{D(u,\bar\omega)}i\bar q\,\varphi(u,-\bar\omega)\,\bar E'(u,\bar\omega)\\
&+\frac{6\cos^2\theta\sin\theta f(u)\theta'(u)\sqrt{G(u)}\left(\bar\omega^2-\bar q^2f(u)\right)}{uD(u,\bar\omega)}\,\varphi(u,-\bar\omega)\,\varphi'(u,\bar\omega)\\
&+\text{non-derivative terms}\Bigg\},
\end{aligned}
$$

where $N = N_f T_{D7} V_{S^3}$. The equations of motion and the action are written in the form that allow one to apply the recipes of section 2.3 directly. To obtain the retarded Green's functions, we solve the coupled system of equations (3.35) and (3.36) with incoming wave boundary conditions at the horizon and combine with the appropriate factors from the action (3.37) as described in section 2.3.

3.A.2 Holographic zero sound attenuation when $T = 0$ and $m \neq 0$

In this appendix we derive the formula for the zero sound attenuation at finite hypermultiplet mass following the approach of Ref. [64]. Note that our notation is different from that used there. At zero temperature and non-zero mass, it will be convenient to use the coordinate system in which the background metric takes the form

$$ds_{10}^2 = \frac{r^2}{R^2}\left(-dt^2 + d\vec{x}^2\right) + \frac{R^2}{r^2}\left(d\rho^2 + \rho^2 ds_{S^3}^2 + d\mathcal{R}^2 + \mathcal{R}^2 d\phi^2\right),$$

where $r^2 = \rho^2 + \mathcal{R}^2$. The background DBI action is given by

$$S_{\text{fund.}} = -N \int_0^\infty d\rho\, d^4x\, \rho^3 \sqrt{1 + \mathcal{R}'(\rho)^2 - A_t'(\rho)^2},$$

where $\mathcal{R}$ is the embedding coordinate of the D7-branes. The background gauge field and embedding coordinate are determined by two conserved charges c and d via

$$A_t(\rho) = \frac{R^2}{6} d \left(d^2 - c^2\right)^{-\frac{1}{3}} \mathcal{B}\left[\frac{\rho^6}{\rho^6 + d^2R^{12} - c^2R^{12}}; \frac{1}{6}, \frac{1}{3}\right],$$
$$\mathcal{R}(\rho) = \frac{R^2}{6} c \left(d^2 - c^2\right)^{-\frac{1}{3}} \mathcal{B}\left[\frac{\rho^6}{\rho^6 + d^2R^{12} - c^2R^{12}}; \frac{1}{6}, \frac{1}{3}\right],$$

where d is the density of fundamental matter and $\mathcal{B}$ is the incomplete beta function. The mass and chemical potential are given by the asymptotic values

$$A_t\left(\rho \to \infty\right) = r_H\, \tilde{\mu}, \qquad \mathcal{R}\left(\rho \to \infty\right) = \frac{r_H}{\sqrt{2}}\, \tilde{m},$$

and are related to the constants d and c via

$$c = r_H^3 \gamma \frac{\tilde{m}}{\sqrt{2}} \left(\tilde{\mu}^2 - \tilde{m}^2/2\right), \qquad d = r_H^3 \gamma \tilde{\mu} \left(\tilde{\mu}^2 - \tilde{m}^2/2\right),$$

where

$$\gamma = \left(\frac{R^2}{6} \mathcal{B}\left[\frac{1}{6}, \frac{1}{3}\right]\right)^{-3}.$$

The equations of motion for the fluctuations of the embedding scalar $\delta\mathcal{R}$ and the fluctuations of the gauge-invariant combination $\delta\mathcal{A} \equiv R^2 \omega a_z + R^2 q a_t$ are coupled.[12] In the near-horizon limit $\rho \to 0$, the solutions take the form

$$\delta\mathcal{A} = A\, \rho\, e^{\pm i\Omega/\rho}, \qquad \delta\mathcal{R} = B\, \rho\, e^{\pm i\Omega/\rho}, \tag{3.38}$$

where $\Omega = R^2 \omega \sqrt{1 - c^2/d^2}$ and the upper sign in the exponent corresponds to the ingoing boundary condition. In the small frequency limit ($\Omega/\rho \ll 1$), the solutions (3.38) can be expanded as

$$\delta\mathcal{A} = \pm i\Omega A + A\rho + \cdots, \qquad \delta\mathcal{R} = \pm i\Omega B + B\rho + \cdots. \tag{3.39}$$

Alternatively, taking first the small frequency limit of the equations of motion, we obtain the following solutions near the boundary

$$\delta\mathcal{A} = C_0 + O\left(1/\rho^2\right), \qquad \delta\mathcal{R} = \tilde{C}_0 + O\left(1/\rho^2\right),$$

whereas near the horizon the corresponding solutions are

$$\begin{aligned} \delta\mathcal{A} &= C_0 + b_1 C_1 + b_2 C_2 + a_1 C_1 \rho + a_2 C_2 \rho, \\ \delta\mathcal{R} &= \tilde{C}_0 + \tilde{b}_1 C_1 + \tilde{b}_2 C_2 + \tilde{a}_1 C_1 \rho + \tilde{a}_2 C_2 \rho, \end{aligned} \tag{3.40}$$

[12] They are given by equations (A.11) of [64], with the replacements $E \to \delta\mathcal{A}$, $\tilde{\xi} \to \delta\mathcal{R}$, $r \to \rho$, $d \to dR^6$, $c \to cR^6$, $L \to R$, $R \to \mathcal{R}$.

where the coefficients are given by

$$a_1 = -\frac{c^2q^2 + (d^2-c^2)\omega^2}{R^2\left(d^2-c^2\right)^{\frac{3}{2}}}, \qquad a_2 = \frac{cdq^2}{R^2\left(d^2-c^2\right)^{\frac{3}{2}}},$$

$$b_1 = \frac{\Gamma\left(\frac{7}{6}\right)\Gamma\left(\frac{4}{3}\right)\left[\left(3c^2-d^2\right)q^2 + 3\left(d^2-c^2\right)\omega^2\right]}{\Gamma\left(\frac{1}{2}\right)\left(d^2-c^2\right)^{\frac{4}{3}}}, \qquad b_2 = -\frac{2cdq^2\Gamma\left(\frac{7}{6}\right)\Gamma\left(\frac{4}{3}\right)}{\Gamma\left(\frac{1}{2}\right)\left(d^2-c^2\right)^{\frac{4}{3}}},$$

$$\tilde{a}_1 = -\frac{cd}{R^6\left(d^2-c^2\right)^{\frac{3}{2}}}, \qquad \tilde{a}_2 = \frac{d^2}{R^6\left(d^2-c^2\right)^{\frac{3}{2}}},$$

$$\tilde{b}_1 = \frac{2cd\Gamma\left(\frac{7}{6}\right)\Gamma\left(\frac{4}{3}\right)}{R^4\Gamma\left(\frac{1}{2}\right)\left(d^2-c^2\right)^{\frac{4}{3}}}, \qquad \tilde{b}_2 = -\frac{\Gamma\left(\frac{7}{6}\right)\Gamma\left(\frac{4}{3}\right)\left(3d^2-c^2\right)}{R^4\Gamma\left(\frac{1}{2}\right)\left(d^2-c^2\right)^{\frac{4}{3}}}.$$

The poles of the retarded Green's function correspond to the quasinormal modes of the system - these are the solutions which obey ingoing boundary conditions near the horizon and vanish near the boundary. Such solutions exist when it is possible to match the expansion (3.39) (with the upper sign) onto the expansion (3.40) with $C_0 = \tilde{C}_0 = 0$. Performing this matching order-by-order in ρ, we find that the coefficients C_1 and C_2 obey the equation

$$\begin{pmatrix} i\Omega a_1 - b_1 & i\Omega a_2 - b_2 \\ i\Omega\tilde{a}_1 - \tilde{b}_1 & i\Omega\tilde{a}_2 - \tilde{b}_2 \end{pmatrix} \begin{pmatrix} C_1 \\ C_2 \end{pmatrix} = \begin{pmatrix} 0 \\ 0 \end{pmatrix}. \tag{3.41}$$

A non-trivial solution exists provided that

$$\begin{vmatrix} i\Omega a_1 - b_1 & i\Omega a_2 - b_2 \\ i\Omega\tilde{a}_1 - \tilde{b}_1 & i\Omega\tilde{a}_2 - \tilde{b}_2 \end{vmatrix} = 0. \tag{3.42}$$

By substituting an expansion of the form $\omega = c_0 + c_1 q + c_2 q^2 + \ldots$, we find that the above determinant vanishes when ω is given by the dispersion relation (3.27). Note that this method only finds the lowest energy quasinormal modes, as it involves taking the small ω limit.

Chapter 4

Collective excitations in the RN-AdS_4 theory

4.1 Introduction

As we have previously mentioned, there have been numerous studies of the excitations present when $T = 0$ and $\omega, q \ll \mu$ in specific strongly-coupled field theories, and one common feature amongst many examples is a propagating, longitudinal 'holographic zero sound' mode with the dispersion relation

$$\bar{\omega} = \pm v_s \bar{q} - i\Gamma_0 \bar{q}^2 + O\left(\bar{q}^3\right), \tag{4.1}$$

where

$$\bar{\omega} = \frac{\omega}{\mu}, \qquad \text{and} \qquad \bar{q} = \frac{q}{\mu}. \tag{4.2}$$

This is a feature of probe brane theories in different dimensions and with different UV symmetries (where the conserved charge is a density of fundamental matter — at least in the case where the background is derived from string theory) [61,64–69,90,97] and also the 4D bulk Einstein-Maxwell theory with a cosmological constant (where the conserved charge is an R-charge density) [70].

In the previous chapter, the behaviour of this zero temperature sound mode in the D3/D7 theory in (3+1) dimensions was analysed as the temperature was increased from $T = 0$ and it was found to behave similarly to the 'zero sound' mode due to the oscillation of the Fermi surface of a Landau Fermi liquid (LFL), despite the fact that some of its other properties are quite different from an LFL (e.g. its heat capacity is proportional to T^6 rather than T) [59]. A natural question to ask is whether similar behaviour is observed in the low temperature sound modes of other holographic theories at large chemical potential and hence whether they can all be characterised in this way as LFL-like 'zero sound' modes or not.

In this chapter, based on the paper [109], we study the strongly-coupled field theory dual to the RN-AdS_4 black hole solution of 4D Einstein-Maxwell theory with a cosmological constant. This is a (2+1)-dimensional field theory whose properties have been investigated in recent years as it is relatively simple and yet has very interesting behaviour.[1] When $T = 0$, the low energy behaviour of the field theory is governed by a CFT_1 dual to the AdS_2 factor of the black hole's $AdS_2 \times \mathbb{R}^2$ near-horizon geometry [105]. If one considers a probe Dirac action for fermions in this background, the field theory operators dual to these fermions exhibit Fermi surfaces of a non-Fermi liquid type [104, 105, 110]. If instead one considers a fermionic action which is the supersymmetric completion of the Einstein-Maxwell action, no such Fermi surfaces are observed [106–108].

The quasinormal modes of the bulk bosonic fields, which correspond to the poles of the retarded Green's functions of the field theory energy-momentum tensor $T^{\mu\nu}$ and U(1) current J^μ, have also been studied at zero temperature. At $T = 0$ the transverse sector (i.e. transport perpendicular to the direction of the momentum flow) contains a branch cut along the negative imaginary frequency axis, and no long-lived modes (by which we mean no modes satisfying $\bar{\omega} \to 0$ as $\bar{q} \to 0$). At very small temperatures $T \ll \mu$, this branch cut becomes a series of poles, one of

[1] Recall that real strange metallic phases are often not (3+1)-dimensional, as mentioned in section 1.3.3.

which has a dispersion relation of the form $\bar{\omega} = -i\mathcal{D}\bar{q}^2 + O(\bar{q}^3)$ [111–113]. This is an analogue of the well-known hydrodynamic shear diffusive mode of the energy-momentum tensor [114].

At $T = 0$, the longitudinal sector (i.e. transport parallel to the direction of the momentum flow) also contains a branch cut along the negative imaginary frequency axis. In addition to this, it has two propagating modes with dispersion relations of the form (4.1) with $v_s = \sqrt{(\partial P/\partial\epsilon)}|_{T=0}$ and $\Gamma_0 \approx \mu\eta_0/2(\epsilon + P)$, where η_0 is the 'zero temperature viscosity' derived via the 'Kubo formula'

$$\eta_0 = -\lim_{\omega\to 0}\frac{1}{\omega}\mathrm{Im}\left[G^R_{T^{xy}T^{xy}}(\omega, 0)\right]\Big|_{T=0}, \tag{4.3}$$

ϵ and P are the field theory's energy density and pressure respectively, and the '$\approx$' signifies that these are equal to within about 10% [70, 115].[2] When $\mu = 0$, an analogous relation between the low frequency limit of $G^R_{T^{xy}T^{xy}}$ and the leading dissipative term of the *hydrodynamic* sound dispersion relation (i.e. the coefficient of the $(q/T)^2$ term in an expansion in q/T) is a standard result for field theories in the hydrodynamic limit (that is, when $ql_{\mathrm{mfp}} = q/T \ll 1$ where l_{mfp} is the mean free path) [5, 7, 116]. A priori, it is not obvious that this relation should be true for the RN-AdS_4 theory at $T = 0$. It suggests that when $T = 0$, μ acts as an 'effective hydrodynamic scale', at least as far as sound propagation is concerned.

In this chapter, we first study numerically the behaviour of the longitudinal poles for a fixed momentum $\bar{q} < 1$ as the temperature is increased from $T = 0$ to $T \gg \mu$. Of particular interest to us is the behaviour of the sound mode and whether there is a collisionless/hydrodynamic crossover as in the D3/D7 theory and Landau's theory of Fermi liquids. We find that the attenuation of the sound mode shows no significant temperature dependence over the range $T \lesssim \mu$ where we may have expected to find LFL-like behaviour and above this it approaches the $\mu = 0$

[2]The sound attenuation Γ_0 is only known numerically and thus an exact comparison cannot be made.

hydrodynamic result [117,118] where the attenuation decreases like T^{-1}. Its speed is approximately $1/\sqrt{2}$ at all temperatures. This is in complete contrast to the results for an LFL (as shown in figure 1.3). Such an outcome is not particularly surprising since all available evidence suggests that this field theory is *not* an LFL. However, this is also true of the D3/D7 theory and yet it possesses an LFL-like zero sound mode. Our results show that this kind of mode is *not* generic to all strongly-coupled field theories at large chemical potential which have a gravitational dual.

The other long-lived, longitudinal mode of the theory corresponds to a purely imaginary pole that forms when the branch cut along the negative imaginary frequency axis dissolves at non-zero temperatures. This mode becomes more stable as the temperature increases and when $T \gg \mu$ its dispersion relation is that of the $\mu = 0$ hydrodynamic charge diffusion mode [118, 119].

In addition to the poles of the Green's functions, we also compute the spectral functions of energy density and charge density as the temperature is increased at fixed $\bar{q} < 1$. The energy density spectral function is dominated by the peak corresponding to sound propagation at all temperatures. In contrast to this, the charge density spectral function undergoes a crossover from being dominated by the sound peak at low temperatures to being dominated by the diffusion peak at high temperatures $T \gg \mu^2/q$. Note that this mechanism is quite different than in the D3/D7 theory where the sound poles collide to form the diffusion pole. Here, the sound and diffusion poles coexist at all non-zero temperatures (that we can access numerically) but their residues change and this results in the crossover. In the D3/D7 theory this crossover was reminiscent of that in an LFL, but here we know of no such comparison — in particular, the RN-AdS_4 crossover occurs outside of the 'quantum liquid' range $T \ll \mu$ where we may expect an LFL-like theory to apply.

As well as the previous results regarding the temperature dependence of the poles and spectral functions at fixed momentum, we have also calculated their momentum dependence at various fixed temperatures. We find that the sound and purely

imaginary modes exist at all non-zero temperatures that we can access numerically ($T \geq 0.0219\mu$) with the dispersion relations

$$\bar{\omega} = \frac{\bar{q}}{\sqrt{2}} - i\Gamma(T/\mu)\bar{q}^2 + O(\bar{q}^3), \tag{4.4}$$

and

$$\bar{\omega} = -iD(T/\mu)\bar{q}^2 + O(\bar{q}^3), \tag{4.5}$$

and we compute the functions $D(T/\mu)$ and $\Gamma(T/\mu)$ numerically. For this reason, and the fact that it becomes the $\mu = 0$ hydrodynamic charge diffusion mode in the $T \gg \mu$ limit, we will refer to this purely imaginary mode as the diffusion mode. When $\bar{q} \gg 1$, these modes no longer dominate the low-energy properties of the theory and we must consider additional poles of the Green's functions also.

Finally, we investigate the properties of sound propagation in the theory, at some fixed momentum q, over the (T, μ) plane. As discussed above, it is known that when $\mu = 0$, T is the hydrodynamic scale and sound will propagate provided its momentum satisfies $q \ll T$. We also know that when $T = 0$, there is an effective hydrodynamic scale μ in that there is a long-lived sound mode provided that $q \ll \mu$. We find that when both of these scales are non-zero, there will be a long-lived sound mode provided that any *one* of them is much larger than the momentum. In other words, sound will propagate for *any* value of μ/T, provided that one considers small enough momenta.

The structure of the chapter is as follows. In section 4.2 we review the RN-AdS_4 solution of the four dimensional Einstein-Maxwell theory with a cosmological constant, and describe some of the properties of its dual holographic quantum liquid state. We also discuss the gauge-invariant fluctuations of the bulk fields that we use to compute the poles of the retarded Green's functions and the spectral functions. Section 4.3 contains the numerical results showing how the properties of the sound mode change as we increase the temperature at fixed $\bar{q} < 1$. In particular, we

demonstrate that these properties are significantly different from those of an LFL and of the D3/D7 theory. In section 4.4, we explore how the other long-lived mode of the system - the diffusion mode - behaves as T is increased for $\bar{q} < 1$. We also examine how the energy density and charge density spectral functions vary with T for $\bar{q} < 1$. Section 4.5 contains results for the poles and spectral functions as a function of $\bar{q}$ at fixed temperature $T < \mu$. We then study the existence of an effective hydrodynamic scale in section 4.6 by examining the properties of the sound mode as a function of both q/μ and q/T. This is followed by our conclusions and a discussion of the behaviour of the sound mode compared to that of the D3/D7 theory in section 4.7. Appendix 4.A.1 contains the equations of motion and off-shell action for the aforementioned gauge-invariant fluctuations and appendix 4.A.2 contains a description of how to compute the Green's function poles at $T = 0$.

4.2 The RN-AdS_4 background and fluctuations

4.2.1 The action and background solution

The gravitational theory we study is the four dimensional Einstein-Maxwell theory with a cosmological constant, which has the action

$$S = \frac{1}{2\kappa_4^2}\left[\int_{\mathcal{M}} d^4x\sqrt{-g}\left(R - 2\Lambda - L^2 F_{\mu\nu}F^{\mu\nu}\right) + 2\int_{\partial\mathcal{M}} d^3x\sqrt{|h|}\left(\mathcal{K} + \text{counterterms}\right)\right], \tag{4.6}$$

where $\Lambda = -3/L^2$, h is the induced metric on the boundary of the spacetime, $\mathcal{K}$ is the extrinsic curvature on this boundary and $F_{\mu\nu}$ is the field strength of a $U(1)$ gauge field A_μ. This is a consistent truncation of $D = 11$ supergravity [28,120]. The counterterms are discussed in appendix 4.A.1.

This theory has a charged, asymptotically-AdS black hole solution with a planar

horizon: the planar AdS_4 Reissner-Nordström black hole (RN-AdS_4)

$$\begin{aligned} ds_4^2 &= -\frac{r^2 f(r)}{L^2}dt^2 + \frac{r^2}{L^2}dx^2 + \frac{r^2}{L^2}dy^2 + \frac{L^2}{r^2 f(r)}dr^2, \\ f(r) &= 1 - (1+Q^2)\left(\frac{r_0}{r}\right)^3 + Q^2\left(\frac{r_0}{r}\right)^4, \\ A_t &= \frac{Qr_0}{L^2}\left(1 - \frac{r_0}{r}\right), \end{aligned} \tag{4.7}$$

where r is the bulk radial co-ordinate, r_0 is the position of the horizon and Q determines the $U(1)$ charge of the black hole. In the full $D = 11$ supergravity theory, it is the decoupling limit of the geometry created by a stack of M2-branes which are rotating (in a specific way) in the directions transverse to their worldvolume [120]. The bulk $U(1)$ gauge field is dual to a $U(1)$ R-current in the field theory on this worldvolume.

This solution has one tunable dimensionless parameter Q which determines the ratio of the chemical potential in the field theory to the temperature

$$\frac{\mu}{T} = \frac{4\pi Q}{3 - Q^2}. \tag{4.8}$$

It takes values between 0 (the zero chemical potential limit) and $\sqrt{3}$ (the zero temperature limit). The thermodynamics of the dual field theory are well-known [28]. In particular, we note that the entropy density has the unusual property of being non-zero when $T = 0$.

Near the horizon of this geometry, the metric is that of Schwarzschild-$AdS_2 \times \mathbb{R}^2$ [105]

$$ds^2_{\rm NH} = -\frac{R_2^2}{\zeta^2}\left(1 - \frac{\zeta^2}{\zeta_0^2}\right)d\tau^2 + \frac{R_2^2}{\zeta^2\left(1 - \frac{\zeta^2}{\zeta_0^2}\right)}d\zeta^2 + \frac{Qr_0^2}{\sqrt{3}R^2}\left(dx^2 + dy^2\right), \tag{4.9}$$

with a non-zero gauge field

$$A_\tau = \frac{1}{2\sqrt{3}\zeta\left(1-\frac{\zeta}{\zeta_0}\right)}, \tag{4.10}$$

where $R_2 = \frac{R}{\sqrt{6}}$. This is obtained by defining

$$r - r_* = \lambda\frac{R_2^2}{\zeta}, \qquad r_0 - r_* = \lambda\frac{R_2^2}{\zeta_0}, \qquad t = \lambda^{-1}\tau, \tag{4.11}$$

where $r_* = \left(\frac{Q^2}{3}\right)^{\frac{1}{4}} r_0$ is the inner horizon of the RN-AdS_4 solution, and then taking the limit $\lambda \to 0$ with ζ and τ fixed.

These limits correspond to the low energy and low temperature limit of the dual field theory: $\omega, T \ll \mu$. Recalling the gauge/gravity dictionary of section 1.2.2, one comes to the conclusion that (at low temperatures $T \ll \mu$) the low energy dynamics of the field theory are governed by a one-dimensional 'IR CFT' (dual to the AdS_2 factor of the geometry) at each point in space. For this reason, this state is an example of a locally quantum critical state.

4.2.2 Fermionic excitations

This notion can be made more precise by computing the correlators of operators at low energies. Consider a charged scalar field of mass m and charge q in the RN-AdS_4 geometry at $T = 0$. Its Green's function at low frequencies is of the form [105]

$$G^R(\omega, k) = K\frac{b_+^{(0)} + \omega b_+^{(1)} + O(\omega^2) + \mathcal{G}_k(\omega)\left(b_-^{(0)} + \omega b_-^{(1)} + O(\omega^2)\right)}{a_+^{(0)} + \omega a_+^{(1)} + O(\omega^2) + \mathcal{G}_k(\omega)\left(a_-^{(0)} + \omega a_-^{(1)} + O(\omega^2)\right)}, \tag{4.12}$$

where the coefficients $a_\pm^{(n)}$ and $b_\pm^{(n)}$ are independent of ω and can be determined numerically by solving the scalar equation of motion in the full spacetime. The

important part of this correlator is the dependence upon

$$\mathcal{G}_k(\omega) = 2\nu_k e^{-i\pi\nu_k} \frac{\Gamma(-2\nu_k)\,\Gamma\left(\frac{1}{2}+\nu_k - i\frac{q}{2\sqrt{3}}\right)}{\Gamma(2\nu_k)\,\Gamma\left(\frac{1}{2}-\nu_k - i\frac{q}{2\sqrt{3}}\right)} (2\omega)^{2\nu_k}, \tag{4.13}$$

where

$$\nu_k = \sqrt{m^2 R_2^2 + k^2 R_2^2 \frac{R^2}{r_*^2} - \frac{q^2}{12} + \frac{1}{4}}. \tag{4.14}$$

This is the retarded Green's function of a scalar operator with an effective mass $m^2_{\text{eff.}} = m^2 + k^2\frac{R^2}{r_*^2}$ and charge q in the near-horizon AdS_2 geometry. The effective mass appearing here is the mass term in the scalar field's equation of motion in the near-horizon limit of the geometry. In the dual field theory, this is the retarded Green's function of a scalar operator $\mathcal{O}_k$ of charge q and scaling dimension $\Delta_+ = \frac{1}{2} + \nu_k$ in the IR CFT.[3]

Thus the expression (4.12) for the two-point function at low frequencies explicitly shows the extent to which the low-energy dynamics of the field theory are controlled by the IR CFT. Analogous results are found for spin-$\frac{1}{2}$ fermions and gauge fields in the RN-AdS_4 background but with a different expression for $\mathcal{G}_k(\omega)$ and ν_k [70, 105, 111]. We note that this approach may be generalised to non-zero temperatures $T \ll \mu$, where the relevant IR CFT state is now in the thermal state at temperature T.

The expression (4.12) for the low frequency Green's function is especially informative when one is considering spin-$\frac{1}{2}$ operators in the field theory. Suppose that, for real ν_k, there is a pole in the Green's function when $\omega = 0$ at a non-zero momentum $k = k_F$, i.e. that $a_+^{(0)}(k = k_F) = 0$.[4] Then in the vicinity of this pole, the denominator of the Green's function may be written

$$G^R(\omega, k)^{-1} = (k - k_F) - \frac{1}{v_F}\omega - h_2 e^{i\gamma_{k_F}} \omega^{2\nu_{k_F}} + O\left(\omega^2\right), \tag{4.15}$$

[3]This is a simple application of equation (1.27) generalised to include a non-zero charge q.
[4]Complex ν_k indicates an instability of the theory.

where v_F is real if $\nu_{k_F} > 0$ and h_2 is always real. These coefficients are constructed from $a_{\pm}^{(n)}$ and $b_{\pm}^{(n)}$. Keeping only the leading terms at low frequencies, we discover that if $\nu_{k_F} > \frac{1}{2}$, the dispersion relation of fermionic excitations around this Fermi surface is of the form

$$\omega(k) = v_F(k - k_F) - v_F h_2 e^{i\gamma_{k_F}} \left(v_F(k - k_F)\right)^{2\nu_{k_F}} + O\left(k^3\right), \tag{4.16}$$

i.e. the decay rate of an excitation around the Fermi surface is much smaller than its propagating frequency. These are thus quasiparticle excitations and this is a Landau-Fermi-like liquid.[5] Conversely, if $\nu_{k_F} < \frac{1}{2}$, the dispersion relation of fermionic excitations is of the form

$$\omega(k) = \left(\frac{k - k_F}{h_2}\right)^{\frac{1}{2\nu_{k_F}}} e^{-i\frac{\gamma_{k_F}}{2\nu_{k_F}}}, \tag{4.17}$$

i.e. the decay rate of the excitation is comparable to its propagating frequency and so they cannot be regarded as long-lived quasiparticles. This is an example of a non-Fermi liquid. For $\nu_{k_F} = \frac{1}{2}$ one obtains the 'marginal Fermi liquid' dispersion relation

$$(k - k_F) + \tilde{c}_1 \omega \log \omega + c_1 \omega = 0, \tag{4.18}$$

where $\tilde{c}_1$ is real and c_1 is complex.

In summary, the character of the fermionic excitations around a Fermi surface in this theory is completely controlled by the scaling dimension of the fermionic operator in the IR CFT [105]. Physically, this is because these excitations decay via a coupling to the IR CFT degrees of freedom. With this understanding, it is much easier to construct holographic quantum liquids with desired properties. For example, if the geometry is cut off in the IR then there are no IR CFT degrees of freedom and the result is an LFL-like liquid (as in e.g. [100]). Alternatively, one can study solutions whose near-horizon geometries are not conformally-invariant but have alternative scaling symmetries (as in e.g. [121]).

[5] For a Landau Fermi liquid, $\omega(k) = v_F(k - k_F) - i\Gamma(k - k_F)^2 + O\left(k^3\right)$.

As outlined above, the kind of excitations obtained depend upon the mass and charge of the bulk fermionic field. They are also dependent upon the precise action of the fermionic field. The fermions of the minimal supersymmetric completion of the action (4.6) do not have any Fermi surfaces [106–108], but more complicated truncations of supergravity exhibit the non-Fermi liquid behaviour described above [122]. In the following sections we will investigate properties of the theory dual to the RN-AdS_4 geometry which are independent of the probe fermions, and compare these properties to those of an LFL.

4.2.3 Fluctuations around equilibrium

We are interested in the response of the field theory to small perturbations around the equilibrium state. This is encoded holographically in the linear response of the black hole to perturbations around the background solution (4.7):

$$\begin{aligned} g_{\mu\nu} &\to g_{\mu\nu} + h_{\mu\nu}, \\ A_\mu &\to A_\mu + a_\mu. \end{aligned} \tag{4.19}$$

We use the rotational invariance in the (x, y)-plane to choose the momentum to flow only in the x-direction of the field theory, without loss of generality. We may then classify fluctuations according to their parity under $y \to -y$. The fluctuations which are even under this operation ($h_{xx},\ h_{yy},\ h_{rr},\ h_{tt},\ h_{rt},\ h_{rx},\ h_{xt},\ a_r,\ a_t$ and a_x) decouple from those which are odd ($h_{yr},\ h_{yx},\ h_{yt}$ and a_y) at linear order [119]. The indices are raised and lowered with the background metric. In the following we are interested only in the even fluctuations which we refer to as 'longitudinal' henceforth, as they encode the response of the fields parallel to the direction of momentum flow. The metric and gauge field fluctuations are coupled within this longitudinal sector which tells us that the retarded Green's functions of the longitudinal components of the field theory energy-momentum tensor $T^{\mu\nu}$ and U(1) conserved current J^μ are not independent.

We are particularly interested in two properties of the retarded Green's functions $G^R_{\mathcal{O}_A\mathcal{O}_B}$ — their poles in the complex frequency plane and their spectral functions. The poles correspond to the field theory excitations — the real part of each pole is its propagating frequency and the imaginary part is its decay rate. We are primarily interested in the long-lived excitations i.e. those with the smallest imaginary part. Note that if any excited bulk fields are coupled, their dual field theory operators share a common set of Green's function poles.

The matrix of spectral functions

$$\chi_{AB}(\omega, q) \equiv i\left(G^R_{\mathcal{O}_A\mathcal{O}_B}(\omega, q) - G^R_{\mathcal{O}_B\mathcal{O}_A}(\omega, q)^*\right), \tag{4.20}$$

tell us the rate of work done on the system by small external sources for $\mathcal{O}_A$ and $\mathcal{O}_B$ with frequency ω (see, for example, [49]). Modes which couple strongly to external sources in this way are visible in the spectral functions as tall, narrow peaks centred on the propagating frequency and with a width proportional to their decay rate. Such a peak will be produced by a pole of the Green's function with small imaginary part provided that the residue of the Green's function is large enough at this pole and that there are no other poles near it in the complex frequency plane. Unlike the existence of a pole, the residue at a pole differs between the Green's functions of a set of coupled operators and hence despite the fact that they have a shared set of Green's function poles, the spectral functions of coupled operators can be very different. We are interested in the energy density spectral function $\chi_{T^{tt}T^{tt}} \equiv \chi_{\epsilon\epsilon}$ and the charge density spectral function $\chi_{J^tJ^t} \equiv \chi_{QQ}$, which are real quantities, and tell us which modes couple strongly to external sources of energy density and charge density respectively.

4.2.4 Gauge-invariant variables and Ward identities

The longitudinal sector of our theory contains ten fields whose excitations are coupled. As we described in section 2.3.2, the equations of motion and on-shell action for the excited longitudinal fields can be simplified considerably by noting that the theory has a U(1) gauge symmetry which acts on the gauge field fluctuations as

$$a_\mu \to a_\mu - \partial_\mu \Lambda, \tag{4.21}$$

and a diffeomorphism symmetry which acts as

$$\begin{aligned} h_{\mu\nu} &\to h_{\mu\nu} - \nabla_\mu \xi_\nu - \nabla_\nu \xi_\mu, \\ a_\mu &\to a_\mu - \xi^\alpha \nabla_\alpha A_\mu - A_\alpha \nabla_\mu \xi^\alpha, \end{aligned} \tag{4.22}$$

to linear order, where ∇ is the covariant derivative with respect to the background metric [58]. We can form two linearly-independent variables which are invariant under these transformations

$$\begin{aligned} Z_1(r,\omega,q) &= \omega a_x(r,\omega,q) + q a_t(r,\omega,q) - \frac{qL^2 A_t'(r)}{2r} h_{yy}, \\ Z_2(r,\omega,q) &= \frac{2\omega q}{r^2} h_{xt} + \frac{\omega^2}{r^2} h_{xx} + \frac{q^2}{r^2} h_{tt} + \frac{q^2 f(r)}{r^2} h_{yy} \left(1 + \frac{r f'(r)}{2f(r)} - \frac{\omega^2}{q^2 f(r)}\right), \end{aligned} \tag{4.23}$$

and to linear order in the fluctuations, we can write our theory in terms of these variables. In particular, this reduces the set of ten coupled equations to a set of two. It also allows us to write the on-shell action in the form

$$S_{\text{on-shell}} = \int_{r\to\infty,\omega>0} \frac{d\omega d^2 q}{(2\pi)^3} \Big[Z_i(r,-\omega,-q)\, \mathcal{G}_{ij} \partial_r Z_j(r,\omega,q) + \phi_I(r,-\omega,-q)\, \mathcal{C}_{IJ} \phi_J(r,\omega,q) \Big], \tag{4.24}$$

where $i = 1, 2$ and ϕ_I denote the fundamental fluctuations $\{h_{tt}, h_{xx}, h_{yy}, h_{tx}, a_t, a_x\}$. The $\mathcal{C}_{IJ}$ terms are analytic in ω, q and hence contribute only contact terms to the retarded Green's functions (i.e. terms analytic in ω, q). These Z_i variables are a

generalisation of those of [57] to non-zero chemical potential (and in 3+1, rather than 4+1, dimensions).

As outlined in section 2.3.2. this property of bulk gauge-invariance thus generates a number of relationships between the retarded Green's functions of the corresponding field theory operators:

$$G^R_{J^x J^t} = \frac{\omega}{q} G^R_{J^t J^t}, \qquad G^R_{J^x J^x} = \frac{\omega^2}{q^2} G^R_{J^t J^t}, \tag{4.25}$$

$$G^R_{T^{xx} J^t} = \frac{\omega^2}{q^2} G^R_{T^{tt} J^t}, \quad G^R_{T^{tx} J^t} = \frac{\omega}{q} G^R_{T^{tt} J^t}, \quad G^R_{T^{yy} J^t} = \left(1 - \frac{\omega^2}{q^2}\right) G^R_{T^{tt} J^t}, \ \ldots, \tag{4.26}$$

$$G^R_{T^{xx} T^{tt}} = \frac{\omega^2}{q^2} G^R_{T^{tt} T^{tt}}, \quad G^R_{T^{tx} T^{tt}} = \frac{\omega}{q} G^R_{T^{tt} T^{tt}}, \ \ldots, \tag{4.27}$$

where the '...' represents other similar relations, and these equations should be understood to hold up to contact terms. These are precisely the Ward identities of the field theory.

The contribution of the contact terms to the diagonal retarded Green's functions is purely real, and thus they don't affect our results for the spectral functions $\chi_{\epsilon\epsilon}$ and χ_{QQ} or for the poles.

We note that these are not the only possible gauge-invariant choice of variables. Another choice is the Kodama-Ishibashi variables which involve radial derivatives of the bulk fields, and have the advantage that the two equations of motion in these variables decouple [123].

4.2.5 Equations of motion and action in dimensionless variables

It is convenient to work with the dimensionless radial co-ordinate $u \equiv r/r_0$. For $T > 0$, we use the gauge-invariant variables

$$\begin{aligned}\bar{Z}_1(u,\omega,q) &= \bar{\omega}a_x + \bar{q}a_t - \frac{\bar{q}\mu}{2u}h_y^y,\\ \bar{Z}_2(u,\omega,q) &= i\mu\left[2\bar{\omega}\bar{q}h_t^x + \bar{\omega}^2 h_x^x - \bar{q}^2 f(u)h_t^t + \bar{q}^2 f(u)\left(1 + \frac{uf'(u)}{2f(u)} - \frac{\bar{\omega}^2}{\bar{q}^2 f(u)}\right)h_y^y\right],\end{aligned} \tag{4.28}$$

where $f(u) = 1-(1+Q^2)/u^3 + Q^2/u^4$. The equations of motion and action in these variables are given in appendix 4.A.1. To compute the poles and spectral functions, we used the numerical procedure described in 2.3.

At $T = 0$, we use the Kodama-Ishibashi variables and follow the method described in appendix 4.A.2. The equations of motion in these variables are given in appendix A of [70]. We could only obtain accurate numerics at $T = 0$ above $\bar{q} \gtrsim 0.1$, and hence we only show $T = 0$ results in this range.

4.3 Temperature dependence of the sound mode

Our primary motivation for studying this theory is that it supports stable, propagating excitations of energy and charge density at zero temperature and large chemical potential $\bar{q} \ll 1$. These sound modes at zero temperature have a dispersion relation of the form (4.1) where the speed is $v_s = 1/\sqrt{2}$ [70]. We want to know what effect the increase of temperature has upon this mode. In particular we are looking to see if it shares the characteristics of the 'zero sound' mode of a Landau Fermi liquid. This comparison can be made by studying the sound attenuation as a function of temperature for $T \ll \mu$ and looking for the three different regimes shown in figure 1.3.

Note that when $\mu = 0$ and $\omega, q \ll T$, there are sound modes with the dispersion

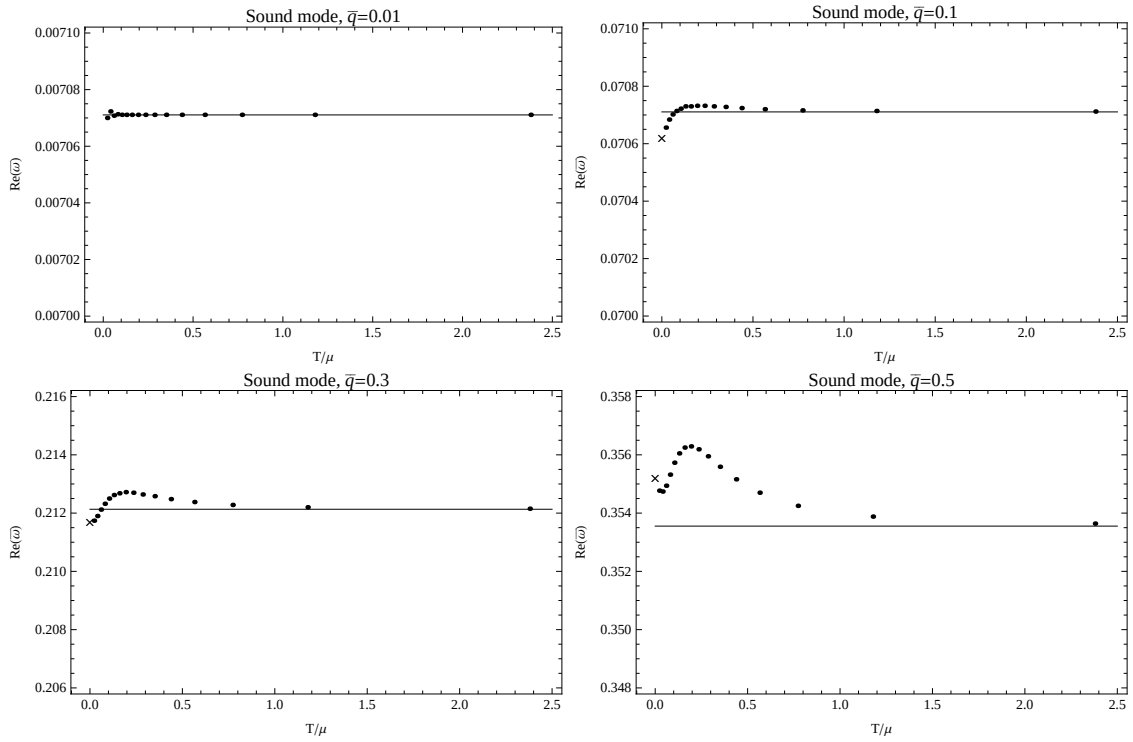

Figure 4.1: Variation of the real part of the sound mode as the temperature is increased. The crosses mark the $T = 0$ numerical results, the dots are the numerical results for $T > 0$, and the solid lines are the $\mu = 0$ analytic result (4.29).

relation

$$\omega = \pm\frac{1}{\sqrt{2}}q - i\frac{1}{8\pi T}q^2 + O(q^3). \tag{4.29}$$

At non-zero μ, we would expect to recover these results when $\mu \ll \omega, q \ll T$, which is outside of the 'quantum liquid' regime $T \ll \mu$ where any LFL-like behaviour would be present.

The temperature dependence of the real and imaginary parts of the sound mode are shown in figures 4.1 and 4.2 for various $\bar{q} < 1$. Our finite temperature numerical results are shown along with $T = 0$ numerical results (for $\bar{q} \geq 0.1$ where we can obtain accurate results) and the $\mu = 0$ analytic result (4.29).

The plots show that both the real and imaginary parts of the mode have a non-trivial temperature dependence. As the temperature is increased from zero, finite temperature corrections cause small changes to the real part of the sound mode whose sign depends upon the value of $\bar{q}$. At sufficiently high temperature,

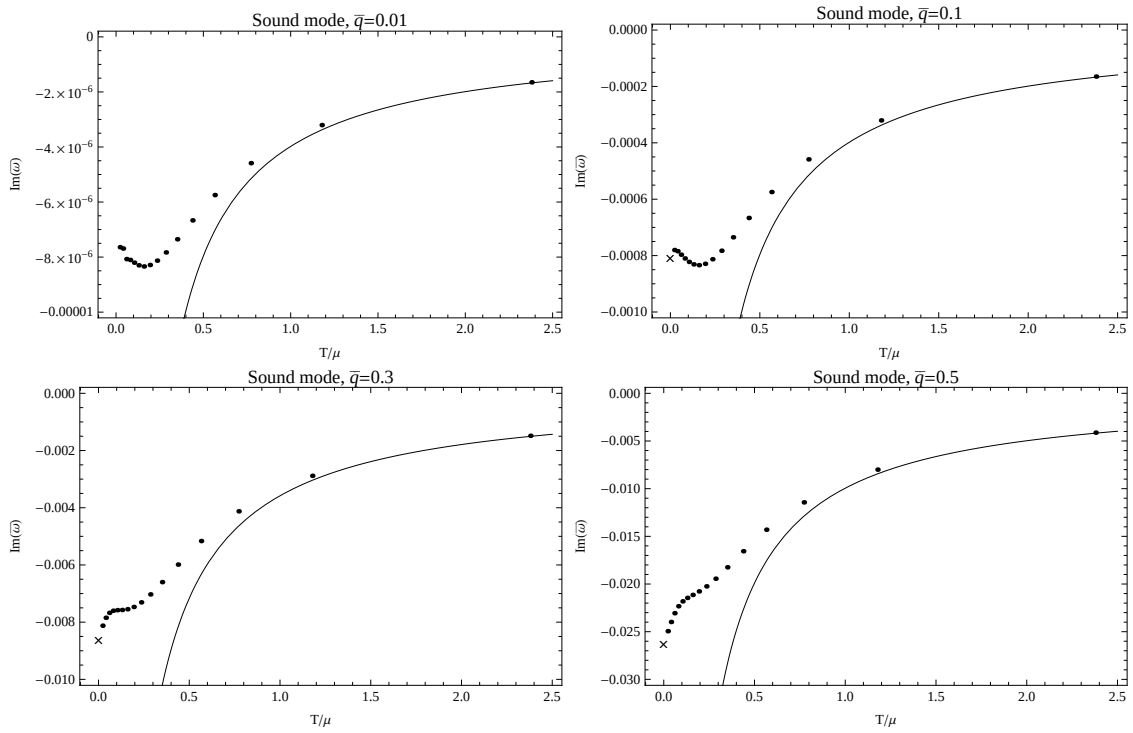

Figure 4.2: Variation of the imaginary part of the sound mode as the temperature is increased. The crosses marks the $T = 0$ numerical results, the dots are the numerical results for $T > 0$, and the solid lines are the $\mu = 0$ analytic result (4.29).

$T/\mu \gtrsim 1$, the real part quickly asymptotes to the $\mu = 0$ hydrodynamic result (4.29). The imaginary part of the sound mode shows similar behaviour. This is slightly surprising — it indicates that the $\mu = 0$ result (4.29) is valid when $q \ll \mu \ll T$. We will comment upon this again in section 4.6.

To make an easier comparison with Landau Fermi liquid theory, we plot the temperature dependence of the imaginary part of the sound mode on a logarithmic scale in figure 4.3. These plots show only the region $T < \mu$ where we may expect such a theory to apply, and the imaginary part of the sound mode is normalised by $\bar{\omega}_0$, its value at the lowest non-zero temperature we can access.

There is a stark contrast between these plots and the results expected for an LFL zero sound mode, shown in figure 1.3.[6] Landau's theory predicts that as the temperature is increased at fixed q and μ, the imaginary part of the zero sound

[6]The magnitude of the frequency of the sound mode in the RN-AdS_4 theory is of the same order as its momentum for the results shown, and thus we compare to the LFL results with $\omega \to q$.

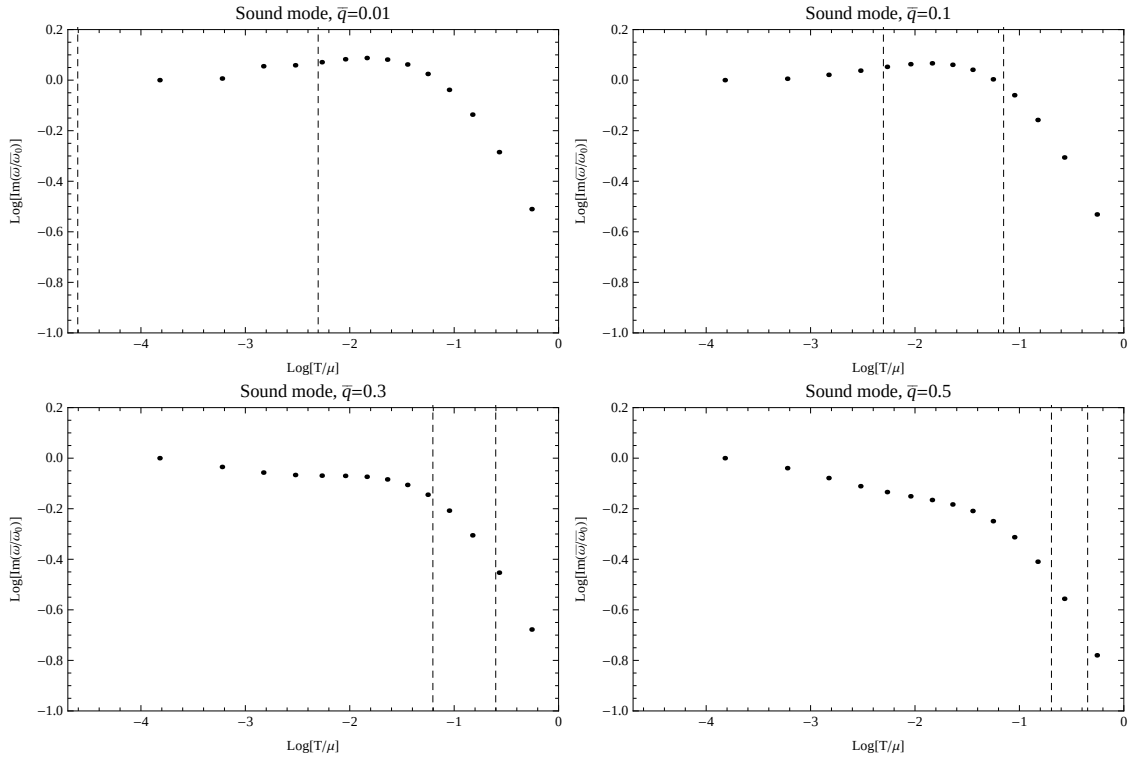

Figure 4.3: Variation of the imaginary part of the sound mode as the temperature is increased, in the regime $T < \mu$. The dots are the numerical results for $T > 0$, and the two dashed lines on each plot denote $T/\mu = q/\mu$ and $T/\mu = \sqrt{q/\mu}$ as one moves to the right along the plot.

mode should be approximately constant up until $T/\mu \sim q/\mu$. Between $T/\mu \sim q/\mu$ and $T/\mu \sim \sqrt{q/\mu}$, it should increase like T^2. Above $T/\mu \sim \sqrt{q/\mu}$ and below $T/\mu \sim 1$, it should decrease like T^2. None of these features are present in our results. The magnitude of the imaginary part of the sound mode in our theory shows no significant temperature dependence until $T \sim \mu$. Above this, it begins to approach the $\mu = 0$, $\omega, q \ll T$ result (4.29) where it decreases as $1/T$.

An explicit comparison between these RN-AdS_4 results and the corresponding D3/D7 results is shown in figure 4.4. This highlights the fact that the D3/D7 sound mode behaves like the LFL zero sound mode, whereas the RN-AdS_4 sound mode does not.

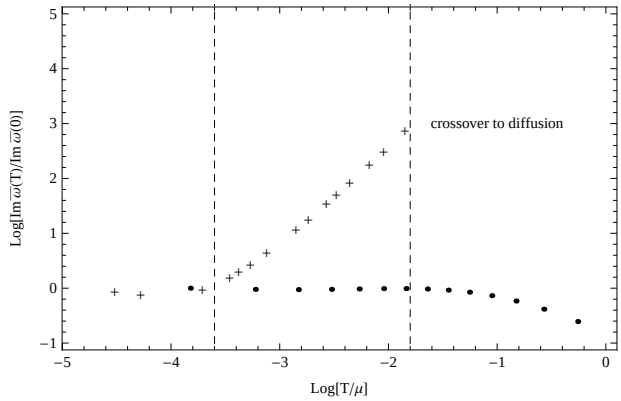

Figure 4.4: A superposition of the plots of the temperature dependence of the normalised imaginary part of the sound mode when $q/\mu = 0.2$ for both the D3/D7 theory and the RN-AdS_4 theory. Crosses denote the D3/D7 numerical results [59] and circles denote the RN-AdS_4 results. Moving from left to right, the dotted lines mark the transition points between the quantum and thermal collisionless regimes, and the thermal collisionless regime and the hydrodynamic regime, in the D3/D7 theory. These occur when $\omega \sim T$ and $\omega \sim T^2/\mu$ respectively. There are no results for the D3/D7 sound mode in the hydrodynamic regime since the hydrodynamic sound mode is suppressed in the probe brane limit. We refer the reader to chapter 3 for a more detailed discussion of these features.

4.4 Further T-dependent properties of the theory when $\bar{q} < 1$

In addition to the sound modes at $T = 0$, there are other propagating modes lying deeper in the complex frequency plane as well as a branch cut along the negative imaginary frequency axis [70]. In this section, we study how this configuration changes as T/μ is increased at a fixed momentum $\bar{q} < 1$. In particular, we concentrate on the longest-lived purely imaginary mode — this exists at non-zero temperatures as the branch cut mentioned above dissolves into a series of poles when $T \neq 0$. We note here that when $\mu = 0$ and $\omega, q \ll T$, the longest-lived purely imaginary mode has the dispersion relation

$$\omega = -i\frac{3}{4\pi T}q^2 + O(q^3), \tag{4.30}$$

corresponding to hydrodynamic charge diffusion [119]. We expect to recover this behaviour at non-zero μ in the limit $\mu \ll \omega, q \ll T$.

We also show in this section how the energy density and charge density spectral functions of the theory change with the temperature, and in particular how the residues of the long-lived modes play an important role in the transition from sound domination of the charge density spectral function to diffusion domination.

4.4.1 Temperature dependence of the diffusion mode

We begin by studying the longitudinal diffusion mode of the theory. At $T = 0$, the negative imaginary frequency axis is a branch cut [70]. At non-zero temperatures, this branch cut dissolves into a series of poles along the axis and generically these become less stable (they recede into the complex plane) as the temperature is increased. However, one of the modes is special in that it becomes more stable as the temperature is increased, and at very high temperatures it becomes the $\mu = 0$ hydrodynamic charge diffusion mode (4.30). Figure 4.5 shows how the imaginary part of this mode changes with the temperature. Its real part is always zero. Unlike for the sound mode, this plot has the same shape for all values of $0.01 \leq \bar{q} \leq 0.5$ and so we show only one for brevity. The decay rate of this mode decreases monatonically as the temperature is increased, and is described well by the $\mu = 0$ result (4.30) when $T \gtrsim \mu$. Again, it is non-trivial that the $\mu = 0$ result holds in the regime $q \ll \mu \ll T$. Note that there is no $T = 0$ point on this plot because it does not make sense to ask where the pole is in that case — the whole negative imaginary frequency axis forms a branch cut.

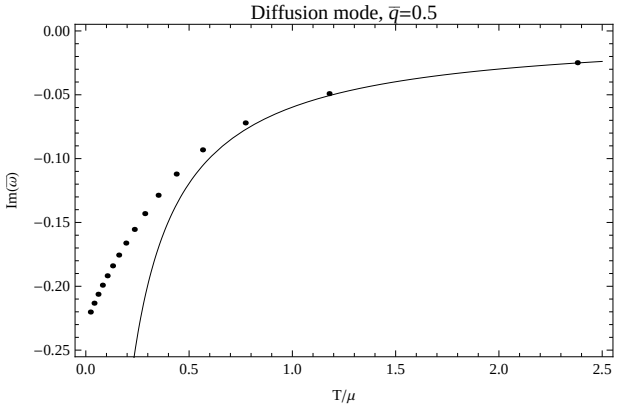

Figure 4.5: Variation of the imaginary part of the longitudinal diffusion mode as the temperature is increased. The dots are the numerical results for $T > 0$, and the solid line is the $\mu = 0$ analytic result (4.30).

4.4.2 Movement of the poles in the complex frequency plane with T

It is instructive to view the simultaneous movement of the Green's function poles described previously in the complex frequency plane as the temperature is increased — this is shown in figure 4.6. As described previously, the sound and diffusion modes both become more stable, approaching the real axis as the temperature is increased. Note that the sound mode is closer to the real axis than the diffusion mode for all values of the temperature and thus it is always the longest-lived mode of the theory. However this does not mean that it always dominates the low-energy properties of the theory, as we shall show in the following subsection. Finally, we note that both the sound and diffusion poles coexist for all non-zero values of the temperature that we can access numerically ($T \gtrsim 0.02\mu$). This is in contrast to the strongly-coupled D3/D7 field theory in which the low temperature sound poles collide to form the high temperature diffusion pole [59].

In addition to the sound and diffusion poles, there are 'secondary' modes corresponding to poles lying deeper in the complex frequency plane. These are much shorter-lived than the sound and diffusion poles when $\bar{q} < 1$ and become less stable as the temperature is increased. They do not have a significant effect on the

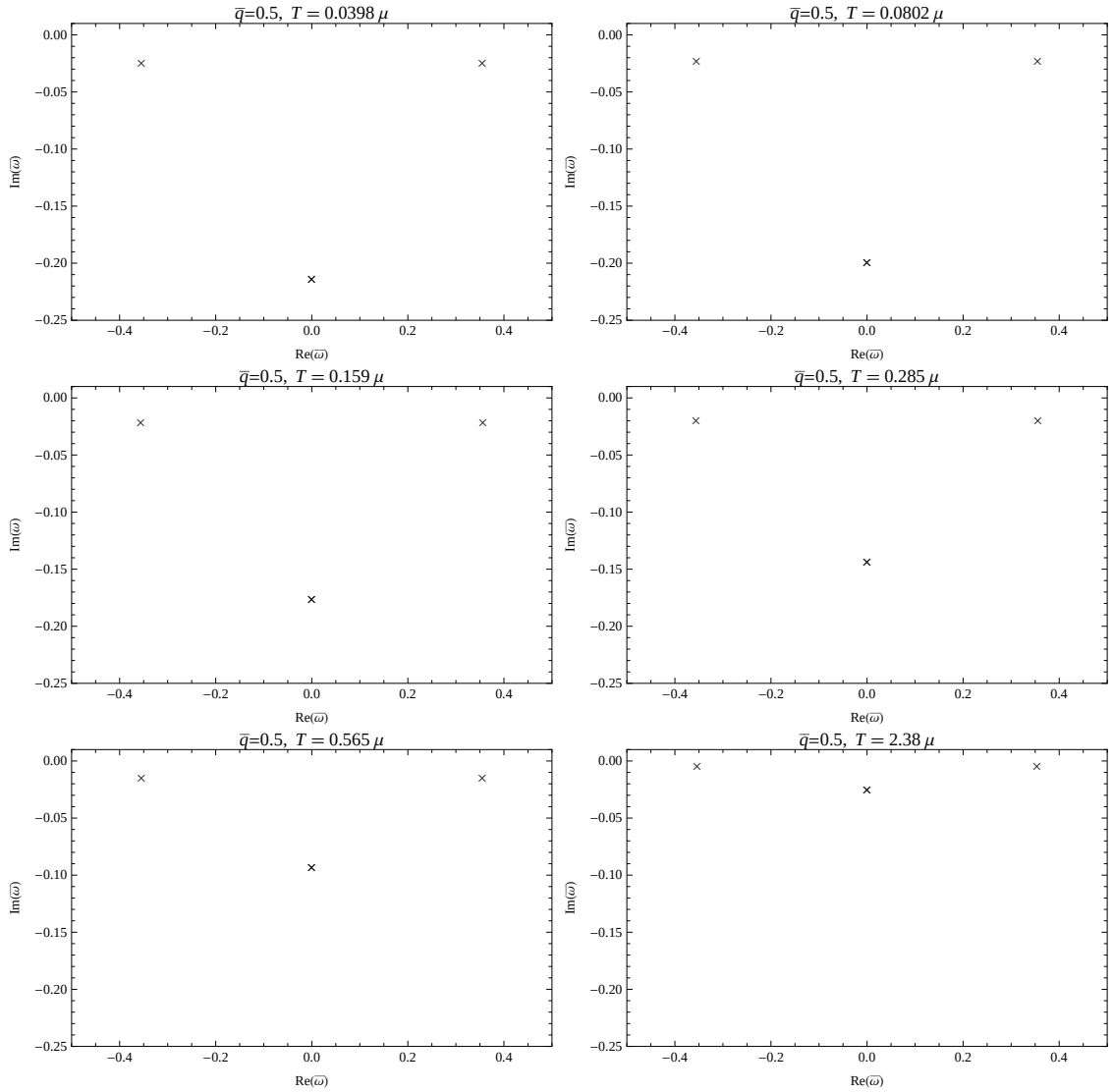

Figure 4.6: Movement of the sound and diffusion poles in the complex frequency plane as the temperature is increased at fixed $\bar{q} = 0.5$. An animated version of this figure is available at `http://www.physics.ox.ac.uk/users/Davison/RNAdS4animations1.html`.

low energy properties of the theory when $\bar{q} < 1$ and hence we do not show their temperature dependence for brevity.

4.4.3 Variation of the spectral functions with T

Until now, we have focused exclusively on the positions of the poles of the retarded Green's functions in the complex frequency plane. While these are interesting, they do not tell us the full story of how charge and energy are transported in the theory.

To investigate this, we now turn our attention to the spectral functions of the energy density and charge density. These determine the average work done on the system when an external source of some frequency is applied to either the energy density or the charge density respectively. Despite the fact that the retarded Green's functions of both of these operators have the same set of poles, their spectral functions are quite different as shown in figures 4.7 and 4.8.

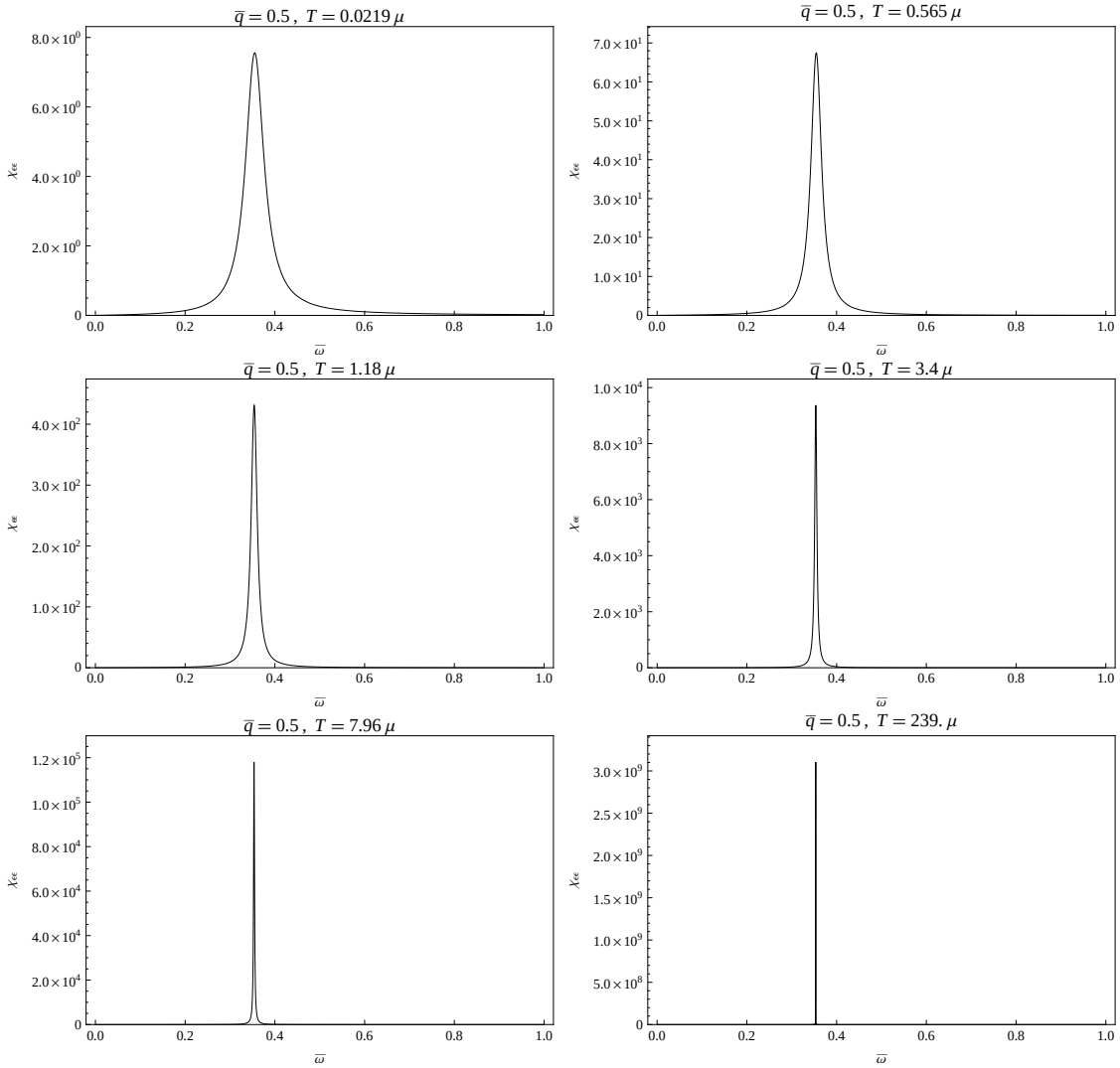

Figure 4.7: The energy density spectral function for $\bar{q} = 0.5$ as the temperature is increased, in units of $2\mu^2 r_0/\kappa_4^2$. The peak due to sound propagation dominates at all temperatures. An animated version of this figure is available at `http://www.physics.ox.ac.uk/users/Davison/RNAdS4animations1.html`.

At very low temperatures, both spectral functions are dominated by the peak

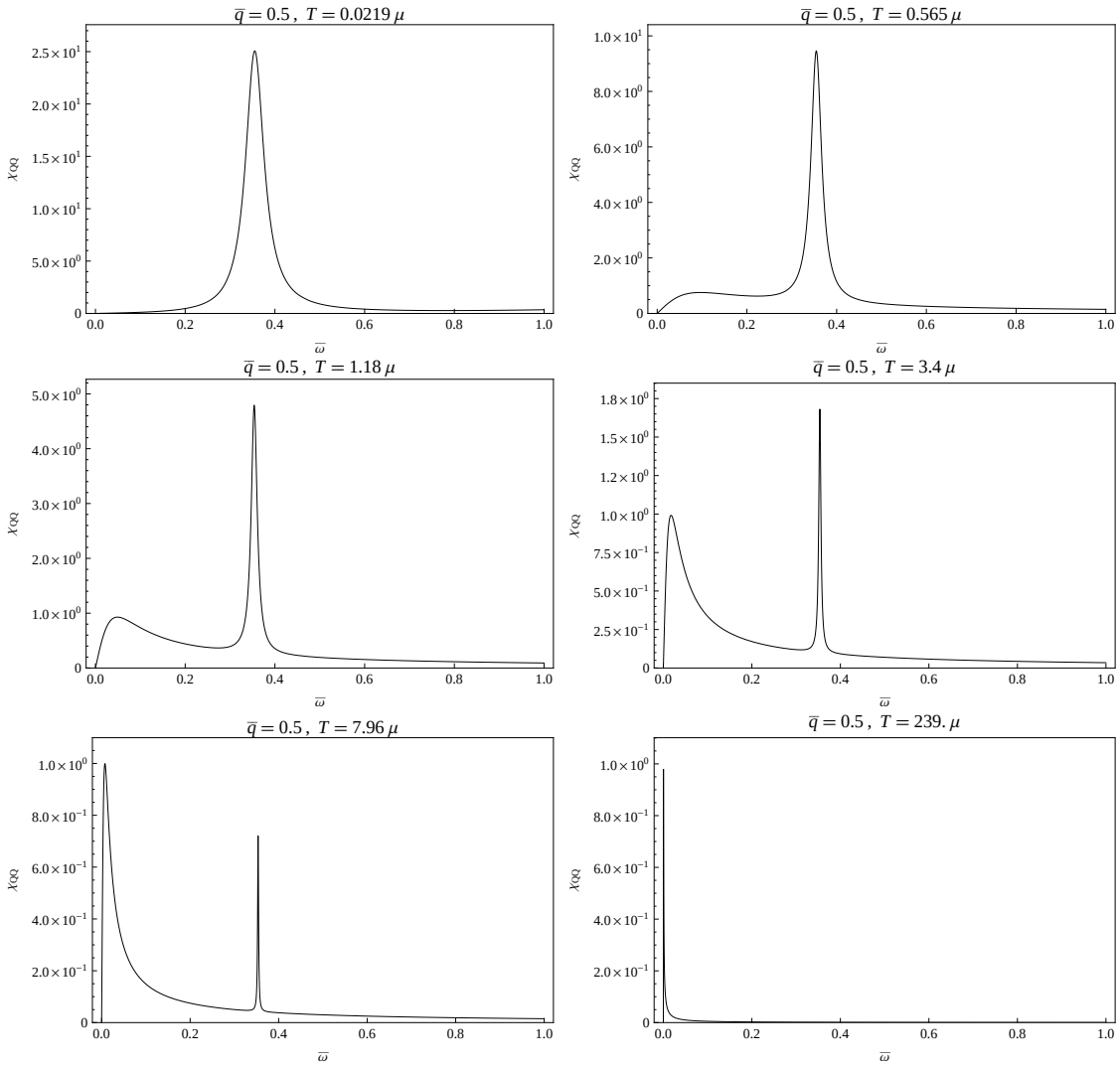

Figure 4.8: The charge density spectral function for $\bar{q} = 0.5$ as the temperature is increased, in units of $2r_0/\kappa_4^2$. There is a crossover between sound domination and diffusion domination at high temperature. An animated version of this figure is available at `http://www.physics.ox.ac.uk/users/Davison/RNAdS4animations1.html`.

corresponding to sound propagation. As the temperature is increased, the spectral function of the energy density undergoes a fairly unremarkable change — the sound peak becomes narrower and taller (corresponding to a longer-lived excitation) but completely dominates at all temperatures. In contrast to this, the sound peak of the charge density spectral function becomes smaller (and narrower) as the temperature increases. At a sufficiently high temperature it becomes so small that the peak around $\bar{\omega} = 0$, corresponding to the high temperature diffusion mode, dominates

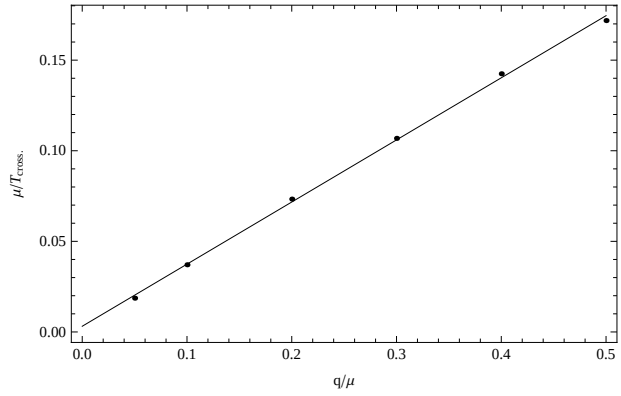

Figure 4.9: The dependence of the crossover value of μ/T upon q/μ. The best fit straight-line to these results has intercept ≈ 0.003 and gradient ≈ 0.34.

the spectral function. At what temperature does this crossover occur? In figure 4.9, we show how the crossover value of μ/T (i.e. the value where the sound and diffusion peaks are of the same height) varies with q/μ. There is a clear linear relationship, signifying that the crossover occurs when

$$T_{\text{cross.}} \sim \mu^2/q, \tag{4.31}$$

and that diffusion dominates when $T \gg \mu^2/q$. Note that since we are studying the range $\bar{q} < 1$, this condition automatically implies that $T \gg \mu$. This crossover is reminiscent of the $\mu \to 0$ limit. In that limit, the fluctuations of $T^{\mu\nu}$ and J^μ decouple resulting in a hydrodynamic sound pole in the $T^{\mu\nu}$ correlators and a hydrodynamic diffusion pole in the J^μ correlators. The charge density spectral function in this limit is shown in [72]. However, we cannot interpret the crossover shown above to be due to approaching this limit, since it corresponds to the limit $\mu \ll q, T$ of our results, whereas the regime we are studying here is $q \ll \mu \ll T$.

In the D3/D7 theory, the corresponding crossover occurred for $T_{\text{cross.}} \sim \sqrt{q\mu}$ and was reminiscent of the collisionless/hydrodynamic crossover in an LFL [59], but we do not have a similar explanation here. In particular, the crossover observed here in the RN-AdS_4 theory occurs outside of the 'quantum liquid' regime $T \ll \mu$.

4.5 Dispersion relations at fixed temperature $T < \mu$

In the previous sections, we established how an increase in temperature affects the sound and diffusion modes that exist at some fixed, low momentum $q \ll \mu$. We now turn our attention to studying the dispersion relations of these modes at a fixed temperature T and chemical potential μ. This is done by fixing T/μ and varying $\bar{q}$.

4.5.1 The sound mode dispersion relation

In [70], the dispersion relation at $T = 0$ and $\bar{q} \ll 1$ was found numerically to be of the form (4.1) with $v_s = 1/\sqrt{2}$ and $\Gamma_0 = 0.083$, which is remarkably close to the dispersion relation expected from the 'zero temperature hydrodynamics' described in the introduction and in [70], which has $\Gamma_0 = 0.072$ rather than 0.083.

We found a dispersion relation of the form (4.4) to be valid for non-zero temperatures also. The quadratic coefficient of the attenuation Γ as a function of temperature is shown in figure 4.10. These results were obtained by fitting over the range $0.01 \leq \bar{q} \leq 0.5$, and an example of the fit for $T = 0.0219\mu$ is shown in figure 4.11.

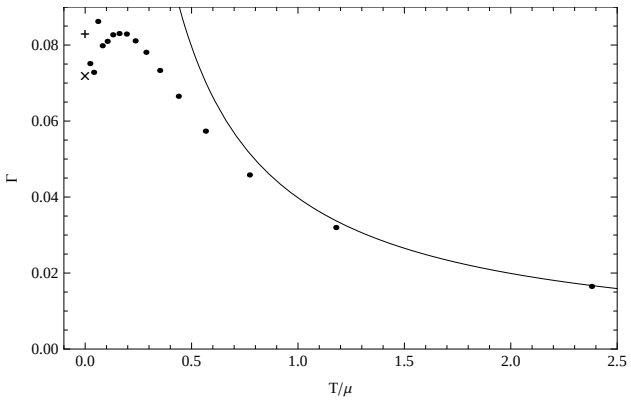

Figure 4.10: The temperature dependence of the quadratic term Γ in the imaginary part of the sound dispersion relation (4.4). Circles show our numerical results, the solid line shows the $\mu = 0$ analytic result (4.29), the '+' shows the $T = 0$ numerical result of [70] and the '×' shows the prediction of '$T = 0$ hydrodynamics'.

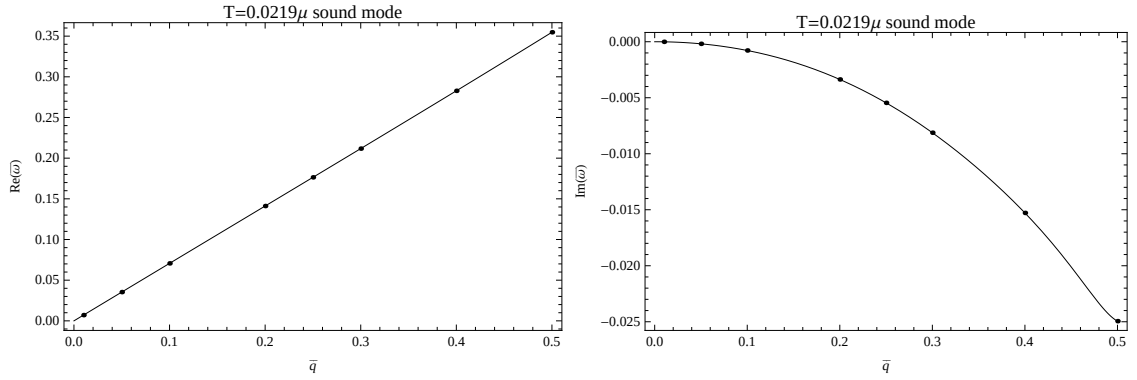

Figure 4.11: The dispersion relation of the sound mode at $T = 0.0219\mu$ for $0.01 \leq \bar{q} \leq 0.5$. The circles show our numerical results and the solid line is the best fit $\bar{\omega} \approx \bar{q}/\sqrt{2} - i0.075\bar{q}^2 + O(\bar{q}^3)$.

At high temperatures $T \gg \mu$, it agrees with the $\mu = 0$ result (4.29), and at low temperatures $T \ll \mu$ it approaches a similar value to the $T = 0$ result of [70]. Although our results at very low T do not match smoothly onto the $T = 0$ numerical result of [70], they differ only by around 10% and we believe that this is most likely caused by numerical inaccuracies, which grow as the temperature is lowered. The proximity of the numerical results to the prediction of '$T = 0$ hydrodynamics' is surprising — ultimately, an analytic calculation will be needed to determine whether these small discrepancies are due to inaccurate numerics, or whether this proximity is in fact a coincidence. The general trend of the results is clear however — as the temperature increases, the sound mode becomes more stable, as was observed in section 4.3.

When $\bar{q} \gtrsim 1$, this series form of the dispersion relation is useless. Figure 4.12 shows the dispersion relation of the sound mode when $q > \mu > T$, at two different temperatures: $T = 0$ and $T = 0.159\mu$. The dispersion relations have the same shape at both temperatures — the real part asymptotes to $\bar{\omega} = \bar{q}$, and the imaginary part tends to a constant, in the region $q \gg \mu > T$.

4.5.2 The diffusion mode dispersion relation

Recall that at non-zero temperatures, the branch cut along the negative imaginary frequency axis becomes a series of poles and that the most stable of these becomes the

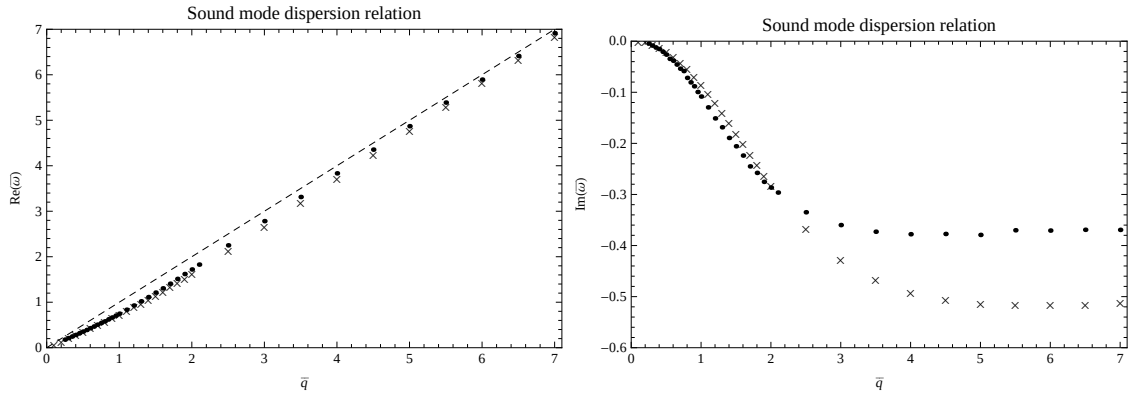

Figure 4.12: The dispersion relation of the sound mode at two different temperatures: $T = 0$ (circles) and $T = 0.159\mu$ (crosses). The dashed line is the line $\mathrm{Re}\,(\bar{\omega}) = \bar{q}$.

$\mu = 0$ diffusion mode at high temperatures. Figure 4.13a shows the imaginary part of the dispersion relation of this pole at two fixed, low temperatures $T = 0.0219\mu$ and $T = 0.159\mu$ (its real part is always zero). At both temperatures, the pole

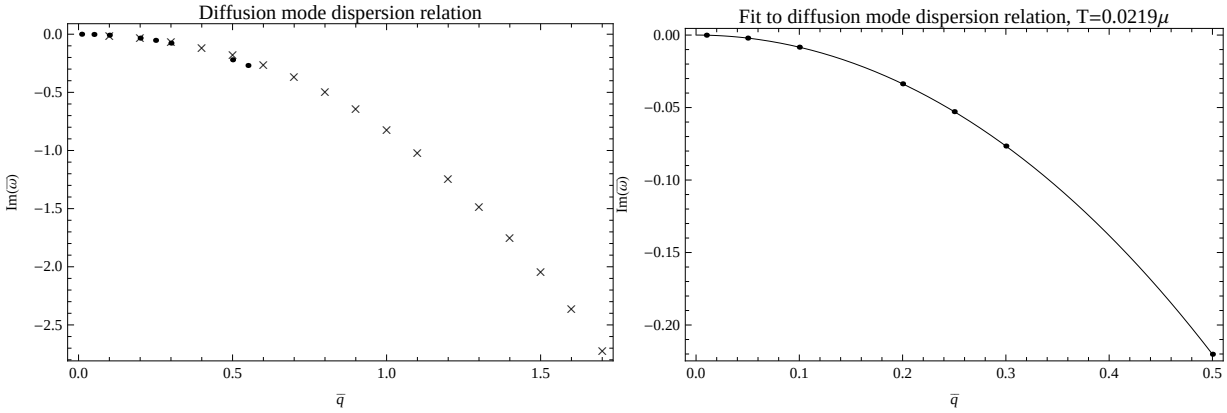

(a) Numerical results (b) Best fit

Figure 4.13: The dispersion relation of the diffusion mode at two different temperatures: $T = 0.0219\mu$ (circles) and $T = 0.159\mu$ (crosses) with the polynomial best fit at $T = 0.0219\mu$ shown also (solid line). We cannot track the $T = 0.0219\mu$ mode for as high momenta as the $T = 0.159\mu$ mode.

recedes quickly into the complex plane as the momentum is increased. Performing a polynomial fit to the imaginary part in the range $0.01 \leq \bar{q} \leq 0.5$ at the very low temperature $T = 0.0219\mu$, we found a dispersion relation of the form (4.5) with $D \approx 0.83$. The fit is shown in figure 4.13b. This therefore is an analogue, at low temperatures $T < q < \mu$, of the $\mu = 0$, $q \ll T$ hydrodynamic charge diffusion mode.

In fact, this quadratic form of the dispersion relation (4.5) is valid for all non-zero temperatures that we could access — the dependence of D upon T is shown in figure 4.14. We extracted D from a fit over the range $0.01 \leq \bar{q} \leq 0.5$. It decreases monatonically as the temperature is raised, in agreement with the results of section 4.4.1, and approaches the $\mu = 0$ result (4.30) in the limit $T \gg \mu$. Again, we note that this is despite the fact that we are studying the regime $\mu \gg q$.

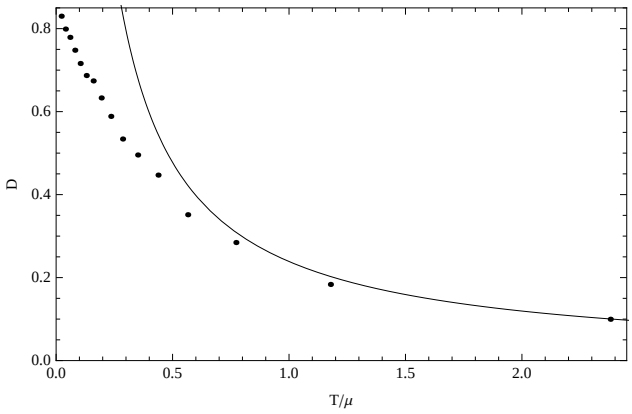

Figure 4.14: The temperature dependence of the quadratic coefficient D in the dispersion relation of the diffusion mode (4.5). The circles show our numerical results and the solid line is the analytic $\mu = 0$ result (4.30).

We could not obtain the numerical accuracy required to access non-zero temperatures lower than $T = 0.0219\mu$ and hence we cannot say whether the mode exists with a quadratic dispersion relation for arbitrarily low non-zero temperatures. We emphasise again that this mode does not exist at $T = 0$ itself (unlike the $T = 0$ 'R-spin diffusion' mode of [97]), as there is a branch cut in that case.

4.5.3 Dispersion relations of the secondary modes

Figures 4.15 and 4.16 show the dispersion relations of the second stablest ('secondary') propagating and purely imaginary modes at two different temperatures. These differ qualitatively from the sound and diffusion modes described above in that $\bar{\omega} \neq 0$ when $\bar{q} = 0$. At high momenta $q \gg \mu > T$, the propagating secondary modes have the same form as the sound modes — their real parts asymptote to

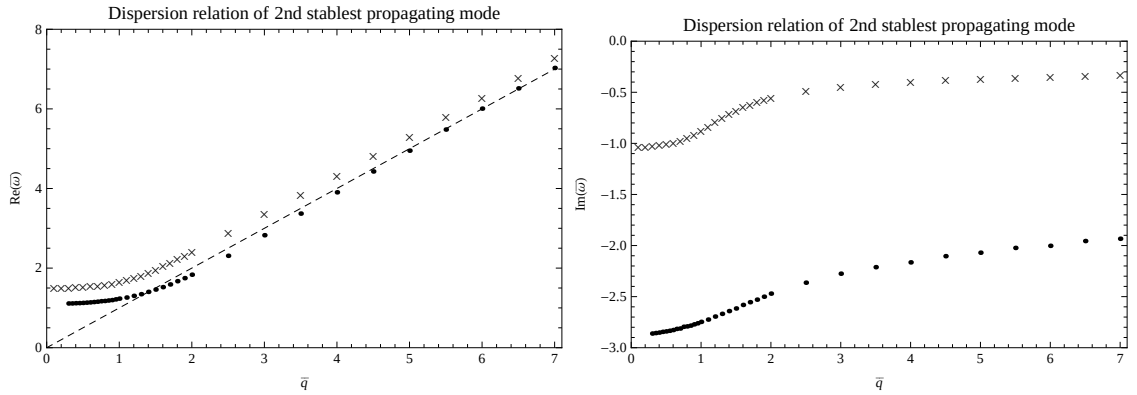

Figure 4.15: The dispersion relation of the second stablest propagating mode at two different temperatures: $T = 0$ (circles) and $T = 0.159\mu$ (crosses). The dashed line is the line $\mathrm{Re}\,(\bar{\omega}) = \bar{q}$.

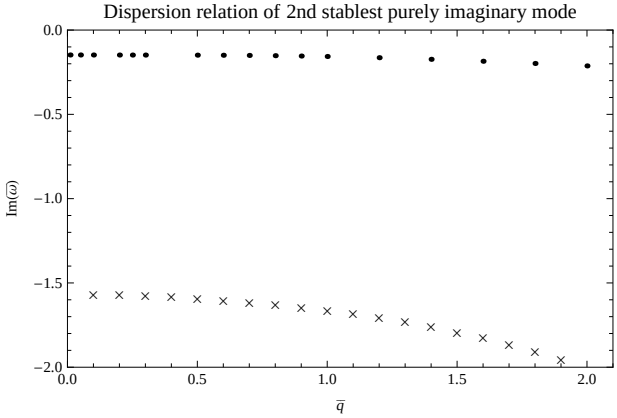

Figure 4.16: The dispersion relation of the second-stablest purely imaginary mode at two different temperatures: $T = 0.0219\mu$ (circles) and $T = 0.159\mu$ (crosses).

$\mathrm{Re}\,(\bar{\omega}) = \bar{q}$ and their imaginary parts tend to a constant. The purely imaginary secondary mode recedes into the complex plane as the momentum is increased, and the rate at which this happens increases with the temperature.

4.5.4 Movement of the poles in the complex frequency plane with q

It is instructive to view the simultaneous movements of these poles in the complex frequency plane as the momentum is increased. This is shown in figure 4.17 for $T = 0.159\mu$. We see that as $\bar{q}$ is increased, the purely imaginary modes both

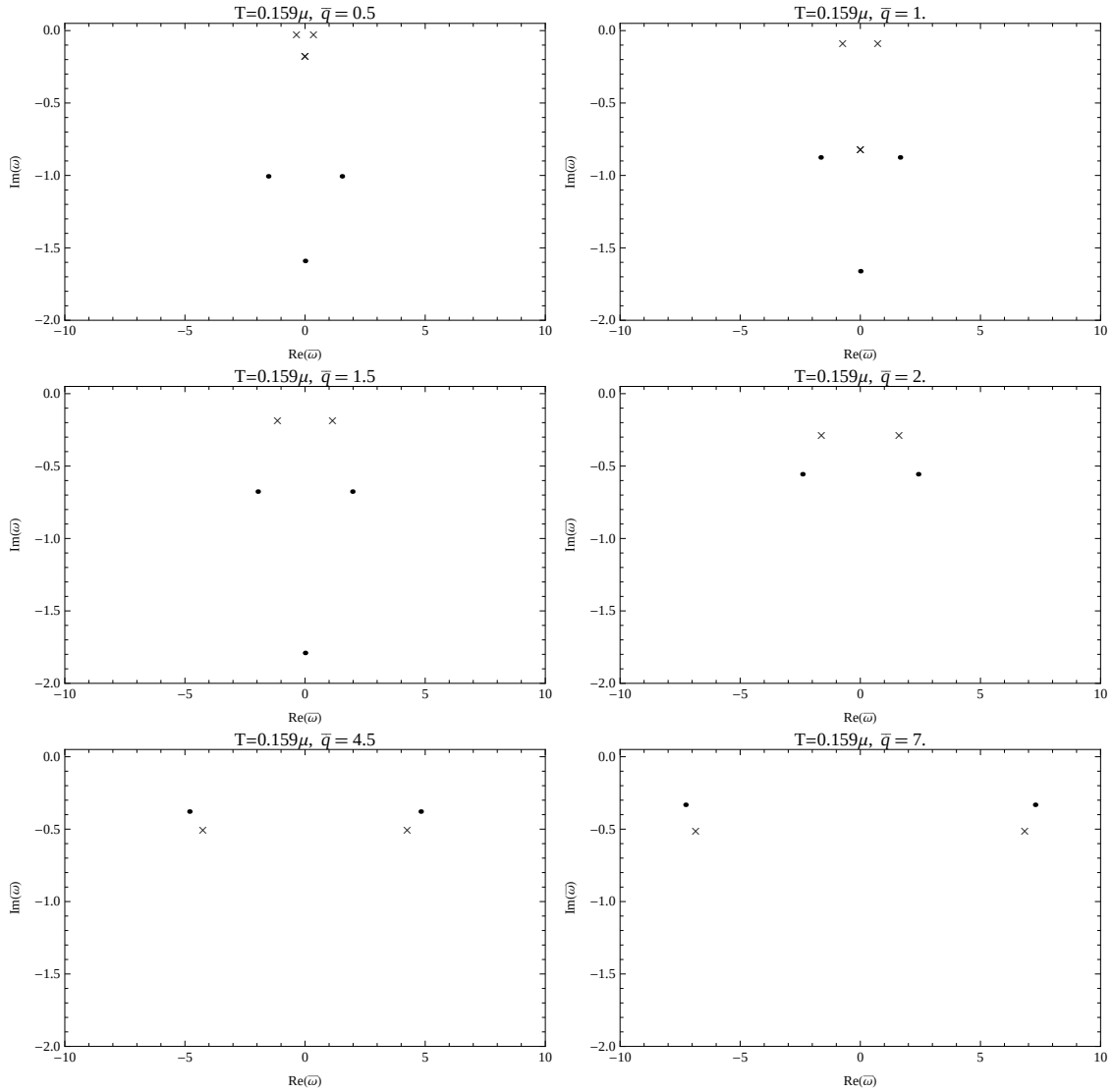

Figure 4.17: Movement of the six longest-lived modes in the complex frequency plane as a function of momentum, for fixed $T = 0.159\mu$. The crosses denote the sound and diffusion modes, and the circles denote the secondary propagating and imaginary modes. An animated version of this figure is available at `http://www.physics.ox.ac.uk/users/Davison/RNAdS4animations2.html`.

become less stable as described previously. This figure shows that the diffusion mode destabilises much quicker than the secondary imaginary mode. The propagating modes show a different behaviour — their speeds both increase but their imaginary parts move in opposite directions and begin to approach each other in the complex plane as $\bar{q}$ increases. They eventually cross, before moving off horizontally together along the relativistic trajectory $\mathrm{Re}\,(\bar{\omega}) = \bar{q}$. At these high values of $\bar{q}$ it is clear

that our original separation of modes into the stablest (sound and diffusion), second stablest etc. is of no value.

4.5.5 Variation of the spectral functions with q

Finally, we turn our attention to the spectral functions of the theory at low temperatures and as a function of the momentum $\bar{q}$. These are shown in figures 4.18 and 4.19 for $T = 0.159\mu$. At $\bar{q} = 0.5$, the lowest momentum shown, both spectral

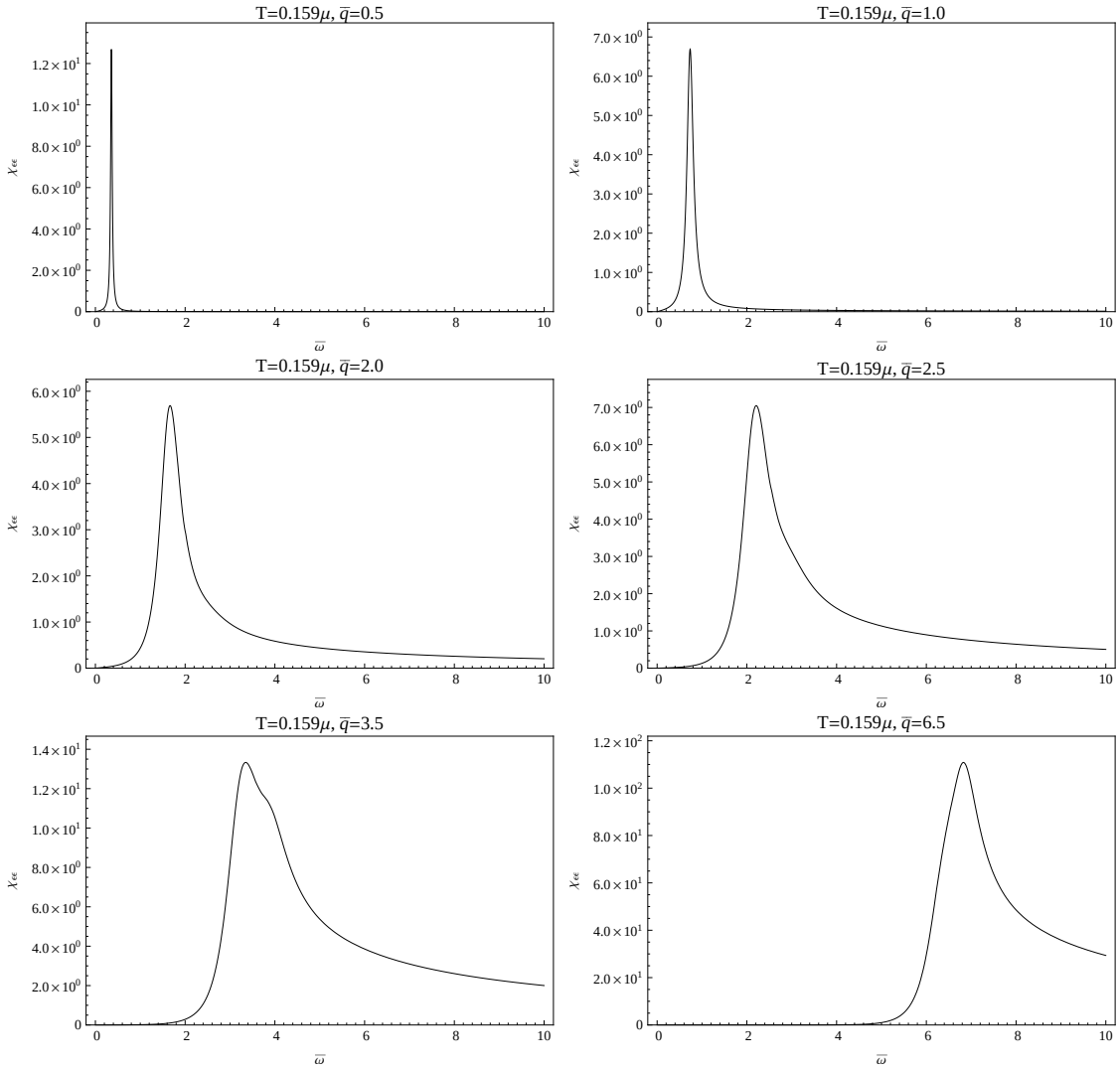

Figure 4.18: The energy density spectral function for $T = 0.159\mu$ as the momentum is increased, in units of $2\mu^2 r_0/\kappa_4^2$. As the momentum is increased, the peak due to sound propagation becomes less dominant. An animated version of this figure is available at `http://www.physics.ox.ac.uk/users/Davison/RNAdS4animations2.html`.

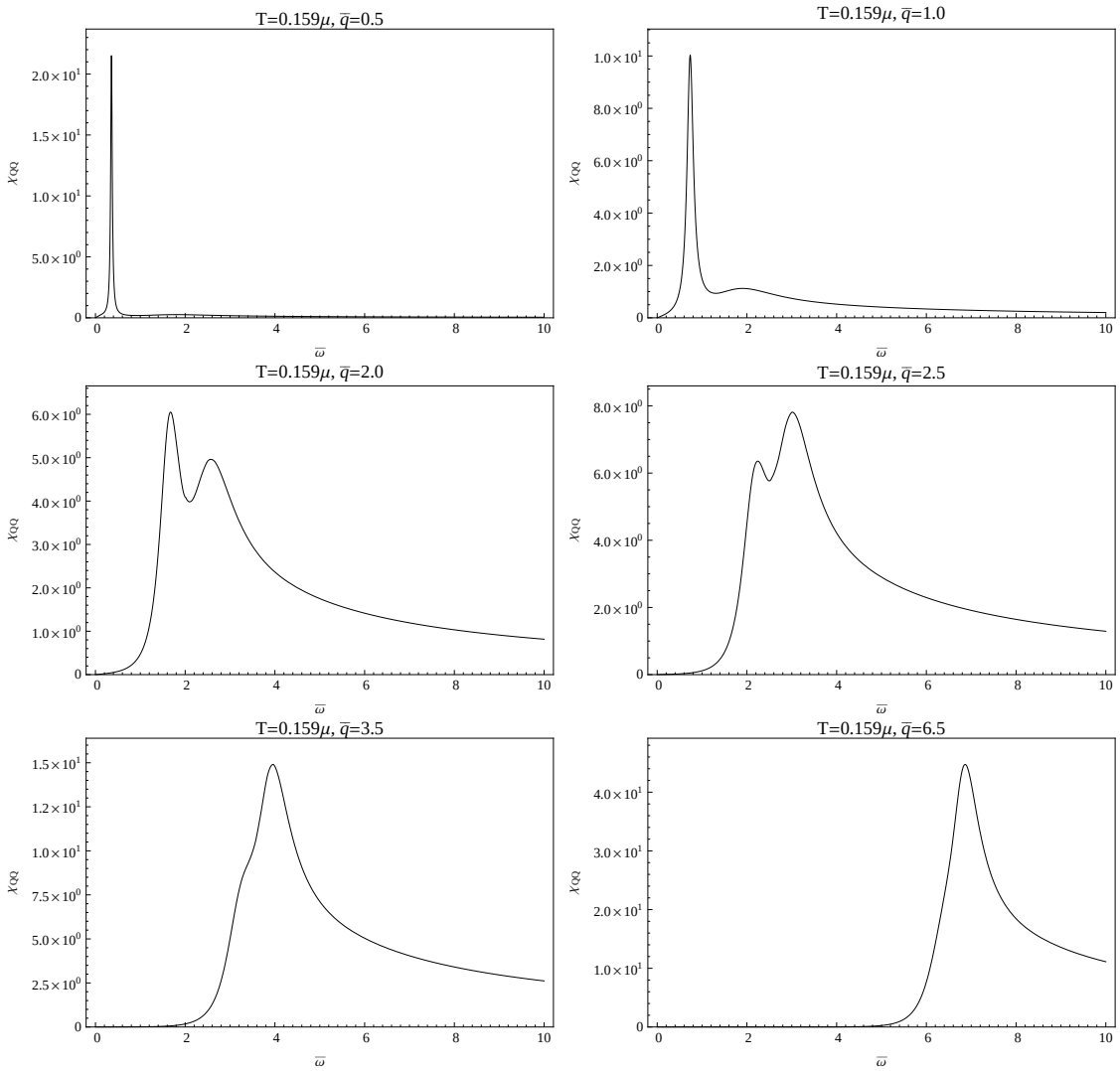

Figure 4.19: The charge density spectral function for $T = 0.159\mu$ as the momentum is increased, in units of $2r_0/\kappa_4^2$. As the momentum is increased, the peak due to sound propagation becomes less dominant. An animated version of this figure is available at `http://www.physics.ox.ac.uk/users/Davison/RNAdS4animations2.html`.

functions are completely dominated by the peak due to sound propagation. As the momentum is increased, this peak becomes smaller and wider and when $q \gtrsim \mu$, it no longer dominates the spectral function — a peak due to the secondary propagating mode also becomes visible. As the momentum is increased further, these two peaks merge into one peak which moves with speed $\mathrm{Re}\,(\bar{\omega}) = \bar{q}$ and constant width. This is a direct reflection of the two corresponding Green's function poles approaching each other in the complex plane. At high momenta, the value of the spectral function is

very small at low frequencies $\bar{\omega} \lesssim \bar{q}$ and it only becomes significant when $\bar{\omega} \gtrsim \bar{q}$. Note that there is no significant difference between the charge density and energy density spectral functions in this regime.

4.6 An effective hydrodynamic scale

As discussed previously, when $\mu = 0$ there is a long-lived sound mode with momentum q provided that $q \ll T$, and when $T = 0$ there is a long-lived sound mode provided that $q \ll \mu$. In the first instance, this is the regime of applicability of hydrodynamics and the condition on the momentum is such that the perturbations occur over much larger distance scales than the mean free path between thermal collisions.

We have studied the behaviour of the sound mode when both T and μ are non-zero, to determine if there is some 'effective hydrodynamic scale' (or effective mean free path) which determines whether sound propagation is possible or not in this more general case. Figure 4.20a is a contour plot showing the value of $|\mathrm{Im}\,(\bar{\omega})\,|/\mathrm{Re}\,(\bar{\omega})$ — which is the ratio of the decay rate to the propagating frequency — for the sound mode as a function of q/μ and q/T. Darker colours correspond to smaller values (i.e. more stable propagation). There is a clear pattern in the plot — provided that *one* of q/T or q/μ is small enough, there is stable sound propagation. It suggests that there is an 'effective hydrodynamic scale' governing sound propagation which is qualitatively of the form $E_{\text{eff.}} = T\left(a_0 + \ldots + a_\alpha\left(\mu/T\right)^\alpha + \ldots + a_1\mu/T\right)$ where $\alpha \in (0, 1)$. This reduces to the correct form in the $T = 0$ and $\mu = 0$ limits separately. A fit of the form $q/(a_0 T + a_1\mu)$ could not quantitatively reproduce the plot above — suggesting that this ansatz is an oversimplification (for example, it neglects almost all terms of the form $(\mu/T)^\alpha$ in the denominator as well as higher order terms in q) — but does give qualitatively the correct features for the sound propagation properties. Figure 4.20b shows the best fit to this form.

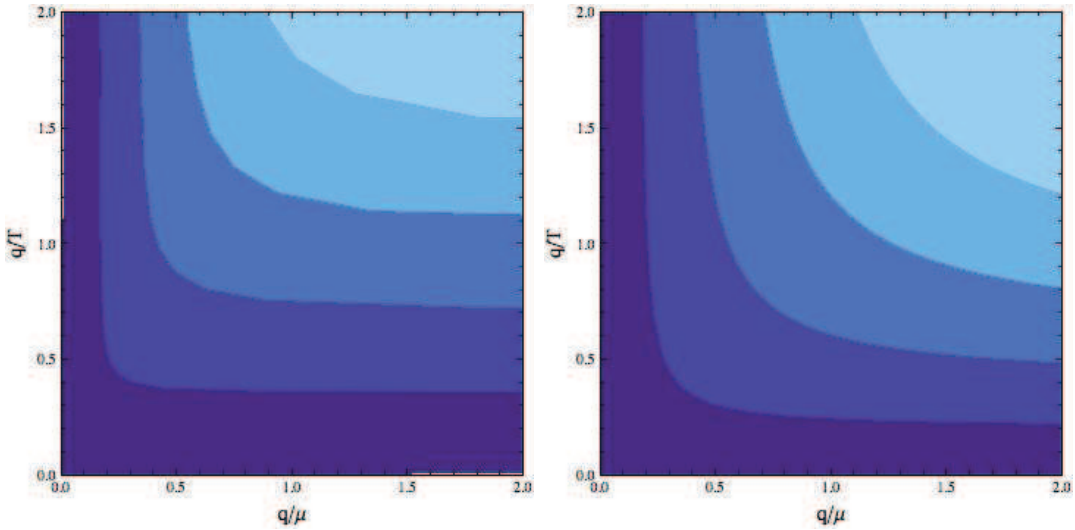

(a) Numerical results (b) Best fit

Figure 4.20: Contour plot showing $|\mathrm{Im}\,(\bar{\omega})\,|/\mathrm{Re}\,(\bar{\omega})$ for the sound mode as a function of q/μ and q/T and the best fit to these results: $a_0 = 10.1$ and $a_1 = 8.3$. Darker colours correspond to smaller values (i.e. more stable propagation) and the contours show the values 0.02, 0.04, 0.06, and 0.08.

An effective hydrodynamic scale of this form is also consistent with the fact that the region $q \ll \mu \ll T$ reproduces the $\mu = 0$, $q \ll T$ results, as we saw in section 4.3.

4.7 Conclusions and discussion

In summary, our main results are as follows:

i) When $q \ll \mu$, the long-lived modes of the charge density and energy density Green's functions are the sound and diffusion-like modes with dispersion relations (4.4) and (4.5) respectively.

ii) When $q \ll \mu$ and $T \ll \mu$, the attenuation of the sound mode shows no significant temperature dependence, unlike in the strongly-coupled D3/D7 field theory and in Landau's theory of Fermi liquids. When $q \ll \mu$ and $T \gg \mu$, the sound and diffusion dispersion relations are well-approximated by the $\mu = 0$ results of [117,119].

iii) When $q \ll \mu$, the energy density spectral function is dominated by the sound

peak at all temperatures, whereas the charge density spectral function undergoes a crossover from sound domination at low temperatures to diffusion domination at high temperatures. This crossover is due to the changing residue at each pole, and occurs at a temperature $T_{\text{cross}} \sim \mu^2/q \gg \mu$.

iv) When $q \gg \mu$ and $T \ll \mu$, the sound and diffusion modes no longer dominate the energy density and charge density spectral functions, and the effects of other modes become important.

v) When both μ and T are non-zero, a long-lived sound mode will propagate provided that its momentum q is much less than either μ or T.

Our results show that although many strongly-coupled field theories at large chemical potential (which have a gravitational dual) possess a $T = 0$ sound mode, these are not all LFL-like 'zero sound' modes (by which we mean that they don't have the properties shown in figure 1.3) as was the case in the D3/D7 theory. However, there is still the possibility that there could be universal behaviour of the sound mode within subsets of strongly-coupled field theories with a gravitational dual. We note that the density-dependent physics in the D3/D7 and RN-AdS_4 theories arise through different holographic mechanisms (see [99, 124] for further discussion of this). In the D3/D7 theory, the background metric is fixed and it is the gauge field action - the DBI action - which alters the equation of motion of the gauge field from the $\mu = 0$ Maxwell equation (whose only long-lived mode is the high temperature charge diffusion mode). In contrast to this, the gauge field equation of motion in the RN-AdS_4 theory departs from the $\mu = 0$ Maxwell equation via couplings to the bulk metric fluctuations. The other major difference between these two field theories is the number of spatial dimensions, but we don't expect that this will have a significant effect on the acoustic properties of the theory (provided that the number of spatial dimensions is greater than one).

It would be very interesting to check whether the low temperature sound modes in other probe brane theories [65–69] share the LFL-like properties of the D3/D7

theory. This would help to establish whether it is the form of the DBI action, which implies that the non-zero density in the field theory is a density of fundamental matter (at least in the cases where the background geometry can be derived from string theory) rather than, for example, the R-charge density in the RN-AdS_4 theory, that generates these interesting properties or not. The effects of metric backreaction (i.e. coupling between the field theory's charge density and energy density) are also yet to be computed for these probe brane theories. These may complete the LFL-like picture of acoustic propagation (by reproducing the full LFL sound attenuation curve - figure 1.3 - including the hydrodynamic regime), or they may result in deviations from it. We cannot gain any insight into this from our backreacted RN-AdS_4 results because of the difference in gauge field actions described previously. Although an expansion of the DBI action in powers of $F_{\mu\nu}$ yields the Maxwell action at lowest order, in field theory quantities this is an expansion in powers of μ/T which is the opposite limit from that in which any LFL-like properties of a theory would be exhibited.

In addition to those mentioned above, there are numerous other field theories with a gravitational dual which may possess interesting sound modes when $T \ll \mu$. Among the most interesting of these are dilatonic black holes (for example [124–126]) and geometries where the bulk charge density is sourced by fermions (for example [100,121,127–129]). It would also be worthwhile to determine the acoustic properties of more general truncations of supergravity which admit more complicated solutions than RN-AdS_4 (for example, those of [120, 125, 130]), to determine whether the specific truncation chosen has a significant effect on these properties.

We have seen that even this relatively simple holographic theory has many non-trivial features in its bosonic excitations. Among the most intriguing are the accuracy of the 'zero temperature hydrodynamics', and the crossover temperature $T_{\text{cross.}} \sim \mu^2/q$ between the charge density spectral function being dominated by the sound mode and the diffusion mode. It would be useful to have a clearer physical

understanding of these properties, and also to determine if they are present in other field theories at non-zero chemical potential.

4.A Appendices

4.A.1 Equations of motion and action

This appendix contains the equations of motion and action used to compute our $T > 0$ numerical results.

Equations of motion

There are two linearly-independent, coupled equations of motion for $\bar{Z}_1(u, \bar{\omega}, \bar{q})$ and $\bar{Z}_2(u, \bar{\omega}, \bar{q})$ which can be written in the form

$$\begin{aligned} \bar{Z}_1''(u) + A_1\bar{Z}_1'(u) + A_2\bar{Z}_2'(u) + A_3\bar{Z}_1(u) + A_4\bar{Z}_2(u) = 0, \\ \bar{Z}_2''(u) + B_1\bar{Z}_1'(u) + B_2\bar{Z}_2'(u) + B_3\bar{Z}_1(u) + B_4\bar{Z}_2(u) = 0, \end{aligned} \tag{4.32}$$

where we have suppressed the dependence of $\bar{Z}_{1,2}$ on $\bar{\omega}$ and $\bar{q}$, and the coefficients are

$$\begin{aligned} A_1 &= \frac{u^5 f'(u)\bar{\omega}^2 + 2f(u)\left[Q^2\bar{q}^2 + u^4\left(\bar{\omega}^2 - f(u)\bar{q}^2\right)\right]}{u^5 f(u)\left(\bar{\omega}^2 - f(u)\bar{q}^2\right)}, \\ A_2 &= -i\bar{q}\frac{u^5 f'(u)\bar{q}^2 + 2\left[Q^2\bar{q}^2 - u^4\left(\bar{\omega}^2 - f(u)\bar{q}^2\right)\right]}{u^6\left(\bar{\omega}^2 - f(u)\bar{q}^2\right)\left[uf'(u)\bar{q}^2 - 4\left(\bar{\omega}^2 - f(u)\bar{q}^2\right)\right]}, \\ A_3 &= \frac{Q^2\left[u^2\left(\bar{\omega}^2 - f(u)\bar{q}^2\right) - 4f(u)\right]}{u^6 f(u)^2} + \frac{4Q^2\bar{q}^2}{u^6\left(\bar{\omega}^2 - f(u)\bar{q}^2\right)} \\ &\quad + \frac{8Q^2\bar{q}^2\left[u^4\left(\bar{\omega}^2 - f(u)\bar{q}^2\right) + Q^2\bar{q}^2\right]}{u^{10}\left(\bar{\omega}^2 - f(u)\bar{q}^2\right)\left[uf'(u)\bar{q}^2 - 4\left(\bar{\omega}^2 - f(u)\bar{q}^2\right)\right]}, \\ A_4 &= i\bar{q}\frac{4Q^2 + u^5 f'(u)}{u^7 f(u)\left[uf'(u)\bar{q}^2 - 4\left(\bar{\omega}^2 - f(u)\bar{q}^2\right)\right]}, \\ B_1 &= -i\bar{q}\frac{2Q^2\left[uf'(u)\bar{q}^2 - 4\left(\bar{\omega}^2 - f(u)\bar{q}^2\right)\right]}{u^4\left(\bar{\omega}^2 - f(u)\bar{q}^2\right)}, \end{aligned} \tag{4.33}$$

$$
\begin{aligned}
B_2 = & \frac{1}{u^5 f(u)\left(\bar{\omega}^2 - f(u)\bar{q}^2\right)\left[uf'(u)\bar{q}^2 - 4\left(\bar{\omega}^2 - f(u)\bar{q}^2\right)\right]}\Bigg\{-16u^4 f(u)^3\bar{q}^4 \\
& + 2f(u)^2\bar{q}^2\left[-4Q^2\bar{q}^2 + 16u^4\bar{\omega}^2 + u^5\left(f'(u) + uf''(u)\right)\bar{q}^2\right] \\
& - f(u)\Big[-8Q^2\bar{q}^2\bar{\omega}^2 + 16u^4\bar{\omega}^4 + u\bar{q}^2\Big\{f'(u)\Big(2Q^2\bar{q}^2 - 2u^4\bar{\omega}^2 + u^5 f'(u)\bar{q}^2\Big) \\
& + 2u^5 f''(u)\bar{\omega}^2\Big\}\Big] + u^5 f'(u)\bar{\omega}^2\left[uf'(u)\bar{q}^2 - 4\bar{\omega}^2\right]\Bigg\}, \\
B_3 = & \frac{8iQ^2\bar{q}}{u^9 f(u)\left(\bar{\omega}^2 - f(u)\bar{q}^2\right)\left[uf'(u)\bar{q}^2 - 4\left(\bar{\omega}^2 - f(u)\bar{q}^2\right)\right]}\Bigg\{u^5 f'(u)\bar{\omega}^2[uf'(u)\bar{q}^2 - 4\bar{\omega}^2] \\
& - f(u)\bar{q}^2\left[-4Q^2\bar{\omega}^2 + uf'(u)\left(Q^2\bar{q}^2 - 3u^4\bar{\omega}^2 + u^5 f'(u)\bar{q}^2\right) + u^6 f''(u)\bar{\omega}^2\right] \\
& + f(u)^2\bar{q}^4\left[-4Q^2 + u^5\left(f'(u) + uf''(u)\right)\right]\Bigg\}, \\
B_4 = & \frac{1}{u^4 f(u)^2\left[uf'(u)\bar{q}^2 - 4\left(\bar{\omega}^2 - f(u)\bar{q}^2\right)\right]}\Bigg\{-4Q^2 f(u)^2\bar{q}^4 + Q^2\bar{\omega}^2\left[uf'(u)\bar{q}^2 - 4\bar{\omega}^2\right] \\
& + f(u)\bar{q}^2\left[8Q^2\bar{\omega}^2 + uf'(u)\left(u^4 f''(u) + 5u^3 f'(u) - Q^2\bar{q}^2\right)\right]\Bigg\}.
\end{aligned}
\tag{4.34}
$$

Action

In these variables, the off-shell action to quadratic order in the fluctuations is of the form

$$
\begin{aligned}
S = \frac{r_0}{2\kappa_4^2}\int_1^\infty du\frac{d\omega d^2q}{(2\pi)^3}\Big[& \mathcal{G}_{11}\partial_u\bar{Z}_1(u,-\bar{\omega},-\bar{q})\partial_u\bar{Z}_1(u,\bar{\omega},\bar{q}) + \mathcal{G}_{12}\partial_u\bar{Z}_1(u,-\bar{\omega},-\bar{q})\partial_u\bar{Z}_2(u,\bar{\omega},\bar{q}) \\
& + \mathcal{G}_{21}\partial_u\bar{Z}_2(u,-\bar{\omega},-\bar{q})\partial_u\bar{Z}_1(u,\bar{\omega},\bar{q}) + \mathcal{G}_{22}\partial_u\bar{Z}_2(u,-\bar{\omega},-\bar{q})\partial_u\bar{Z}_2(u,\bar{\omega},\bar{q}) \\
& + \ldots\Big],
\end{aligned}
\tag{4.35}
$$

where the coefficients are

$$
\begin{aligned}
\mathcal{G}_{11} &= \frac{2u^2 f(u)}{\bar{\omega}^2 - f(u)\bar{q}^2}, \\
\mathcal{G}_{12} &= -\frac{2i\bar{q}uf(u)}{\left(\bar{\omega}^2 - f(u)\bar{q}^2\right)\left[-4\left(\bar{\omega}^2 - f(u)\bar{q}^2\right) + uf'(u)\bar{q}^2\right]}, \\
\mathcal{G}_{21} &= -\mathcal{G}_{12},
\end{aligned}
\tag{4.36}
$$

$$\mathcal{G}_{22} = \frac{2u^4 f(u)\left[(\bar{\omega}^2 - f(u)\bar{q}^2) + \frac{\bar{q}^2 Q^2}{u^4}\right]}{Q^2\left(\bar{\omega}^2 - f(u)\bar{q}^2\right)\left[-4\left(\bar{\omega}^2 - f(u)\bar{q}^2\right) + \bar{q}^2 u f'(u)\right]^2}, \tag{4.37}$$

and the ellipsis represents terms with less than two u derivatives (which cannot generically be written in terms of these gauge-invariant variables). These coefficients, combined with the equations of motion listed previously, allow us to compute the Green's function's poles and spectral functions $\chi_{\epsilon\epsilon}$, χ_{QQ} by following the method of section 2.3. Note that the counterterms in (4.6) (listed, for example, in [70]) do not affect these quantities.

The numerical check described in section 2.3 relies on the coefficients of the one-derivative terms in the action in addition to the two-derivative terms. Hence to obtain a numerical check in our gauge-invariant formalism, we added a boundary 'counterterm' (distinct from those mentioned previously) to the off-shell action of the form

$$S^{\text{c.t.}} = \frac{r_0}{2\kappa_4^2}\int du \frac{d\omega d^2 q}{(2\pi)^3}\frac{d}{du}\left[\phi_I\left(u,-\bar{\omega},-\bar{q}\right)\mathcal{D}^{\text{c.t.}}_{IJ}\left(u,\bar{\omega},\bar{q}\right)\phi_J\left(u,\bar{\omega},\bar{q}\right)\right], \tag{4.38}$$

where $\mathcal{D}^{\text{c.t.}}_{IJ}\left(u,\bar{\omega},\bar{q}\right)$ was chosen such that the full off-shell action could then be written in terms of the gauge-invariant variables $\bar{Z}_{1,2}$. This boundary term does not alter the equations of motion and as the coefficients $\mathcal{D}^{\text{c.t.}}_{IJ}$ are purely real, it does not have any effect upon the poles of the Green's functions or the diagonal spectral functions $\chi_{\epsilon\epsilon}$ and χ_{QQ}. We do not list the coefficients here as they are very lengthy and do not directly affect the results presented. For our numerical computations, we found it more convenient to use the radial co-ordinate $z \equiv 1/u$.

4.A.2 Leaver's Method

As was discussed in section 2.3, the case of a $T = 0$ horizon is qualitatively different to that of a $T \neq 0$ horizon as the radial position of the horizon r_H becomes an irregular singular point of the differential equations governing the fluctuations of

the fields in this limit. To avoid the difficulties of numerically integrating around an irregular singular point, one can use 'Leaver's method' — a discretised approach that does not involve numerical integration [131, 132].[7]

To illustrate Leaver's method, let us begin with the simple case of a single field $\varphi(r, \bar{\omega}, \bar{q})$ which has been normalised such that its leading term near the boundary of the AdS spacetime is a constant. A quasinormal mode of the gravitational theory (i.e. a pole of the Green's function in the dual field theory) is then a solution to the equation of motion for $\varphi(r, \bar{\omega}, \bar{q})$ which satisfies ingoing boundary conditions near the horizon and whose leading (constant) term near the boundary vanishes. For a fixed momentum, we expect such quasinormal modes to exist for a discrete set of frequencies.

Leaver's method works as follows. One should first choose a radial co-ordinate $\mathfrak{r}$ such that the radial direction now spans the range $\mathfrak{r} : 0 \to 1$ where $\mathfrak{r} = 1$ is the horizon of the spacetime and $\mathfrak{r} = 0$ is the boundary. We assume that $\mathfrak{r} = \frac{1}{2}$ is an ordinary point of the ordinary differential equation for $\varphi(\mathfrak{r}, \bar{\omega}, \bar{q})$. One should then make the ansatz for a quasinormal mode solution to the fluctuation equation

$$\varphi(\mathfrak{r}, \bar{\omega}, \bar{q}) = \varphi_{\text{in}}(\mathfrak{r}, \bar{\omega})\, \varphi_{\text{QNM}}(\mathfrak{r}, \bar{\omega}, \bar{q}) \sum_{n=0}^{n_{\text{max.}}} \varphi_n(\bar{\omega}, \bar{q}) \left(\mathfrak{r} - \frac{1}{2}\right)^n , \tag{4.39}$$

where $\varphi_{\text{in}}(\mathfrak{r}, \bar{\omega})$ is the ingoing solution in the near-horizon limit $\mathfrak{r} \to 1$, $\varphi_{\text{QNM}}(\mathfrak{r}, \bar{\omega}, \bar{q})$ is the solution in the near-boundary limit $\mathfrak{r} \to 0$ whose leading (constant) term vanishes and the coefficients of the power series expansion φ_n are independent of $\mathfrak{r}$. By ansatz this is a quasinormal mode and we expect such solutions to exist only for certain $\bar{\omega}$ and $\bar{q}$. To search for these solutions, one should substitute this ansatz into the equation of motion for φ and expand this equation in a power series around $\mathfrak{r} = \frac{1}{2}$ to order $n_{\text{max.}}$. This gives $n_{\text{max.}} + 1$ equations for the $n_{\text{max.}} + 1$ coefficients $\varphi_n(\bar{\omega}, \bar{q})$. These may be written in a matrix form $L_{mn}(\bar{\omega}, \bar{q})\, \varphi_n(\bar{\omega}, \bar{q}) = 0$ where $L(\bar{\omega}, \bar{q})$ is an $(n_{\text{max.}} + 1) \times (n_{\text{max.}} + 1)$ square matrix with coefficients $L_{mn}(\bar{\omega}, \bar{q})$ equal to the

[7] This method works equally when the singular point is not irregular.

coefficient of $\left(\mathfrak{r}-\frac{1}{2}\right)^m \varphi_n$ in the equation of motion. A non-trivial quasinormal mode solution thus exists when

$$\det\left[L\left(\bar{\omega},\bar{q}\right)\right]=0. \tag{4.40}$$

This is Leaver's method for finding the quasinormal modes. In practice, one constructs det$L$ numerically over a range of $\bar{\omega}$ and $\bar{q}$, and searches for zeroes of this determinant. The accuracy of the procedure can be increased by increasing $n_{\text{max.}}$

Note that Leaver's method only works *if there are no singular points in the differential equation lying within the circle with radius* $\frac{1}{2}$ *centred on the point* $\mathfrak{r}=\frac{1}{2}$ *in the complex* $\mathfrak{r}$ *plane.* If this condition is not satisfied, the power series expansion around $\mathfrak{r}=\frac{1}{2}$ is not convergent up to $\mathfrak{r}=0,1$ where we require the relevant boundary conditions to be satisfied.

The equations for the fundamental fluctuations $h_{\mu\nu}$ and a_μ may be written in a form amenable to the application of Leaver's method by first writing the equations for the gauge-invariant Kodama-Ishibashi variables, which are formed from the fundamental fluctuations and their radial derivatives, and then using new variables consisting of linear combinations of the Kodama-Ishibashi variables and their derivatives. This yields two decoupled equations of motion from which the poles of the Green's functions may be obtained. We refer the reader to [70] for more details.

Chapter 5

Conclusions

In this thesis, we have reviewed the concept of gauge/gravity duality and explained how it can be used to compute the properties of strongly-interacting field theories from classical theories of gravity. In particular, we have described in detail how to determine the thermodynamic properties and low-energy excitations of holographic quantum liquids — strongly-interacting theories with a large density of matter.

Holographic quantum liquids are a very useful theoretical laboratory for studying strongly-coupled phases of matter, which are inaccessible via the usual perturbative tools of condensed matter physics. Of particular interest is what kinds of properties are possible in such phases, and how these compare to those of the conventional quantum liquids and to the unexplained phases of matter observed experimentally.

In chapters 3 and 4, we have presented original results of an investigation of the low-energy charge density excitations in two holographic quantum liquids. The first of these, studied in chapter 3, is the theory dual to N_f D7-branes embedded in the Schwarzschild-AdS_5 background generated by N_c D3-branes, in the probe limit $N_f \ll N_c$. We found that the charge density excitations of this theory are remarkably similar to those in a Landau Fermi liquid. At low temperatures $\omega \gg T^2/\mu$, the dominant charge density excitation in this liquid is a propagating holographic zero sound mode. The speed of this mode is equal to the speed of hydrodynamic sound,

and its attenuation is of the form $\sim \omega^2 + T^2$. In contrast to this, the charge density response is dominated by a diffusion mode at high temperatures $\omega \ll T^2/\mu$. When $\omega \sim T^2/\mu$, there is a crossover between these two regimes which is most explicitly seen by examining the poles of the charge density correlator in the complex ω plane — the holographic zero sound poles collide and form a diffusive pole.

These properties are remarkably similar to those of a Landau Fermi liquid, which has a low-temperature 'zero sound' mode due to an oscillation of the Fermi surface. The attenuation of this mode $\sim \omega^2 + T^2$ is a result of the quantum and thermal interactions of the fermionic quasiparticles, and when the thermal interactions become sufficiently frequent (at $\omega \sim T^2/\mu$), the liquid undergoes a collisionless/hydrodynamic crossover in which the zero sound mode becomes highly unstable and is replaced by hydrodynamic sound and diffusion modes. This similarity is puzzling, as the holographic quantum liquid is *not* a Landau Fermi liquid. Although the comparison above yields a nice interpretation of its charge density excitations, it is unknown if this holographic quantum liquid even possesses a Fermi surface.

In chapter 4, we studied the coupled charge density and energy density excitations of a qualitatively different holographic quantum liquid — that which is dual to the Reissner-Nordström-AdS_4 black hole solution to Einstein-Maxwell theory with a cosmological constant. We found that the holographic zero sound mode present in this theory at $T = 0$ does *not* behave like that of a Landau Fermi liquid as one increases the temperature. For example, the attenuation of this mode is approximately temperature independent when $T \ll \mu$, and there is no analogue of a collisionless/hydrodynamic crossover. This is consistent with the other properties of this theory which indicate that it is not a Landau Fermi liquid. We performed a detailed analysis of the poles of the charge density and energy density Green's functions and spectral functions in this theory, emphasising the link between them.

Bibliography

[1] J. M. Maldacena, *The Large N limit of superconformal field theories and supergravity*, *Adv.Theor.Math.Phys.* **2** (1998) 231–252, [hep-th/9711200].

[2] G. 't Hooft, *Dimensional reduction in quantum gravity*, gr-qc/9310026.

[3] L. Susskind, *The World as a hologram*, *J.Math.Phys.* **36** (1995) 6377–6396, [hep-th/9409089].

[4] R. Bousso, *The Holographic principle*, *Rev.Mod.Phys.* **74** (2002) 825–874, [hep-th/0203101].

[5] G. Policastro, D. Son, and A. Starinets, *The Shear viscosity of strongly coupled N=4 supersymmetric Yang-Mills plasma*, *Phys.Rev.Lett.* **87** (2001) 081601, [hep-th/0104066].

[6] P. Kovtun, D. Son, and A. Starinets, *Viscosity in strongly interacting quantum field theories from black hole physics*, *Phys.Rev.Lett.* **94** (2005) 111601, [hep-th/0405231].

[7] D. T. Son and A. O. Starinets, *Viscosity, Black Holes, and Quantum Field Theory*, *Ann.Rev.Nucl.Part.Sci.* **57** (2007) 95–118, [arXiv:0704.0240].

[8] S. Sachdev, *What can gauge-gravity duality teach us about condensed matter physics?*, *Ann.Rev.Condensed Matter Phys.* **3** (2012) 9–33, [arXiv:1108.1197].

[9] J. Polchinski, *String theory. Vol. 2: Superstring theory and beyond.* Cambridge University Press, Cambridge, 1998.

[10] C. Johnson, *D-branes.* Cambridge University Press, Cambridge, 2003.

[11] K. Becker, M. Becker, and J. Schwarz, *String theory and M-theory: A modern introduction.* Cambridge University Press, Cambridge, 2007.

[12] I. R. Klebanov, *TASI lectures: Introduction to the AdS / CFT correspondence*, `hep-th/0009139`.

[13] E. D'Hoker and D. Z. Freedman, *Supersymmetric gauge theories and the AdS / CFT correspondence*, `hep-th/0201253`.

[14] G. T. Horowitz and J. Polchinski, *Gauge/gravity duality*, `gr-qc/0602037`.

[15] H. Nastase, *Introduction to AdS-CFT*, `arXiv:0712.0689`.

[16] J. McGreevy, *Holographic duality with a view toward many-body physics*, *Adv.High Energy Phys.* **2010** (2010) 723105, [`arXiv:0909.0518`].

[17] E. Witten, *Bound states of strings and p-branes*, *Nucl.Phys.* **B460** (1996) 335–350, [`hep-th/9510135`].

[18] I. R. Klebanov, *World volume approach to absorption by nondilatonic branes*, *Nucl.Phys.* **B496** (1997) 231–242, [`hep-th/9702076`].

[19] S. S. Gubser, I. R. Klebanov, and A. A. Tseytlin, *String theory and classical absorption by three-branes*, *Nucl.Phys.* **B499** (1997) 217–240, [`hep-th/9703040`].

[20] S. Kovacs, *N=4 supersymmetric Yang-Mills theory and the AdS / SCFT correspondence*, `hep-th/9908171`.

[21] G. T. Horowitz and A. Strominger, *Black strings and P-branes*, *Nucl.Phys.* **B360** (1991) 197–209.

[22] O. Aharony, S. S. Gubser, J. M. Maldacena, H. Ooguri, and Y. Oz, *Large N field theories, string theory and gravity*, *Phys.Rept.* **323** (2000) 183–386, [hep-th/9905111].

[23] S. Gubser, I. R. Klebanov, and A. M. Polyakov, *Gauge theory correlators from noncritical string theory*, *Phys.Lett.* **B428** (1998) 105–114, [hep-th/9802109].

[24] E. Witten, *Anti-de Sitter space and holography*, *Adv.Theor.Math.Phys.* **2** (1998) 253–291, [hep-th/9802150].

[25] K. Skenderis, *Lecture notes on holographic renormalization*, *Class.Quant.Grav.* **19** (2002) 5849–5876, [hep-th/0209067].

[26] P. Breitenlohner and D. Z. Freedman, *Positive Energy in anti-De Sitter Backgrounds and Gauged Extended Supergravity*, *Phys.Lett.* **B115** (1982) 197.

[27] E. Witten, *Anti-de Sitter space, thermal phase transition, and confinement in gauge theories*, *Adv.Theor.Math.Phys.* **2** (1998) 505–532, [hep-th/9803131].

[28] A. Chamblin, R. Emparan, C. V. Johnson, and R. C. Myers, *Charged AdS black holes and catastrophic holography*, *Phys.Rev.* **D60** (1999) 064018, [hep-th/9902170].

[29] M. Cvetic and S. S. Gubser, *Phases of R charged black holes, spinning branes and strongly coupled gauge theories*, *JHEP* **9904** (1999) 024, [hep-th/9902195].

[30] D. T. Son and A. O. Starinets, *Minkowski space correlators in AdS / CFT correspondence: Recipe and applications*, *JHEP* **0209** (2002) 042, [hep-th/0205051].

[31] C. Herzog and D. Son, *Schwinger-Keldysh propagators from AdS/CFT correspondence*, *JHEP* **0303** (2003) 046, [hep-th/0212072].

[32] L. D. Landau, *Oscillations in a Fermi liquid*, *Zh. Eksp. Teor. Fiz.* **32** (1957) 59. Soviet Phys. - JETP **5**, 101 (1959).

[33] A. A. Abrikosov and I. M. Khalatnikov, *The theory of a fermi liquid (the properties of ^{3}He at low temperatures)*, *Rep. Prog. Phys.* **22** (1959) 329.

[34] D. Pines and P. Nozières, *The theory of quantum liquids*. W. A. Benjamin, New York, 1966.

[35] A. A. Abrikosov, L. P. Gorkov, and I. E. Dzyaloshinski, *Methods of quantum field theory in statistical physics*. Dover, New York, 1968.

[36] P. Morel and P. Nozieres, *Lifetime Effects in Condensed Helium-3*, *Phys.Rev.* **126** (1962) 1909–1918.

[37] W. Abel, A. Anderson, and J. Wheatley, *Propagation of Zero Sound in Liquid He-3 at Low Temperatures*, *Phys.Rev.Lett.* **17** (1966) 74–78.

[38] E. R. Dobbs, *Helium Three*. Oxford University Press, Oxford, 2000.

[39] J. Polchinski, *Effective field theory and the Fermi surface*, `hep-th/9210046`.

[40] R. Shankar, *Renormalization group approach to interacting fermions*, *Rev.Mod.Phys.* **66** (1994) 129–192.

[41] S. Sachdev and B. Keimer, *Quantum Criticality*, *Phys.Today* **64N2** (2011) 29, [`arXiv:1102.4628`].

[42] S. Kasahara, T. Shibauchi, K. Hashimoto, K. Ikada, S. Tonegawa, R. Okazaki, H. Ikeda, H. Takeya, K. Hirata, T. Terashima, and Y. Matsuda, *Evolution from Non-Fermi to Fermi Liquid Transport Properties by Isovalent Doping in $BaFe_2(As_{1-x}P_x)_2$ Superconductors*, *Phys. Rev.* **B81** (2010) 184519, [`arXiv:0905.4427`].

[43] N. Doiron-Leyraud, P. Auban-Senzier, S. R. de Cotret, C. Bourbonnais, D. Jérome, K. Bechgaard, and L. Taillefer, *Correlation between linear resistivity and T_c in the Bechgaard salts and the pnictide superconductor $Ba(Fe_{1-x}Co_x)_2As_2$*, *Phys. Rev.* **B80** (2009) 214531, [arXiv:0912.0559].

[44] R. Cooper, Y. Wang, B. Vignolle, O. Lipscombe, S. Hayden, Y. Tanabe, T. Adachi, Y. Koike, M. Nohara, H. Takagi, C. Proust, and N. Hussey, *Anomalous Criticality in the Electrical Resistivity of $La_{2-x}Sr_xCuO_4$*, *Science* **323** (2009) 603.

[45] S. Grigera, R. Perry, A. Schofield, M. Chiao, S. Julian, G. Lonzarich, S. Ikeda, Y. Maeno, A. Millis, and A. Mackenzie, *Magnetic Field-Tuned Quantum Criticality in the Metallic Ruthenate $Sr_3Ru_2O_7$*, *Science* **294** (2001) 329.

[46] J. Bardeen, *Electrical conductivity of metals*, *Journal of Applied Physics* **11** (1940) 88.

[47] S. Sachdev, M. A. Metlitski, Y. Qi, and C. Xu, *Fluctuating spin density waves in metals*, *Phys.Rev.* **B80** (2009) 155129, [arXiv:0907.3732].

[48] C. P. Herzog, *Lectures on Holographic Superfluidity and Superconductivity*, *J.Phys.A* **A42** (2009) 343001, [arXiv:0904.1975].

[49] S. A. Hartnoll, *Lectures on holographic methods for condensed matter physics*, *Class.Quant.Grav.* **26** (2009) 224002, [arXiv:0903.3246].

[50] G. T. Horowitz, *Introduction to Holographic Superconductors*, arXiv:1002.1722.

[51] N. Iqbal, H. Liu, and M. Mezei, *Lectures on holographic non-Fermi liquids and quantum phase transitions*, arXiv:1110.3814.

[52] S. A. Hartnoll, *Horizons, holography and condensed matter*, arXiv:1106.4324.

[53] S. S. Gubser, *Breaking an Abelian gauge symmetry near a black hole horizon*, *Phys.Rev.* **D78** (2008) 065034, [arXiv:0801.2977].

[54] S. A. Hartnoll, C. P. Herzog, and G. T. Horowitz, *Building a Holographic Superconductor*, *Phys.Rev.Lett.* **101** (2008) 031601, [arXiv:0803.3295].

[55] S. A. Hartnoll, C. P. Herzog, and G. T. Horowitz, *Holographic Superconductors*, *JHEP* **0812** (2008) 015, [arXiv:0810.1563].

[56] M. Kaminski, K. Landsteiner, J. Mas, J. P. Shock, and J. Tarrio, *Holographic Operator Mixing and Quasinormal Modes on the Brane*, *JHEP* **1002** (2010) 021, [arXiv:0911.3610].

[57] P. K. Kovtun and A. O. Starinets, *Quasinormal modes and holography*, *Phys.Rev.* **D72** (2005) 086009, [hep-th/0506184].

[58] R. M. Wald, *General Relativity*. The University of Chicago Press, Chicago, 1984.

[59] R. A. Davison and A. O. Starinets, *Holographic zero sound at finite temperature*, *Phys.Rev.* **D85** (2012) 026004, [arXiv:1109.6343].

[60] A. Karch and E. Katz, *Adding flavor to AdS / CFT*, *JHEP* **0206** (2002) 043, [hep-th/0205236].

[61] A. Karch, D. Son, and A. Starinets, *Zero Sound from Holography*, arXiv:0806.3796.

[62] E. M. Lifshitz and L. P. Pitaevskii, *Course of theoretical physics vol. 9: Statistical physics part 2*. Pergamon Press, Oxford, 1980.

[63] E. M. Lifshitz and L. P. Pitaevskii, *Course of theoretical physics vol. 10: Physical kinetics*. Pergamon Press, Oxford, 1981.

[64] M. Kulaxizi and A. Parnachev, *Comments on Fermi Liquid from Holography*, *Phys.Rev.* **D78** (2008) 086004, [arXiv:0808.3953].

[65] M. Kulaxizi and A. Parnachev, *Holographic Responses of Fermion Matter*, *Nucl.Phys.* **B815** (2009) 125–141, [arXiv:0811.2262].

[66] L.-Y. Hung and A. Sinha, *Holographic quantum liquids in 1+1 dimensions*, *JHEP* **1001** (2010) 114, [arXiv:0909.3526].

[67] O. Bergman, N. Jokela, G. Lifschytz, and M. Lippert, *Striped instability of a holographic Fermi-like liquid*, *JHEP* **1110** (2011) 034, [arXiv:1106.3883].

[68] C. Hoyos-Badajoz, A. O'Bannon, and J. M. Wu, *Zero Sound in Strange Metallic Holography*, *JHEP* **1009** (2010) 086, [arXiv:1007.0590].

[69] B.-H. Lee, D.-W. Pang, and C. Park, *Zero Sound in Effective Holographic Theories*, *JHEP* **1011** (2010) 120, [arXiv:1009.3966].

[70] M. Edalati, J. I. Jottar, and R. G. Leigh, *Holography and the sound of criticality*, *JHEP* **1010** (2010) 058, [arXiv:1005.4075].

[71] K.-Y. Kim and I. Zahed, *Baryonic Response of Dense Holographic QCD*, *JHEP* **0812** (2008) 075, [arXiv:0811.0184].

[72] C. P. Herzog, P. Kovtun, S. Sachdev, and D. T. Son, *Quantum critical transport, duality, and M-theory*, *Phys.Rev.* **D75** (2007) 085020, [hep-th/0701036].

[73] I. Amado, C. Hoyos-Badajoz, K. Landsteiner, and S. Montero, *Residues of correlators in the strongly coupled N=4 plasma*, *Phys.Rev.* **D77** (2008) 065004, [arXiv:0710.4458].

[74] I. Amado, C. Hoyos-Badajoz, K. Landsteiner, and S. Montero, *Hydrodynamics and beyond in the strongly coupled N=4 plasma*, *JHEP* **0807** (2008) 133, [arXiv:0805.2570].

[75] M. Kaminski, K. Landsteiner, F. Pena-Benitez, J. Erdmenger, C. Greubel, *et. al.*, *Quasinormal modes of massive charged flavor branes*, *JHEP* **1003** (2010) 117, [arXiv:0911.3544].

[76] C. P. Herzog, *An Analytic Holographic Superconductor*, *Phys.Rev.* **D81** (2010) 126009, [arXiv:1003.3278].

[77] S. Kobayashi, D. Mateos, S. Matsuura, R. C. Myers, and R. M. Thomson, *Holographic phase transitions at finite baryon density*, *JHEP* **0702** (2007) 016, [hep-th/0611099].

[78] J. Mas, J. P. Shock, and J. Tarrio, *A Note on conductivity and charge diffusion in holographic flavour systems*, *JHEP* **0901** (2009) 025, [arXiv:0811.1750].

[79] J. Erdmenger, N. Evans, I. Kirsch, and E. Threlfall, *Mesons in Gauge/Gravity Duals - A Review*, *Eur.Phys.J.* **A35** (2008) 81–133, [arXiv:0711.4467].

[80] P. Chesler and A. Vuorinen, *Heavy flavor diffusion in weakly coupled N=4 super Yang-Mills theory*, *JHEP* **0611** (2006) 037, [hep-ph/0607148].

[81] M. Kruczenski, D. Mateos, R. C. Myers, and D. J. Winters, *Meson spectroscopy in AdS / CFT with flavor*, *JHEP* **0307** (2003) 049, [hep-th/0304032].

[82] A. Karch and A. O'Bannon, *Holographic thermodynamics at finite baryon density: Some exact results*, *JHEP* **0711** (2007) 074, [arXiv:0709.0570].

[83] M. C. Wapler, *Massive Quantum Liquids from Holographic Angel's Trumpets*, *JHEP* **1005** (2010) 019, [arXiv:1002.0336].

[84] D. Mateos, R. C. Myers, and R. M. Thomson, *Thermodynamics of the brane*, *JHEP* **0705** (2007) 067, [hep-th/0701132].

[85] S. Nakamura, Y. Seo, S.-J. Sin, and K. Yogendran, *Baryon-charge Chemical Potential in AdS/CFT*, *Prog.Theor.Phys.* **120** (2008) 51–76, [arXiv:0708.2818].

[86] K. Ghoroku, M. Ishihara, and A. Nakamura, *D3/D7 holographic Gauge theory and Chemical potential*, *Phys.Rev.* **D76** (2007) 124006, [arXiv:0708.3706].

[87] T. Faulkner and H. Liu, *Condensed matter physics of a strongly coupled gauge theory with quarks: Some novel features of the phase diagram*, arXiv:0812.4278.

[88] D. Mateos, S. Matsuura, R. C. Myers, and R. M. Thomson, *Holographic phase transitions at finite chemical potential*, *JHEP* **0711** (2007) 085, [arXiv:0709.1225].

[89] R. C. Myers, A. O. Starinets, and R. M. Thomson, *Holographic spectral functions and diffusion constants for fundamental matter*, *JHEP* **0711** (2007) 091, [arXiv:0706.0162].

[90] D. Nickel and D. T. Son, *Deconstructing holographic liquids*, *New J.Phys.* **13** (2011) 075010, [arXiv:1009.3094].

[91] D. Mateos, R. C. Myers, and R. M. Thomson, *Holographic phase transitions with fundamental matter*, *Phys.Rev.Lett.* **97** (2006) 091601, [hep-th/0605046].

[92] C. Hoyos-Badajoz, K. Landsteiner, and S. Montero, *Holographic meson melting*, *JHEP* **0704** (2007) 031, [hep-th/0612169].

[93] A. Paredes, K. Peeters, and M. Zamaklar, *Mesons versus quasi-normal modes: Undercooling and overheating*, *JHEP* **0805** (2008) 027, [arXiv:0803.0759].

[94] J. Erdmenger, M. Kaminski, and F. Rust, *Holographic vector mesons from spectral functions at finite baryon or isospin density*, *Phys.Rev.* **D77** (2008) 046005, [arXiv:0710.0334].

[95] R. C. Myers and A. Sinha, *The Fast life of holographic mesons*, *JHEP* **0806** (2008) 052, [arXiv:0804.2168].

[96] J. Mas, J. P. Shock, J. Tarrio, and D. Zoakos, *Holographic Spectral Functions at Finite Baryon Density*, *JHEP* **0809** (2008) 009, [arXiv:0805.2601].

[97] M. Ammon, J. Erdmenger, S. Lin, S. Muller, A. O'Bannon, *et. al.*, *On Stability and Transport of Cold Holographic Matter*, *JHEP* **1109** (2011) 030, [arXiv:1108.1798].

[98] F. Bigazzi, A. L. Cotrone, J. Mas, D. Mayerson, and J. Tarrio, *D3-D7 Quark-Gluon Plasmas at Finite Baryon Density*, *JHEP* **1104** (2011) 060, [arXiv:1101.3560].

[99] S. A. Hartnoll, J. Polchinski, E. Silverstein, and D. Tong, *Towards strange metallic holography*, *JHEP* **1004** (2010) 120, [arXiv:0912.1061].

[100] S. Sachdev, *A model of a Fermi liquid using gauge-gravity duality*, *Phys.Rev.* **D84** (2011) 066009, [arXiv:1107.5321].

[101] N. Iqbal and H. Liu, *Luttinger's Theorem, Superfluid Vortices, and Holography*, arXiv:1112.3671.

[102] M. Goykhman, A. Parnachev, and J. Zaanen, *Fluctuations in finite density holographic quantum liquids*, arXiv:1204.6232.

[103] W. Kohn, *Cyclotron Resonance and de Haas-van Alphen Oscillations of an Interacting Electron Gas*, *Phys.Rev.* **123** (1961) 1242–1244.

[104] H. Liu, J. McGreevy, and D. Vegh, *Non-Fermi liquids from holography*, *Phys.Rev.* **D83** (2011) 065029, [arXiv:0903.2477].

[105] T. Faulkner, H. Liu, J. McGreevy, and D. Vegh, *Emergent quantum criticality, Fermi surfaces, and AdS(2)*, *Phys.Rev.* **D83** (2011) 125002, [arXiv:0907.2694].

[106] R. Belliard, S. S. Gubser, and A. Yarom, *Absence of a Fermi surface in classical minimal four-dimensional gauged supergravity*, *JHEP* **1110** (2011) 055, [arXiv:1106.6030].

[107] J. P. Gauntlett, J. Sonner, and D. Waldram, *Universal fermionic spectral functions from string theory*, *Phys.Rev.Lett.* **107** (2011) 241601, [arXiv:1106.4694].

[108] J. P. Gauntlett, J. Sonner, and D. Waldram, *Spectral function of the supersymmetry current*, *JHEP* **1111** (2011) 153, [arXiv:1108.1205].

[109] R. A. Davison and N. K. Kaplis, *Bosonic excitations of the AdS_4 Reissner-Nordstrom black hole*, *JHEP* **1112** (2011) 037, [arXiv:1111.0660].

[110] M. Cubrovic, J. Zaanen, and K. Schalm, *String Theory, Quantum Phase Transitions and the Emergent Fermi-Liquid*, *Science* **325** (2009) 439–444, [arXiv:0904.1993].

[111] M. Edalati, J. I. Jottar, and R. G. Leigh, *Shear Modes, Criticality and Extremal Black Holes*, *JHEP* **1004** (2010) 075, [arXiv:1001.0779].

[112] D. K. Brattan and S. A. Gentle, *Shear channel correlators from hot charged black holes*, *JHEP* **1104** (2011) 082, [arXiv:1012.1280].

[113] X.-H. Ge, K. Jo, and S.-J. Sin, *Hydrodynamics of RN AdS_4 black hole and Holographic Optics*, *JHEP* **1103** (2011) 104, [arXiv:1012.2515].

[114] G. Policastro, D. T. Son, and A. O. Starinets, *From AdS / CFT correspondence to hydrodynamics*, *JHEP* **0209** (2002) 043, [hep-th/0205052].

[115] M. Edalati, J. I. Jottar, and R. G. Leigh, *Transport Coefficients at Zero Temperature from Extremal Black Holes*, *JHEP* **1001** (2010) 018, [arXiv:0910.0645].

[116] G. Policastro, D. T. Son, and A. O. Starinets, *From AdS / CFT correspondence to hydrodynamics. 2. Sound waves*, *JHEP* **0212** (2002) 054, [hep-th/0210220].

[117] C. P. Herzog, *The Sound of M theory*, *Phys.Rev.* **D68** (2003) 024013, [hep-th/0302086].

[118] A. S. Miranda, J. Morgan, and V. T. Zanchin, *Quasinormal modes of plane-symmetric black holes according to the AdS/CFT correspondence*, *JHEP* **0811** (2008) 030, [arXiv:0809.0297].

[119] C. P. Herzog, *The Hydrodynamics of M theory*, *JHEP* **0212** (2002) 026, [hep-th/0210126].

[120] M. Cvetic, M. Duff, P. Hoxha, J. T. Liu, H. Lu, *et. al.*, *Embedding AdS black holes in ten-dimensions and eleven-dimensions*, *Nucl.Phys.* **B558** (1999) 96–126, [hep-th/9903214].

[121] S. A. Hartnoll and A. Tavanfar, *Electron stars for holographic metallic criticality*, *Phys.Rev.* **D83** (2011) 046003, [arXiv:1008.2828].

[122] O. DeWolfe, S. S. Gubser, and C. Rosen, *Fermi Surfaces in Maximal Gauged Supergravity*, arXiv:1112.3036.

[123] H. Kodama and A. Ishibashi, *Master equations for perturbations of generalized static black holes with charge in higher dimensions*, *Prog.Theor.Phys.* **111** (2004) 29–73, [hep-th/0308128].

[124] C. Charmousis, B. Gouteraux, B. Kim, E. Kiritsis, and R. Meyer, *Effective Holographic Theories for low-temperature condensed matter systems*, *JHEP* **1011** (2010) 151, [arXiv:1005.4690].

[125] S. S. Gubser and F. D. Rocha, *Peculiar properties of a charged dilatonic black hole in AdS_5*, *Phys.Rev.* **D81** (2010) 046001, [arXiv:0911.2898].

[126] K. Goldstein, S. Kachru, S. Prakash, and S. P. Trivedi, *Holography of Charged Dilaton Black Holes*, *JHEP* **1008** (2010) 078, [arXiv:0911.3586].

[127] S. A. Hartnoll and P. Petrov, *Electron star birth: A continuous phase transition at nonzero density*, *Phys.Rev.Lett.* **106** (2011) 121601, [arXiv:1011.6469].

[128] V. M. Puletti, S. Nowling, L. Thorlacius, and T. Zingg, *Holographic metals at finite temperature*, *JHEP* **1101** (2011) 117, [arXiv:1011.6261].

[129] N. Iqbal, H. Liu, and M. Mezei, *Semi-local quantum liquids*, *JHEP* **1204** (2012) 086, [arXiv:1105.4621].

[130] M. Duff and J. T. Liu, *Anti-de Sitter black holes in gauged $N = 8$ supergravity*, *Nucl.Phys.* **B554** (1999) 237–253, [hep-th/9901149].

[131] E. W. Leaver, *Quasinormal modes of Reissner-Nordstrom black holes*, *Phys.Rev.* **D41** (1990) 2986–2997.

[132] F. Denef, S. A. Hartnoll, and S. Sachdev, *Quantum oscillations and black hole ringing*, *Phys.Rev.* **D80** (2009) 126016, [arXiv:0908.1788].